ISSN: 2153-1196 Volume 15, Number 2, February 2024

Scientific Research Publishing

# Journal of Modern Physics

## Gravitation, Astrophysics and Cosmology

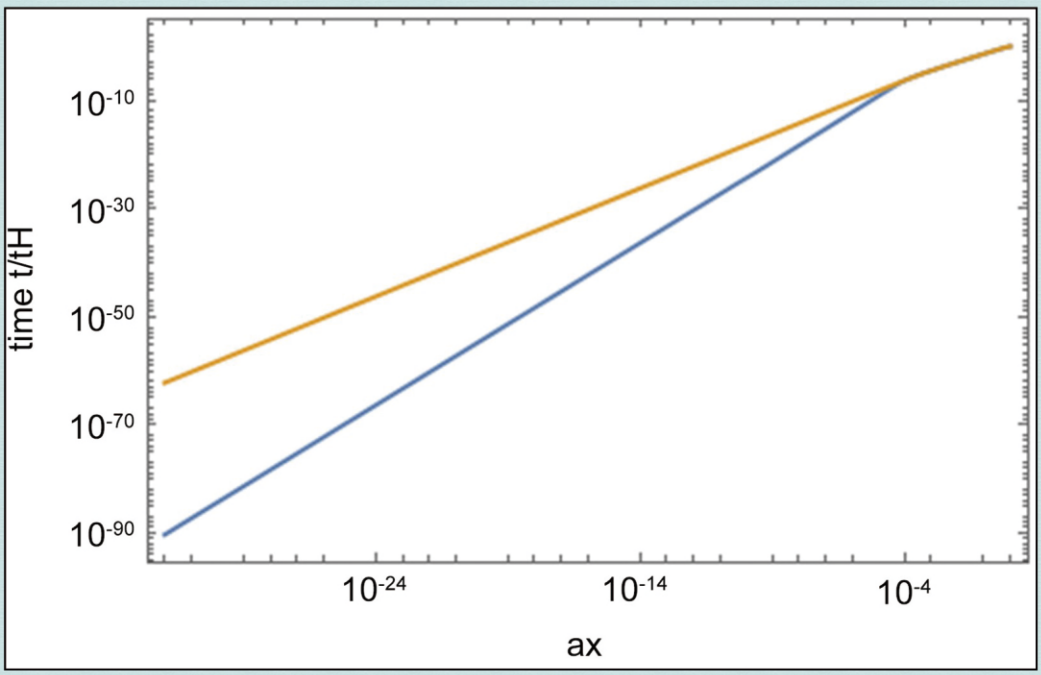


ISSN: 2153-1196
9 772153 119007 02

https://www.scirp.org/journal/jmp

# Journal Editorial Board

ISSN: 2153-1196 (Print) ISSN: 2153-120X (Online)
https://www.scirp.org/journal/jmp

## Editorial Board

Scientific Research Publishing

Journal of Modern Physics, 2024, 15, 159-238
https://www.scirp.org/journal/jmp
ISSN Online: 2153-120X
ISSN Print: 2153-1196

# Table of Contents

Volume 15 Number 2 February 2024



The figure on the front cover is from the article published in Journal of Modern Physics, 2024, Vol. 15, No. 2, pp. 193-238 by Jan Helm.

# Journal of Modern Physics (JMP)
# Journal Information

## SUBSCRIPTIONS

The *Journal of Modern Physics* (Online at Scientific Research Publishing, https://www.scirp.org/) is published monthly by Scientific Research Publishing, Inc., USA.

**Subscription rates:**
Print: $89 per issue.
To subscribe, please contact Journals Subscriptions Department, E-mail: sub@scirp.org

## SERVICES

**Advertisements**
Advertisement Sales Department, E-mail: service@scirp.org

**Reprints (minimum quantity 100 copies)**
Reprints Co-ordinator, Scientific Research Publishing, Inc., USA.
E-mail: sub@scirp.org

## COPYRIGHT



## PRODUCTION INFORMATION

For manuscripts that have been accepted for publication, please contact:
E-mail: jmp@scirp.org

Journal of Modern Physics, 2024, 15, 159-166
https://www.scirp.org/journal/jmp
ISSN Online: 2153-120X
ISSN Print: 2153-1196

# A Solution to the Cosmological Constant Problem Using the Holographic Principle (A Brief Note)

**Eugene Terry Tatum**

Independent Researcher, Bowling Green, Kentucky, USA
Email: ett@twc.com

**How to cite this paper:** Tatum, E.T. (2024) A Solution to the Cosmological Constant Problem Using the Holographic Principle (A Brief Note). *Journal of Modern Physics*, **15**, 159-166.
https://doi.org/10.4236/jmp.2024.152006

**Received:** December 9, 2023
**Accepted:** February 3, 2024
**Published:** February 6, 2024





## Abstract

This paper integrates a quantum conception of the Planck epoch early universe with FSC model formulae and the holographic principle, to offer a reasonable explanation and solution of the cosmological constant problem. Such a solution does not appear to be achievable in cosmological models which do not integrate black hole formulae with quantum formulae such as the Stephan-Boltzmann law. As demonstrated herein, assuming a constant value of Lambda over the great span of cosmic time appears to have been a mistake. It appears that Einstein's assumption of a *constant*, in terms of vacuum energy *density*, was not only a mistake for a statically-balanced universe, but also a mistake for a dynamically-expanding universe.

## Keywords

Quantum Cosmology, Planck Scale, Cosmological Constant, Black Holes, Holographic Principle, Flat Space Cosmology, AdS-CFT, ER = EPR, Cosmology Model

## 1. Introduction and Background

It appears that the correct mathematical treatment of our visible universe as an expanding black hole-like global object was first *successfully* achieved in 2015 [1] [2]. To achieve this, a thermodynamic formula *slightly different* from the Hawking black hole temperature formula was necessary. This was accomplished primarily due to the incorporation of a geometric mean refinement of Hawking's black hole temperature formula taking the following form:

$$T_t \cong \frac{\hbar c^3}{8\pi G k_B \sqrt{M_t M_{pl}}} \cong \frac{\hbar c}{4\pi k_B \sqrt{R_t R_{pl}}} \tag{1}$$

wherein $T_t$ is time-dependent cosmic temperature, $M_t$ is temperature-dependent cosmic mass, $R_t$ is temperature-dependent cosmic Schwarzschild radius, $R_{pl}$ is the Planck radius (to be defined below), and all other symbols are well-known physical constants. A stunning result was the *prediction*, in 2015, of today's most precise (*i.e.*, low uncertainty) Hubble constant measurement derived from a CMB temperature study reported in 2023 by Dhal *et al.* [3]. In the current paper, we will hereafter refer to Equation (1) as the Tatum *et al.* thermodynamic formula.

Although implied by the assumptions of the 2015 Flat Space Cosmology (FSC) model, their quantum cosmology equations were not published explicitly until 2018 [4]. These equations are repeated herein for the convenience of the reader:

$$R \cong \frac{\hbar^{3/2}c^{7/2}}{32\pi^2 k_B^2 T^2 G^{1/2}} \qquad R_0 \cong \frac{\hbar^{3/2}c^{7/2}}{32\pi^2 k_B^2 T_0^2 G^{1/2}} \tag{2}$$

$$H \cong \frac{32\pi^2 k_B^2 T^2 G^{1/2}}{\hbar^{3/2}c^{5/2}} \qquad H_0 \cong \frac{32\pi^2 k_B^2 T_0^2 G^{1/2}}{\hbar^{3/2}c^{5/2}} \tag{3}$$

$$t \cong \frac{\hbar^{3/2}c^{5/2}}{32\pi^2 k_B^2 T^2 G^{1/2}} \qquad t_0 \cong \frac{\hbar^{3/2}c^{5/2}}{32\pi^2 k_B^2 T_0^2 G^{1/2}} \tag{4}$$

$$M \cong \frac{\hbar^{3/2}c^{11/2}}{64\pi^2 k_B^2 T^2 G^{3/2}} \qquad M_0 \cong \frac{\hbar^{3/2}c^{11/2}}{64\pi^2 k_B^2 T_0^2 G^{3/2}} \tag{5}$$

$$Mc^2 \cong \frac{\hbar^{3/2}c^{15/2}}{64\pi^2 k_B^2 T^2 G^{3/2}} \qquad M_0c^2 \cong \frac{\hbar^{3/2}c^{15/2}}{64\pi^2 k_B^2 T_0^2 G^{3/2}} \tag{6}$$

The right-hand column equations are for correlation with current cosmological observations, using the 2009 Fixsen Cosmic Microwave Background (CMB) temperature of 2.72548 K as $T_0$, the only observational input [5]. The remarkably good correlations between these FSC quantum cosmology equations and current observations have been well-documented [6] The FSC model has proven to be quite useful in its predictive capacity [7] [8].

It is the purpose of the present paper to show how the FSC model can employ the holographic principle to offer a solution of the cosmological constant problem, whereas this appears to be extremely difficult or impossible using the standard ΛCDM cosmology model. This difficulty can be expressed by quantifying the discrepancy between the quantum field theory estimate of the value of the cosmological constant and observational estimates of its value. The discrepancy is a factor roughly on the order of $10^{121}$! This has often been referred to as the most embarrassing problem in all of modern physics [9] [10].

## 2. The Solution

It is theorized that the Big Bang may have started with what is likely to be the smallest possible micro black hole, the Planck mass particle, $m_P$. Since the Planck mass has a density at or near what is referred to as the "Planck density," one customarily derives its value according to $m_P/l_P^3$, which equals $5.155 \times 10^{96}$ kg·m$^{-3}$ using the NIST 2018 CODATA [11] [12]. However, we can also treat the

Planck mass particle as a micro black hole with a Schwarzschild radius of two Planck lengths ($2l_P$). In FSC, this is referred to as the "Planck radius" $R_{pl}$ [see Equation (1)]. If we divide the $m_P$ value of $2.17643424 \times 10^{-8}$ kg by the volume of a sphere of Schwarzschild radius $2l_P$, we get a result of $1.538322 \times 10^{95}$ kg·m$^{-3}$. This corresponds to a Planck energy density value of $1.382584 \times 10^{112}$ J·m$^{-3}$. These are almost certainly more realistic values for a micro black hole Planck density, and will be taken as such in the calculations below.

Furthermore, given its Schwarzschild radius $2l_P$, we can assume that the sphere of the Planck mass micro black hole has a surface area of $4\pi R_{pl}^2$, which is $16\pi l_P^2$. This implies a starting Hubble surface area value for the Planck epoch black hole universe of $1.3130 \times 10^{-68}$ m$^2$. We can then compare this starting Hubble horizon surface area value with that of the current Hubble surface. This would be according to the $4\pi R_0^2$ spherical surface formula. In FSC, the current Hubble radius value $R_0$ is $1.382894 \times 10^{26}$ *m*. Thus, the current value of $4\pi R_0^2$ would be $2.40318 \times 10^{53}$ m$^2$. Interestingly, the ratio of $2.40318 \times 10^{53}$ m$^2$ to $1.3130 \times 10^{-68}$ m$^2$ is $1.8303 \times 10^{121}$, which also can be expressed as $10^{121.26}$. This is the longstanding FSC magnitude of the cosmological constant problem. This can hardly be a coincidence with respect to the magnitude of the standard cosmology problem.

It is reasonable to treat the expanding cosmic black hole horizon at radius $R_t$ (the time-dependent Schwarzschild radius correlated to the increasing Schwarzschild mass $M_t$) as a membrane of area $4\pi R_t^2$. One can view this boundary surface (hereafter referred to as the "boundary") as continually radiating a Hawking temperature (see Haug & Tatum for details). Thus, this temperature smoothly declines as the cosmic black hole smoothly grows in mass and expands adiabatically.

We can also, according to the holographic principle of Susskind and 't Hooft [13], treat the boundary as a conceptually separate entity in comparison to the black hole interior (hereafter referred to as the "bulk"). Therefore, we are entitled to view the boundary as starting out, in the Planck mass epoch, with the Planck energy value of a single Planck mass micro black hole equal to $m_Pc^2$ equal to $1.9561 \times 10^9$ J. The Planck epoch temperature $T_P$ of this $16\pi l_P^2$ membrane is equal to $5.65 \times 10^{30}$ K (see Haug & Tatum, their Equation (6)), which can be compared to a $4\pi l_P^2$ (*i.e.*, according to a single Planck length Schwarzschild radius) boundary membrane temperature of $h^{1/2}c^{5/2}G^{-1/2}k_b^{-1}$ equal to $1.4168 \times 10^{32}$ *K*, the classical Planck temperature (see Buczyna *et al.* reference [12] on Planck units).

One can now use the holographic principle to create a one-to-one correspondence of energy densities between the boundary and the bulk. The energy density within the current boundary surface area should be the Planck energy density of $1.382584 \times 10^{112}$ J·m$^{-3}$ (as calculated above for the micro black hole epoch) divided by $1.8303 \times 10^{121}$ for the current cosmological epoch, to obtain the current FSC energy density within the boundary and bulk. The resulting energy density is $7.554 \times 10^{-10}$ J·m$^{-3}$ (see reference [6]). This is also quite consistent with the

current *observed* cosmological constant value of $P$vac = 5.3566 × $10^{-10}$ J·$m^{-3}$ from the 2015 Planck Collaboration data set [14]. In the FSC model, another cosmological conundrum, called the cosmological *coincidence* problem, is also solved. This is because, in FSC, the matter and vacuum densities are *always* highly correlated. This *cannot* be true for the standard ΛCDM model.

## 3. Discussion

The standard ΛCDM cosmological model is vexed by many conundrums, not the least of which are the cosmological constant problem and the cosmological coincidence problem. There has been a suspicion, for several decades now, that this may be because the ΛCDM model is not a fully-integrated quantum cosmology model. This appears to be true. On the other hand, the FSC model of Tatum *et al.* has derived some extremely useful Planck scale quantum cosmology formulae which, so far, appear to be accurate over a wide cosmic time and temperature range. An exciting recent development was Haug & Wojnow's derivation of the Tatum *et al.* thermodynamic formulae of Equation (1) using the Stephan-Boltzmann law [15].

Thus, FSC appears to be usefully integrating the general relativity of black holes with certain quantum formulae. This is what is meant by referring to FSC as a "quantum cosmology model." It may be the first of many similar models to follow. To this author's knowledge, no particularly useful quantum cosmology model preceded FSC, presumably because there was insufficient development of the appropriate cosmic thermodynamic formulae, which have always been a key feature of FSC.

The purpose of the present paper has been to use the black hole holographic principle of Susskind and 't Hooft to provide a solution to the cosmological constant problem. Maldacena's AdS-CFT and ER = EPR hypotheses [16] [17] and the related holographic principle appear to have been the biggest cosmological breakthroughs in recent decades. They have a firmly-established mathematical basis, so that cosmologists can have some confidence in their careful application or, at the least, a direction in which to look for a new breakthrough, such as presented herein.

Importantly, in just the last few years, some respected physicists and cosmologists have joined in the speculation that our universe might very well be an evolving and expanding black hole-like object [18] [19] [20] [21]. It is good to now have them joining the conversation. Siegel's summary on this topic is especially nice. Lineweaver and Patel make some excellent points as well. Objections that such speculations should be forbidden by general relativity are simply short-sighted. Black holes and related objects, such as white holes, are clearly allowed by general relativity and still too mysterious for us to forestall a debate on related cosmological models. The apparent successes of the FSC Schwarzschild cosmological model are also in support of this viewpoint. Our visible universe has a surprising number of mathematical similarities to a gigantic black hole. As

discussed in a comprehensive summary of the FSC model peer-reviewed publications [22], not the least of these are the mass-to-radius ratio and the current average density of the visible universe. For instance, the mass-to-radius ratio of the visible universe (if we include dark matter mass) and a Schwarzschild black hole are both in the range of $c^2/2G$ [23] [24]. Furthermore, the visible universe appears to be at or very near critical density. Surprisingly, this is the *average* density of a Schwarzschild black hole with a radius of approximately 14 billion light-years or very slightly larger (14.62 billion light-years in the FSC model). As a perpetual matter-generating model, FSC specifically models a universe at perpetual critical density. It appears, from CMB observations, that our visible universe has shown this spatial flatness feature (*i.e.*, critical density) as far back in cosmic time as we can observe to date. Thus, it appears to be an effective model for what we can see at present.

In their holographical principle hypothesis, Susskind and 't Hooft make separate distinctions between the horizon boundary of a black hole and its bulk. If their principle is correct, there is a one-to-one correspondence between properties of the boundary (a two-dimensional membrane of curved space-time) and the conventional 3-D bulk. As shown above, the original Planck mass energy (not density) within the boundary membrane is what is dispersed throughout the Hubble horizon boundary membrane during cosmic expansion. The resulting energy *density* dilutional effect is quantitively the same as observed in the 3D bulk. So, as often mentioned in previous papers, there is no cosmological constant problem in FSC. Finally, although some theorists [25] have speculated that there is no need to introduce a cosmological constant, the current paper accepts the presence of such a constant, despite its small value. Otherwise, it would be most difficult to explain why the universal expansion is not decelerating.

As for a way to potentially falsify the solution presented in the present paper, the best way to do so would be to measure the cosmic vacuum energy density so precisely that the calculated model density presented herein is *consistently* five or more standard deviations outside of the observational determination. At present, this does not appear to be the case. The two numbers are very close to one another, and there is yet too much uncertainty in the value of the Hubble constant. However, the coming decade of more precise dark energy observations and more precise Hubble constant determinations should be a good test of the hypothesis presented herein.

## 4. Summary and Conclusions

The current paper integrates a quantum conception of the Planck epoch early universe with FSC model formulae and the holographic principle, to offer a reasonable theoretical explanation and solution of the cosmological constant problem. Such a solution does not appear to be achievable in cosmological models which do not integrate black hole formulae with quantum formulae, such as the Stephan-Boltzmann law.

Einstein's "cosmological constant" was created *only* to achieve a statically-balanced universe (*i.e.*, neither contracting nor expanding). This was a mistake which he admitted to as his greatest blunder [26]. What was particularly erroneous about his blunder is well-described by Bodanis. The assumption that our universe could be kept perpetually in static balance by any sort of energy force in opposition to that of attractive gravity was simply unrealistic in the face of any perturbations to such a precarious balance.

However, in a dynamically-expanding universe, assuming the value of Lambda to remain constant *over the great span of cosmic time*, in terms of energy *density*, also appears to have been a mistake. At the very least, this possibility has been a topic of serious discussion in a number of recent scientific papers [27] [28] [29] [30]. And now, with the aid of the FSC model, the cosmological constant problem appears to be understandable and solved. We humbly and respectfully request that other investigators in the field carefully consider the above mathematical arguments and accept or attempt to refute the results.

## Dedications and Acknowledgements

This paper is dedicated to the late Dr. Stephen Hawking and to Dr. Roger Penrose for their groundbreaking work on black holes and their possible application to cosmology. Dr. Tatum also thanks Dr. Rudolph Schild of the Harvard-Smithsonian Center for Astrophysics for his past support and encouragement. Most importantly, he thanks his friend and colleague, U.V.S. Seshavatharam, for his co-authorship on selected previous FSC publications.

## Conflicts of Interest

The author declares no conflicts of interest regarding the publication of this paper.

## References

[1] Tatum, E.T., Seshavatharam, U.V.S. and Lakshminarayana, S. (2015) *International Journal of Astronomy and Astrophysics*, **5**, 116-124. https://doi.org/10.4236/ijaa.2015.52015

[2] Tatum, E.T., Seshavatharam, U.V.S. and Lakshminarayana, S. (2015) *Frontiers of Astronomy, Astrophysics and Cosmology*, **1**, 98-104. http://pubs.sciepub.com/faac/1/2/3

[3] Dhal, S., *et al.* (2023) *Experimental Astronomy*, **612**, 86.

[4] Tatum, E.T. (2018) *Journal of Modern Physics*, **9**, 1867-1882. https://doi.org/10.4236/jmp.2018.910118

[5] Fixsen, D.J., *et al.* (2009) *Astrophysical Journal*, **707**, 916. https://doi.org/10.1088/0004-637X/707/2/916

[6] Tatum, E.T. (2020) A Heuristic Model of the Evolving Universe Inspired by Hawking and Penrose. In: Tatum, E.T., Ed., *New Ideas Concerning Black Holes and the Universe*, IntechOpen, London, 5-21. https://doi.org/10.5772/intechopen.75238

[7] Tatum, E.T., Haug, E.G. and Wojnow, S. (2023) Predicting High Precision Hubble

Constant Determinations Based upon a New Theoretical Relationship between CMB Temperature and $H_0$. https://hal.science/hal-04268732v2

[8] Haug, E.G. and Tatum, E.T. (2023) The Hawking Hubble Temperature as a Minimum Temperature, the Planck Temperature as a Maximum Temperature and the CMB Temperature as Their Geometric Mean Temperature. https://hal.science/hal-04308132v2

[9] Weinberg, S. (1989) *Reviews of Modern Physics*, **61**, 1-23. https://doi.org/10.1103/RevModPhys.61.1

[10] Carroll, S. (2001) *Living Reviews in Relativity*, **4**, 5-56. https://doi.org/10.12942/lrr-2001-1

[11] Tiesinga, E., Mohr, P., Newell, D. and Taylor, B. (2022) *Reviews of Modern Physics*, **93**, Article ID: 025010.

[12] Buczyna, J.R., Unnikrishnan, C.S. and Gillies, G.T. (2011) *Gravitation and Cosmology*, **17**, 339-343. https://doi.org/10.1134/S0202289311040037

[13] Susskind, L. (1995) *Journal of Mathematical Physics*, **36**, 6377-6396. https://doi.org/10.1063/1.531249

[14] Planck Collaboration (2016) *Astronomy & Astrophysics*, **594**, A13. https://doi.org/10.1051/0004-6361/201629543

[15] Haug, E.G. and Wojnow, S. (2023) How to Predict the Temperature of the CMB Directly Using the Hubble Parameter and the Planck Scale Using the Stephan-Boltzmann Law. https://doi.org/10.21203/rs.3.rs-3576675/v1

[16] Maldacena, J.M. (1998) *Advances in Theoretical Mathematical Physics*, **2**, 231-252. https://doi.org/10.4310/ATMP.1998.v2.n2.a1

[17] Maldacena, J. and Susskind, L. (2013) *Fortschritte der Physik*, **61**, 781-811. https://doi.org/10.1002/prop.201300020

[18] Siegel, E. (2022, January 27) Are We Living in a Baby Universe That Looks like a Black Hole to Outsiders? *Forbes*. https://bigthink.com/hard-science/baby-universes-black-holes-dark-matter/

[19] Lineweaver, C.H. and Patel, V.M. (2023) *American Journal of Physics*, **91**, 819-825. https://doi.org/10.1119/5.0150209

[20] Rovelli, C. and Vidotto, F. (2018) *Universe*, **4**, Article No. 127. https://doi.org/10.3390/universe4110127

[21] Poplawski, N. (2016) *The Astrophysical Journal*, **832**, 96. https://doi.org/10.3847/0004-637X/832/2/96

[22] Tatum, E.T. and Seshavatharam, U.V.S. (2021) Flat Space Cosmology—A New Model of the Universe Incorporating Astronomical Observations of Black Holes, Dark Energy and Dark Matter. Universal Publishers, Irvine.

[23] Tatum, E.T. (2015) *Journal of Cosmology*, **25**, 13061-13080. https://ui.adsabs.harvard.edu/abs/2015JCos...2513063T/abstract

[24] Tatum, E.T. (2015) *Journal of Cosmology*, **25**, 13081-13111. https://ui.adsabs.harvard.edu/abs/2015JCos...2513073T

[25] Yarman, T. and Kholmetskii, A.L. (2013) *European Physics Journal Plus*, **128**, Article No. 8. https://doi.org/10.1140/epjp/i2013-13008-2

[26] Bodanis, D. (2016) Einstein's Greatest Mistake: A Biography. Houghton Mifflin Harcourt, New York.

[27] Kragh, H.S. and Overduin, J.M. (2014) Variable Cosmological Constants and Quintessence. In: Kragh, H.S. and Overduin, J.M., Eds., *The Weight of the Vacuum*, Sprin-

ger, Berlin, 77-87. https://doi.org/10.1007/978-3-642-55090-4_10

[28] Xu, L.X., Lu, J.B. and Li, W.B. (2010) *Physics Letters B*, **690**, 333-336. https://doi.org/10.1016/j.physletb.2010.05.058

[29] Blanco-Pérez, C. and Fernández-Guerrero, A. (2015) *Zeitschrift für Naturforschung A*, **70**, 905-911. https://doi.org/10.1515/zna-2015-0314

[30] Ahmed, N. and Alamri, S.Z. (2018) *Research in Astronomy and Astrophysics*, **18**, 123. https://doi.org/10.1088/1674-4527/18/10/123

Journal of Modern Physics, 2024, 15, 167-173
https://www.scirp.org/journal/jmp
ISSN Online: 2153-120X
ISSN Print: 2153-1196

# Upsilon Constants and Their Usefulness in Planck Scale Quantum Cosmology

**Eugene Terry Tatum**

Independent Researcher, Bowling Green, Kentucky, USA
Email: ett@twc.com

**How to cite this paper:** Tatum, E.T. (2024) Upsilon Constants and Their Usefulness in Planck Scale Quantum Cosmology. *Journal of Modern Physics*, **15**, 167-173.
https://doi.org/10.4236/jmp.2024.152007

**Received:** November 6, 2023
**Accepted:** February 3, 2024
**Published:** February 6, 2024



## Abstract

This paper introduces the two Upsilon constants to the reader. Their usefulness is described with respect to acting as coupling constants between the CMB temperature and the Hubble constant. In addition, this paper summarizes the current state of quantum cosmology with respect to the Flat Space Cosmology (FSC) model. Although the FSC quantum cosmology formulae were published in 2018, they are only rearrangements and substitutions of the other assumptions into the original FSC Hubble temperature formula. In a real sense, this temperature formula was the first quantum cosmology formula developed since Hawking's black hole temperature formula. A recent development in the last month proves that the FSC Hubble temperature formula can be derived from the Stephan-Boltzmann law. Thus, this Hubble temperature formula effectively *unites* some quantum developments with the general relativity model inherent in FSC. More progress towards unification in the near-future is expected.

## Keywords

Quantum Cosmology, Hubble Constant, Planck Scale, Upsilon Constant, Flat Space Cosmology, Black Holes, CMB Temperature, ΛCDM Cosmology, Quantum Gravity, Unification

## 1. Introduction and Background

To the best of this author's knowledge, Planck scale quantum cosmology effectively originated with the publication of the seminal papers of Flat Space Cosmology (FSC) in 2015 [1] [2] [3] [4]. By incorporating our model Hubble constant definition and the Schwarzschild formula into our unique Hubble temperature formula, we *predicted* in 2015 a Hubble constant value of 66.89 km/s/Mpc. A subsequent study in 2023 [5] yielded a nearly identical result (66.87117) to a

precision of ±0.00043.

The only input of our 2015 FSC Hubble constant determination formula was Fixsen's 2009 CMB temperature $T_0$ value of 2.72548 K [6]. Our particularly useful *scaling* cosmological black hole temperature formula is:

$$\left.\begin{aligned} & k_B T_t \cong \frac{\hbar c^3}{8\pi G\sqrt{M_t M_{pl}}} \cong \frac{\hbar c}{4\pi\sqrt{R_t R_{pl}}} \\ & \begin{cases} M_t \cong \left(\dfrac{\hbar c^3}{8\pi G k_B T_t}\right)^2 \dfrac{1}{M_{pl}} & (\mathrm{A}) \\ R_t \cong \dfrac{1}{R_{pl}}\left(\dfrac{\hbar c}{4\pi k_B}\right)^2\left(\dfrac{1}{T_t}\right)^2 & (\mathrm{B}) \\ R_t T_t^2 \cong \dfrac{1}{R_{pl}}\left(\dfrac{\hbar c}{4\pi k_B}\right)^2 & (\mathrm{C}) \\ t \cong \dfrac{R_t}{c} & (\mathrm{D}) \end{cases} \end{aligned}\right\} \quad (1)$$

One can readily see that this FSC Temperature formula (top left equation) is a slight (but *important*) modification of Hawking's black hole temperature formula in terms of the product inside the radical of our denominator. It is also apparent that our FSC temperature formula and Hawking's temperature formula give the same value for the Planck mass epoch universe, presumably at or near the beginning of universal expansion. Both formulae would also agree if the half Planck mass (correlating to a single Planck length Schwarzschild radius) were inserted for both terms inside the radical. The half Planck mass can also be referred to as the "instanton".

It is of great interest that Haug and Wojnow [7] have recently confirmed the importance of the FSC temperature formula by deriving it from the Stephan-Boltzmann law! This is a tremendous breakthrough in further certifying FSC as a useful model of quantum cosmology. One can then realize that the FSC temperature formula is a major step forward in uniting the general relativity of black holes with their quantum physics, as Hawking attempted to do.

Since the October 23, 2023 pre-print of Haug and Wojnow as described above, Tatum *et al.* [8] have derived two useful formulae using the Greek and Latin versions of letter Upsilon as a compound constant coupling the Hubble constant to the CMB temperature. They employ the Greek Upsilon symbol ϒ and the Latin Capital Upsilon symbol Ʊ as new constants defined below.

*In 2018, FSC quantum cosmology equations were fully derived* by Tatum and published in several venues [9] [10] [11]. This was achieved by rearranging the FSC Hubble temperature formula and substituting *c/R* with the Hubble constant. Moreover, the Schwarzschild formula was used in order to substitute *R* with its definition in terms of *M*. The resulting quantum cosmology formulae are as follows, using only the standard cosmological and quantum symbols:

$$R \cong \frac{\hbar^{3/2} c^{7/2}}{32\pi^2 k_B^2 T^2 G^{1/2}} \qquad R_0 \cong \frac{\hbar^{3/2} c^{7/2}}{32\pi^2 k_B^2 T_0^2 G^{1/2}} \quad (2)$$

$$H \cong \frac{32\pi^2 k_B^2 T^2 G^{1/2}}{\hbar^{3/2} c^{5/2}} \qquad H_0 \cong \frac{32\pi^2 k_B^2 T_0^2 G^{1/2}}{\hbar^{3/2} c^{5/2}} \tag{3}$$

$$t \cong \frac{\hbar^{3/2} c^{5/2}}{32\pi^2 k_B^2 T^2 G^{1/2}} \qquad t_0 \cong \frac{\hbar^{3/2} c^{5/2}}{32\pi^2 k_B^2 T_0^2 G^{1/2}} \tag{4}$$

$$M \cong \frac{\hbar^{3/2} c^{11/2}}{64\pi^2 k_B^2 T^2 G^{3/2}} \qquad M_0 \cong \frac{\hbar^{3/2} c^{11/2}}{64\pi^2 k_B^2 T_0^2 G^{3/2}} \tag{5}$$

$$Mc^2 \cong \frac{\hbar^{3/2} c^{15/2}}{64\pi^2 k_B^2 T^2 G^{3/2}} \qquad M_0 c^2 \cong \frac{\hbar^{3/2} c^{15/2}}{64\pi^2 k_B^2 T_0^2 G^{3/2}} \tag{6}$$

As per convention, the $T_0$ equations in the right-hand column are for currently observed cosmological values, where the current and most precise value of the CMB temperature (Fixsen's 2.72548 K) is used as the sole $T_0$ input. The 2018 NIST CODATA values for the constants are updated, in place of the 2014 NIST CODATA values used in 2015. These 2018 values are either identical (as in most cases) or minimally different (as for $G$) in comparison to those used in 2015. Therefore, the calculated results of the standard cosmological parameters remain essentially of the same values (see Section 3).

## 2. The Upsilon Formulae for Calculating $H_0$

One can readily recognize that the $H_0$ value calculated above can also be expressed as:

$$H_0 = \Upsilon T_0^2 \tag{7}$$

wherein all of the constants on the right-hand side of the $H_0$ Equation in (3) can be replaced with the Greek Upsilon term. Thus, it becomes quite clear that *there is an extremely interesting and simple relationship between the Hubble constant and the current CMB temperature in FSC which dates back to* 2015. *One can think of them as essentially two sides of the same cosmological coin*! *Given this new insight*, $H_0$ *can be reconsidered as a scaling cosmic thermodynamic parameter*.

Equation (7), which we refer to as the first of our cosmological "Upsilon equations", expresses the current Hubble constant in reciprocal seconds ($s^{-1}$). Using the 2009 Fixsen CMB temperature value $T_0$ of 2.72548 K, one gets a Hubble constant value of:

$$H_0 = 2.167899530268314 \times 10^{-18}\ s^{-1} \tag{8}$$

The value for $\Upsilon$ in Equation (7) reduces to:

$$\Upsilon = 2.918456015397301274664047080 16 \times 10^{-19}\ s^{-1} \cdot K^{-2} \tag{9}$$

One can then use the conversion factor for arriving at $H_0$ in units of km/s/Mpc by multiplying $\Upsilon$ by 3.08567758149137 × $10^{19}$ km/Mpc. A further simplification of the $\Upsilon$ term, intended for immediate conversion of CMB temperature $T_0$ to $H_0$ in units of km/s/Mpc, utilizes the most precise km/Mpc conversion number used by the IAU (International Astronomical Union). The Latin Capital Upsilon term $\mho$ is then used instead of the Greek Upsilon term $\Upsilon$ so that the second Upsilon

formula is:

$$H_0 = \mho T_0^2 \tag{10}$$

The value for $H_0$ is then *converted directly to km/s/Mpc*, without requiring an intermediate km/Mpc multiplication step.

$$H_0 = \mho T_0^2 = 66.894389794746 \text{ km/s/Mpc} \tag{11}$$

The value for $\mho$ in Equation (11) reduces to:

$$\mho = 9.005414299280081 \text{ km/s/Mpc/K}^2 \tag{12}$$

Or, if one chooses, the units of $\mho$ can be expressed in $\text{km}\cdot\text{s}^{-1}\cdot\text{Mpc}^{-1}\cdot\text{K}^{-2}$

So, a quick and useful approximation of $H_0$ can be obtained by simply multiplying the square of the CMB temperature by 9. If anyone among our modern cosmologists has already found this quick rule-of-thumb CMB temperature-to-Hubble constant conversion method to km/s/Mpc, this paper provides, for the first time, the theoretical basis for this conversion method. Even using a $\mho$ conversion value of 9.0054143 km/s/Mpc/K$^2$ gives an almost exact Hubble constant value. In such case, the extra decimal places in the above numbers add relatively little more value. The strength of the current paper is simply to provide the FSC rationale for generating such precise and accurate Hubble constant values from knowing only the best modern measurement of the CMB temperature.

## 3. Results: Using FSC Formulae to Calculate Parameters

Standard cosmological formulae are typically calculated using the current Hubble constant $H_0$ customarily given in S.I. units. Thus, the Hubble constant value in reciprocal seconds ($\text{s}^{-1}$) is used. Below are the most commonly-used formulae in ΛCDM and FSC:

$$t_0 \cong \frac{1}{H_0} = 4.61275989\times10^{17} \text{ s} = 14.617 \text{ billion years} \tag{13}$$

$$R_0 \cong \frac{c}{H_0} = 1.38287063\times10^{26} \text{ m} = 14.617 \text{ billion lt-yrs} \tag{14}$$

$$M_0 = \frac{c^3}{2GH_0} = 9.3108051513\times10^{52} \text{ kg} \tag{15}$$

$$M_0c^2 = \frac{c^5}{2GH_0} = 8.3681343479\times10^{69} \text{ J} \tag{16}$$

$$\rho_0 = \frac{3H_0^2}{8\pi G} = 8.40531461467\times10^{-27} \text{ kg}\cdot\text{m}^{-3} \tag{17}$$

$$\rho_0c^2 = \frac{3H_0^2c^2}{8\pi G} = 7.554320039\times10^{-10} \text{ J}\cdot\text{m}^{-3} \tag{18}$$

The above results are similar to the ΛCDM values, allowing for some theoretical differences and observational uncertainties. ΛCDM apparently doesn't use the exact cosmological time formula given above, unless they are using a different $H_0$ value than that obtained from the Planck satellite CMB observations. It is

particularly puzzling that standard model cosmologists insist on a cosmic age of approximately 13.8 billion years, despite the current best estimate of the age of the Milky Way's "Methuselah star" (HD 140283). This estimate has a reported value of 14.27 ± 0.38 billion years [12]. Furthermore, astrophysicists are deeply puzzled as to how the early galaxies could have become so large, if the universe was actually only 13.8 billion years old. Nevertheless, the difference between the "observed" cosmic age of about 13.8 billion years and the FSC calculation of about 14.6 billion years is only about 5.8%, which could well be within the margin of observational error (thinking again of the Methuselah star!).

## 4. Discussion

This paper has been written with several purposes in mind. First, in light of recent breakthroughs having to do with uniting quantum physics with general relativity, this paper provides a wider historical perspective which places the FSC model at the center of these developments. Our 2015 FSC papers introduced readers to our new cosmological model which incorporates formulae representing reasonable speculations concerning the fact *that our expanding universe has a number of parameter relationships not unlike a* Schwarzschild *black hole*. First and foremost among these is the mass-to-radius ratio of our visible universe, which is very close to, if not exactly, the ratio of a *Schwarzschild* black hole, once one adds in the dark matter, which is at least five times the visible matter. In addition, it is almost unimaginable that the average density measurement of our universe is essentially that of a black hole with a radius of about 14 billion light-years. One only has to plug the numbers in and calculate *M/R* ratio and the average mass density calculated in this paper. If one compares these two figures with those of a Schwarzschild black hole of similar mass and radius, it certainly raises a number of interesting questions. These observations, among many others, led to our development of the FSC model. We were curious as to what a model of reasonable black hole assumptions might produce. The result was the eventual development of what we believe are the first useful quantum cosmology formulae, some of which are repeated in this paper. Later publications [13] [14] [15] have suggested similar lines of development, perhaps inspired by the success of FSC. As for any possible significance of the Upsilon constants with respect to quantum symmetry in cosmology, or implications concerning a bouncing quantum cosmology, this is unknown at the present time.

Second, this paper introduces to readers the discovery by Tatum *et al.* [8] concerning the use of the two Upsilon compound coupling constants relating the Hubble constant to the square of the CMB temperature in a surprisingly simple way. In a sense, the Hubble constant and the CMB temperature *appear* to be permanently bound together by our Upsilon constants. Apparently, one cannot consider one without considering the other. If this turns out to be true, then the Hubble constant is no more a cosmic constant (over time) than the CMB temperature is a cosmic constant. Unless they violate the perfect cosmological prin-

ciple (*i.e.*, no particular cosmic time is *particularly special* for us as observers), they are *both* most likely better regarded as *scaling thermodynamic cosmic parameters*. Maybe it is true that "only time will tell".

## 5. Summary and Conclusion

To summarize, this paper clearly defines a fascinating relationship between the CMB temperature and the Hubble constant. With the aid of FSC quantum cosmology formulae (in particular, the formula for the current Hubble constant value), it is apparent that there is a compound constant which couples these two universal parameters at present, and most likely for other cosmic times since the decoupling epoch. Tatum *et al.*, in a recent paper [8], have named the first coupling constant Upsilon, using the Greek symbol ϒ. At about the same time, Tatum independently arrived at a different coupling constant which automatically gives the Hubble constant in km/s/Mpc, without having to convert reciprocal seconds to km/s/Mpc. This conversion is already accomplished with the use of the second Upsilon symbol, the Latin Capital Upsilon symbol ʊ. Since the reader might be interested in the historical development of quantum cosmology to the present, this paper has also provided some context concerning the FSC model and its extremely useful Hubble temperature equation with much resemblance to the Hawking black hole temperature formula. In retrospect, and in a real sense, our slightly modified formula appears to be the very first *useful* quantum cosmology formula.

Comment: It should be noted here that this paper in no way attempts to address the current "Hubble tension" problem. Because of dramatically different methods for measuring the Hubble constant value, there are a myriad of factors to consider before usefully comparing the CMB method and the nearby universe methods employed by the SHoES project [16] and Freedman [17].

## Dedications and Acknowledgements

This paper is dedicated to the late Dr. Stephen Hawking and Dr. Roger Penrose for their groundbreaking work on black holes and their possible application to cosmology. Dr. Tatum thanks Dr. Rudolph Schild of the Harvard-Smithsonian Center for Astrophysics for his past encouragement and support. Most importantly, he also thanks his friend and colleague, U.V.S. Seshavatharam, for his co-authorship on selected FSC publications.

## Conflicts of Interest

The author declares no conflicts of interest regarding the publication of this paper.

## References

[1] Tatum, E.T., Seshavatharam, U.V.S. and Lakshminarayana, S. (2015) *Journal of Modern Physics*, **5**, 116-124. http://dx.doi.org/10.4236/ijaa.2015.52015

[2] Tatum, E.T., Seshavatharam, U.V.S. and Lakshminarayana, S. (2015) *Journal of Applied Physical Science International*, **4**, 18-26.

[3] Tatum, E.T., Seshavatharam, U.V.S. and Lakshminarayana, S. (2015) *International Journal of Astronomy and Astrophysics*, **5**, 133-140. http://dx.doi.org/10.4236/ijaa.2015.53017

[4] Tatum, E.T., Seshavatharam, U.V.S. and Lakshminarayana, S. (2015) *Frontiers of Astronomy, Astrophysics and Cosmology*, **1**, 98-104. http://pubs.sciepub.com/faac/1/2/3

[5] Dhal, S. *et al.* (2023) *Experimental Astronomy*, **56**, 715-726. https://doi.org/10.1007/s10686-023-09904-w

[6] Fixsen, D.J. *et al.* (2009) *Astrophysical Journal*, **707**, 916. https://doi.org/10.1088/0004-637X/707/2/916

[7] Haug, E.G and Wojnow, S. (2023) Planck Scale Quantum Cosmology Predicts the Temperature of the Cosmic Microwave Background. https://doi.org/10.13140/RG.2.2.19811.12328

[8] Tatum, E.T., Haug, E.G. and Wojnow, S. (2023). Predicting High Precision Hubble Constant Determinations Based Upon a New Theoretical Relationship between CMB Temperature and $H_0$. https://hal.science/hal-04268732

[9] Tatum, E.T. (2018) Why Flat Space Cosmology Is Superior to Standard Inflationary Cosmology. *Journal of Modern Physics*, **9**, 1867. https://dx.doi.org/10.4236/jmp.2018.910118

[10] Tatum, E.T. (2019) A Heuristic Model of the Evolving Universe Inspired by Hawking and Penrose. IntechOpen. http://dx.doi.org/10.5772/intechopen.87019

[11] Tatum, E.T. and Seshavatharam, U.V.S. (2021) Flat Space Cosmology—A New Model of the Universe Incorporating Astronomical Observations of Black Holes, Dark Energy and Dark Matter. Universal Publishers, Irvine, California.

[12] Vandenberg, D.A. *et al.* (2014) *Astrophysical Journal*, **792**, Article No. 110. https://doi.org/10.1088/0004-637X/792/2/110

[13] Christillin, P. (2023) *Journal of Modern Physics*, **14**, 666-669. https://doi.org/10.4236/jmp.2023.145037

[14] Fèvre, R. (2021) *Journal of High Energy Physics, Gravitation and Cosmology*, **7**, 377-390. https://doi.org/10.4236/jhepgc.2021.72021

[15] Lineweaver, C.H. and Patel, V.M. (2023) *American Journal of Physics*, **91**, 819-825. https://doi.org/10.1119/5.0150209

[16] Reiss, A.G., *et al.* (2021) *Astrophysical Journal*, **934**, L7. https://doi.org/10.3847/2041-8213/ac5c5b

[17] Freedman, W.L. *et al.* (2019) *Astrophysical Journal*, **882**, 34. https://doi.org//10.3847/1538-4357/ab2f73

Journal of Modern Physics, 2024, 15, 174-178
https://www.scirp.org/journal/jmp
ISSN Online: 2153-120X
ISSN Print: 2153-1196

# How the Flat Space Cosmology Model Correlates the Recombination CMB Temperature of 3000 K with a Redshift of 1100

**Eugene Terry Tatum[1], U. V. S. Seshavatharam[2]**

[1]Independent Researcher, Bowling Green, Kentucky, USA
[2]I-SERVE, Hitech City, Hyderabad, India
Email: ett@twc.com, seshavatharam.uvs@gmail.com

**How to cite this paper:** Tatum, E.T. and Seshavatharam, U.V.S. (2024) How the Flat Space Cosmology Model Correlates the Recombination CMB Temperature of 3000 K with a Redshift of 1100. *Journal of Modern Physics*, **15**, 174-178.
https://doi.org/10.4236/jmp.2024.152008

**Received:** November 23, 2023
**Accepted:** February 3, 2024
**Published:** February 6, 2024





## Abstract

This paper shows how the Flat Space Cosmology model correlates the recombination epoch CMB temperature of 3000 K with a cosmological redshift of 1100. This proof is given in support of the recent publication that the Tatum and Seshavatharam Hubble temperature formulae can be derived using the Stephan-Boltzmann dispersion law. Thus, as explained herein, the era of high precision Planck scale quantum cosmology has arrived.

## Keywords

Hubble Constant, Cosmic Microwave Background, Quantum Cosmology, Stephan-Boltzmann, Upsilon Coupling Constant, Flat Space Cosmology, ΛCDM Cosmology

## 1. Introduction and Background

It has long been established that the cosmic recombination epoch Cosmic Microwave Background (CMB) temperature of 3000 K correlates with a cosmological redshift $z$ value of around 1100. This has been especially true since Fixsen updated his fitting of the CMB black body radiation spectrum with a peak temperature of 2.72548 K [1]. Given the black body nature of the 3000 K universe, it is perhaps not surprising that one can successfully apply the Stephan-Boltzmann dispersion law to derive the Tatum and Seshavatharam Hubble temperature $T_H$ formulae [2]:

$$\left.\begin{aligned} & k_B T_t \cong \frac{\hbar c^3}{8\pi G\sqrt{M_t M_{pl}}} \cong \frac{\hbar c}{4\pi\sqrt{R_t R_{pl}}} \\ & M_t \cong \left(\frac{\hbar c^3}{8\pi G k_B T_t}\right)^2 \frac{1}{M_{pl}} \qquad (\mathrm{A}) \\ & R_t \cong \frac{1}{R_{pl}}\left(\frac{\hbar c}{4\pi k_B}\right)^2 \left(\frac{1}{T_t}\right)^2 \qquad (\mathrm{B}) \\ & R_t T_t^2 \cong \frac{1}{R_{pl}}\left(\frac{\hbar c}{4\pi k_B}\right)^2 \qquad (\mathrm{C}) \\ & t \cong \frac{R_t}{c} \qquad (\mathrm{D}) \end{aligned}\right\} \tag{1}$$

Proof of the Stephan-Boltzmann derivation was given recently [3].

While the Tatum and Seshavatharam temperature formulae are modeled for a Planck scale quantum cosmology for the entire history of universal expansion, we will specifically show in the present paper the correlation between the CMB temperature of 3000 K and the redshift $z$ value of 1100. Our particular Planck scale quantum cosmology model is called Flat Space Cosmology (FSC) [4].

## 2. Relevant Equations for Our CMB Temperature and Redshift Calculations

This section provides the relevant FSC equations useful for correlating a given Hubble CMB temperature $T_X$ with its predicted redshift $z$ and predicted Hubble parameter value $H_T$.

The usual cosmology redshift formula with regard to past and current cosmic temperatures is:

$$z \cong \frac{T_x}{T_0} - 1 \tag{2}$$

wherein $z$ is the redshift, $T_x$ is any given Hubble CMB temperature, and $T_0$ is the 2009 current Fixsen CMB temperature of 2.72548 K.

To correlate the predicted $z$ value with the predicted temperature-dependent Hubble parameter value $H_T$, the following FSC Hubble quantum cosmology formulae [5] are used:

$$H \cong \frac{32\pi^2 k_B^2 T^2 G^{1/2}}{\hbar^{3/2} c^{5/2}} \qquad H_0 \cong \frac{32\pi^2 k_B^2 T_0^2 G^{1/2}}{\hbar^{3/2} c^{5/2}} \tag{3}$$

wherein the latest NIST 2018 CODATA [6] are used for all constants, and $T_0$ is the 2009 Fixsen CMB temperature, the only observational input to the right-hand equation.

To correlate the FSC cosmic radius value $R_T$ at a given CMB temperature, the top equation in formulae (1) is used (see the right-hand term):

$$T_t \cong \frac{\hbar c^3}{8\pi G k_B \sqrt{M_t M_{pl}}} \cong \frac{\hbar c}{4\pi k_B \sqrt{R_t R_{pl}}} \tag{4}$$

Results of calculations made using Equations (2) thru (4) are presented in Table 1.

## 3. Discussion

Beginning in 2015, FSC has proven to be one of the most successful Planck scale quantum cosmology models to date. In fact, the Hubble parameter quantum cosmology formulae [current Equation (3)] and the top equation of the Tatum and Seshavatharam Hubble temperature $T_X$ formulae [current Equation (4)] have been used to predict, with high precision, the most recent Hubble parameter values derived from CMB studies published in 2023 [7].

Reference [7] mentions a "deeper theoretical understanding" of the relationship between the Hubble parameter and the CMB temperature. One can see in our $H_X/T_X^2$ column of Table 1 that there is an obvious coupling constant linking $H_X$ and $T_X^2$. There is slight variation in the value of this coupling constant in Table 1, but this is only because abbreviated numbers are used in order to fit them into the table. This coupling constant first appeared in 2015 in Equation (3) of FSC reference [2]. It has now been calculated out to 29 decimal places [7], using Mathematica software and the NIST 2018 CODATA [6]. However, the number of decimal places is not nearly as important as the expected reduction in the uncertainty of $H_0$ in terms of standard deviation. The result of this new coupling constant precision should be high precision in Hubble parameter determinations going forward. Any cosmology formulae using a Hubble parameter value and incorporating this newer and more precise FSC coupling constant (tentatively called "Upsilon") would be expected to vastly improve cosmological model predictions. Many such "Hubble formulae" are used in standard ΛCDM cosmology, in the same way that they are used in FSC.

The "deeper theoretical understanding" mentioned above is now revealed to be inherent in the FSC model. As clearly alluded to by Lineweaver and Patel [8], the modeling of our universe as an expanding black hole-like object is not such an outlandish idea after all.

**Table 1.** Correlations between radii, temperatures, redshift and Hubble parameter.

| $\log\left(\frac{R_0}{R_x}\right)$ | $T_x$ | $T_x^2$ | $\frac{H_x}{T_x^2}$ | $z$ | $H_x$ |
|---|---|---|---|---|---|
| 0 | 2.72548 | 7.4282412304 | 2.917245E-19 | 0 | 2.167E-18 |
| 0 | 2.7 | 7.29 | 3.049643E-19 | 0 | 2.167E-18 |
| 1.08 | 9.5 | 90.25 | 2.967313E-19 | 2.49 | 2.678E-17 |
| 1.95 | 25.8 | 665.64 | 2.955051E-19 | 8.47 | 1.967E-16 |
| 2.16 | 33.2 | 1102.24 | 2.944005E-19 | 11.18 | 3.245E-16 |
| 2.38 | 42.7 | 1823.29 | 2.936998E-19 | 14.67 | 5.355E-16 |
| 2.6 | 55.0 | 3025 | 2.920992E-19 | 19.18 | 8.836E-16 |
| 2.87 | 70.8 | 5012.64 | 2.908647E-19 | 24.98 | 1.458E-15 |
| **6.08** | **3000.0** | **9000000** | **2.918444E-19** | **1099.72** | **2.6266E-12** |

## 4. Summary and Conclusions

This paper shows the exquisite FSC correlation between a CMB temperature of 3000 K and a cosmological redshift of 1100.

Furthermore, by revealing the obvious coupling constant linking $H_X$ and $T_X^2$, this paper shows the continued value of FSC as an accurate Planck scale quantum cosmology model. Although the most useful FSC quantum cosmology formulae were first published in 2018 (reference [5], Section 2.9), they have been inherent in FSC since its 2015 inception. Thus, a theoretical model which is now more than eight years old continues to show its value with respect to observational correlations.

The "deeper theoretical understanding" mentioned in reference [7] comes from the gradual recognition in the astrophysics and cosmology community that modeling our universe as an expanding black hole-like object is likely to be *necessary*, in order to achieve high precision Hubble cosmology. Such a cosmology, which *requires* the use of the Hubble parameter in its formulae, also requires an exquisitely high precision in its CMB-derived Hubble parameter determinations. This appears to have now been achieved. FSC provides this "deeper theoretical understanding".

## Acknowledgements

Both authors would like to acknowledge Sir Roger Penrose and the late Stephan Hawking for the inspiration provided by their enormous contributions to the field of cosmology. U.V.S. Seshavatharam is indebted to professors Madugula Nagaphani Sarma, Chairman, Institute of Scientific Research in Vedas (I-SERVE), Hyderabad, India and Shri K.V.R.S. Murthy, former scientist IICT (CSIR), Govt. of India, Director, Research and Development, I-SERVE, for their valuable guidance and great support in developing this subject. Dr. Tatum would also like to thank Dr. Rudy Schild, Harvard-Smithsonian Center for Astrophysics, for his past support and encouragement in developing this subject.

## Conflicts of Interest

The authors declare no conflicts of interest regarding the publication of this paper.

## References

[1] Fixsen, D.J. (2009) *Astrophysical Journal*, **707**, 916. https://doi.org/10.1088/0004-637X/707/2/916

[2] Tatum, E.T., Seshavatharam,U.V.S. and Lakshminarayana, S. (2015) *International Journal of Astronomy and Astrophysics*, **5**, 116-124. http://dx.doi.org/10.4236/ijaa.2015.52015

[3] Haug, E.G. and Wojnow, S. (2023) How to Predict the Temperature of the CMB Directly Using the Hubble Parameter and the Planck Scale Using the Stephan-Boltzmann Law. https://hal.science/hal-04269991

[4] Tatum, E.T. (2020) A Heuristic Model of the Evolving Universe Inspired by Hawk-

ing and Penrose. In: Tatum, E.T., Ed., *New Ideas Concerning Black Holes and the Universe,* IntechOpen, London, 5-21. http://dx.doi.org/10.5772/intechopen.87019

[5] Tatum, E.T. (2018) *Journal of Modern Physics*, **9**, 1867-1882. https://doi.org/10.4236/jmp.2018.910118

[6] Tiesinga, E., *et al.* (2019) The 2018 CODATA Recommended Values of the Fundamental Physical Constants (Web Version 8.1). National Institute of Standards and Technology, Gaithersburg. http://physics.nist.gov/constants

[7] Tatum, E.T., Haug, E.G. and Wojnow, S. (2023) Predicting High Precision Hubble Constant Determinations Based Upon a New Theoretical Relationship between CMB Temperature and $H_o$. https://hal.science/hal-04268732v2

[8] Lineweaver, C.H. and Patel, V.M. (2023) *American Journal of Physics*, **91**, 819-825. https://doi.org/10.1119/5.0150209

Scientific Research Publishing

Journal of Modern Physics, 2024, 15, 179-183
https://www.scirp.org/journal/jmp
ISSN Online: 2153-120X
ISSN Print: 2153-1196

# On Our Peculiar Black Hole Universe

**Paolo Christillin**

Department of Physics, University of Pisa, Pisa, Italy
Email: christ.pao@gmail.com

**How to cite this paper:** Christillin, P. (2024) On Our Peculiar Black Hole Universe. *Journal of Modern Physics*, **15**, 179-183.
https://doi.org/10.4236/jmp.2024.152009

**Received:** November 17, 2023
**Accepted:** February 4, 2024
**Published:** February 7, 2024



## Abstract

The black hole model of the Universe evolution, accompanied by matter creation, already successfully accounting for many features of the past is discussed and further justified. It is once more stressed that even a very large object but with a big mass is in its own right a black hole. As a consequence, the extrapolation of the past predicts for the future no big crunch, nor big bounce but a steady expansion with smaller matter density.

## Keywords

Universe Expansion, Black Hole Model, Matter Creation, Gravitational Self Energy

## 1. Introduction

The inadequacy of the GR Friedman equations [1] for the description of the Universe evolution has to be attributed to the fact that in the one for the acceleration, the potential, due to the Hubble expansion, is not a state function [2]. Thus in its derivative another term enters in addition to the usual Newtonian one and the corresponding mass variation (matter non conservation) produces a totally different scenario corresponding to a black hole one (b.h.).

This description of the Universe evolution as a gigantic and evolving black hole, which successfully combines gravitation and QM, in spite of its successes (prediction of the time dependent Universe age [3], inertial forces and gravitational radiation, causality [4], and the relevance to the problem of the existence of dark energy and of the cosmological constant), has encountered many criticisms which can be summarized by the following referee's report "the universe and black holes are fundamentally different, and one should explain why the universe is expanding from the viewpoint of a black hole." Indeed one is traditionally attached to the picture of a small very dense object, eventually shrinking, and one can view the numerical agreement of the model with present data at

most as a mere coincidence.

The aim of the present work is to argue that this is not so.

Starting from the "elementary" observation by Feynman [5] many people [6]-[14] have tried to elucidate the problem about what is known and what not about black holes. However with different degrees of sophistication (adding rotation for instance) they remain essentially attached to General Relativity whose basic assumption *i.e.* "matter conservation" has been disproved [3] mainly because of the obvious time dependence of the Universe age.

We therefore proceed with very simple arguments to the justification of **this unconventional black hole of a big mass in a large volume obeying however the same relation** $M/R = c^2/G$ **of a conventional tiny and very dense one.**

## 2. Discussion

The basic relation, backed up **at present** by "data" [15] ( $M \simeq 10^{80} m_N$ , $R \simeq 10^{26}$ m ) is as well known

$$Mc^2 = \frac{GM^2}{R} \tag{1}$$

or

$$\varepsilon = \frac{GM}{c^2 R} = 1 \tag{2}$$

When taken to describe the Universe evolution, *i.e.* as an equation, down to the *Planck epoch* (*whose quantities represents the smallest quantum b.h.*, *where contrary to a wide spread opinion QM and gravitation successfully combine*) **this equation is not stable.** In fact this condition which essentially corresponds to energy conservation does not correspond to a minimum in energy. Indeed if we allow a perturbation in R at the Planck era

$$R \to R + dR$$

we cannot have shrinking with a radius smaller than the Planck one and a bigger one naturally entails a correspondingly increase in the mass.

The same argument also holds true also for later times even if a smaller radius cannot be discarded in principle. However the same observation remains valid: no restoring force!

Consider indeed the radiation dominated era where the mass is given by [2]

$$M \simeq (kT)^4 R^3 \tag{3}$$

Of course in principle both possibilities exist *i.e.* increase and decrease in $R$ with constant $M/R \simeq (kT)^4 R^2$ . In the first case $M/R$ remains constant at the price of a decreasing temperature ( $(KT)^2 \simeq 1/R$ ) which is what is actually observed. In the second case the opposite should happen in contrast to actuality.

The possibility of perturbing to a smaller radius (at constant mass) would result in energy violation since the negative self energy would overcompensate the mass. In other words again only a bigger radius is possible (smaller self energy) and mass creation is demanded to restore energy balance.

In the case of the matter dominated era even if photons are a very small fraction of nucleons the above argument remains true. A contraction would decrease the photon wavelength (anti CMB) and this implies that also for nucleons expansion is the only possibility. Thus the particle mass content simply increases.

Therefore expansion in the radiation dominated era would correspond, loosely speaking, to the Boltzmann thermal death whereas in the matter dominated era (where **nucleons are non relativistic**) the negative heat capacity would allow the birth of structures.

In the b.h. model where $\varepsilon$ must be constant in time as proved in Ref. [4] the mass variation required by Equation (2) has therefore another fundamental effect in the equations of motion

$$d\varepsilon = 0 = -\frac{GM}{R^2} + \frac{GdM}{RdR} \tag{4}$$

where the first term represents the well known Newtonian acceleration counterbalanced by the second one, due to mass variation. So **self energy is seen to provide the repulsive force since it increases the total energy when particles move away and thus demands matter creation. This is the missing dark energy at present represented by the cosmological constant.**

Consider now the density given in the b.h. model by

$$\rho_{b.h.} = \frac{3}{4\pi G}\frac{c^2}{r^2} \tag{5}$$

which, in line with the previous arguments, reads

$$\rho_{b.h.} = \frac{3H^2}{4\pi G}$$

This has to be compared with the critical density of the standard GR treatment in flat space

$$\rho_{cr} = \frac{3H^2}{8\pi G} \tag{6}$$

$$\rho_{b.h.} = 2\rho_{cr} \tag{7}$$

This represents probably a rather unexpected result in the sense, first, that it seems to suggest that a sort of black hole description is contained also in a particular GR formulation, but with a numerical difference. This point can be understood by remembering that (probably inspired by a non relativistic origin) $H^2$ appears in GR with the coefficient 1/2 and that in the given case (without the cosmological constant) also GR describes the same situation of the black hole model *i.e.* indefinite expansion consistent with energy conservation determined only by the density. Of course the difference between the two theories lies in the acceleration equation where the mass variation, necessary to account mainly for the time dependent age of the Universe provides the repulsive agent. The doubled $\rho$ has implications for the amount of the presumed dark energy in that it proves how this quantity be model dependent.

In the b.h. model there is no such critical density. The given one, smaller than

the GR's, is just of the right amount predicted by the model and the expansion, accompanied by matter creation and density decrease in time, happens independent of the Universe curvature. That must have evolved becoming flatter and flatter from the Planck radius to the present one ($1/R_c^2 \simeq G\rho/c^2$ , $R_C$ standing for the curvature radius) *i.e.* a Universe in the matter era essentially flat. A totally different scenario than the GR one, which in connection with curvature probably suffers from being an essentially static, matter conserving, one. This also determines the fate of the Universe: no big crunch, nor big bounce but a density decrease which might anyway foresee the possibility of structure formation due to the negative heat capacity of gravitation.

So an innocent looking, unassuming relation turns out to produce two equations which reproduce and correct the cherished GR ones in the Friedman's metric without the epicycle add-ons criticized by Perlmutter [16].

## 3. Conclusion

An elementary argument has been presented to show that in the black hole model, the Universe is not stable and expands according to the arrow of time accompanied by mass creation.

## Acknowledgements

It is a pleasure to thank once more P.Amato, L.Bonci and E.Cataldo (ABC) for continuous help and support.

## Conflicts of Interest

The author declares no conflicts of interest regarding the publication of this paper.

## References

[1] Friedman, A. (1922) *Zeitschrift fuer Physik*, **10**, 377-386. https://doi.org/10.1007/BF01332580

[2] Christillin P. (2023) *Journal of Modern Physics*, **14**, 18-30. https://doi.org/10.4236/jmp.2023.141002

[3] Christillin P. (2023) *Journal of Modern Physics*, **14**, 1452-1457. https://doi.org/10.4236/jmp.2023.1411084

[4] Christillin P. (2022) Gravitation for the Simple Mind(ed). Aracne, Roma.

[5] Feynman R. (1999) Feynman Lectures on Gravitation. Penguin Books Ltd., London.

[6] Pathria, R.K. (1972) *Nature*, **240**, 298-299. https://doi.org/10.1038/240298a0

[7] Seshavatharam, U.V.S. (2010) *Progress in Physics*, **2**, 7-14.

[8] Poplawski, N.J. (2010) *Physics Letters B*, **694**, 181-185. https://doi.org/10.1016/j.physletb.2010.09.056

[9] Poplawski, N.J. (2010) *Physics Letters B*, **687**, 110-113. https://doi.org/10.1016/j.physletb.2010.03.029

[10] Melia, F. and Shevchuk, A.S.H. (2012) *Monthly Notices of the Royal Astronomical Society*, **419**, 2579-2586. https://doi.org/10.1111/j.1365-2966.2011.19906.x

[11] Tatum, E.T. (2015) *Journal of Cosmology*, **25**, 13081-13111.

[12] Tatum E.T., Seshavatharam U.V.S., and Lakshminarayana, S. (2015) *Frontiers of Astronomy, Astrophysics and Cosmology*, **1**, 98-104.

[13] Tatum, E.T. and Seshavatharam, U.V.S. (2021) Flat Space Cosmology A New Model of the Universe Incorporating Astronomical Observations of Black Holes, Dark Energy and Dark Matter. Universal Publishers, Irvine, California.

[14] Tatum, E.T. (2023) *Journal of Modern Physics*, **14**, 573-582. https://doi.org/10.4236/jmp.2023.145033

[15] Kittel, C., Knight, W.D. and Ruderman, M.A. (1962) The Berkeley Physics Course, Mechanics. Mc Graw-Hill, New York.

[16] Perlmutter S. et al. (1999) *The Astrophysical Journal*, **517**, 565. http://dx.doi.org/10.1086/307221

Journal of Modern Physics, 2024, 15, 184-192
https://www.scirp.org/journal/jmp
ISSN Online: 2153-120X
ISSN Print: 2153-1196

# Black Hole Complementarity in Terms of the Outsider and Insider Perspectives

**Eugene Terry Tatum**

Independent Researcher, Bowling Green, Kentucky, USA
Email: ett@twc.com

**How to cite this paper:** Tatum, E.T. (2024) Black Hole Complementarity in Terms of the Outsider and Insider Perspectives. *Journal of Modern Physics*, **15**, 184-192.
https://doi.org/10.4236/jmp.2024.152010

**Received:** January 5, 2024
**Accepted:** February 6, 2024
**Published:** February 9, 2024



## Abstract

A complementarity hypothesis concerning outsider and insider perspectives of a gargantuan black hole is proposed. The two thought experiments presented herein are followed by a brief discussion of a new interpretation of black hole interior "space-and-time-reversal". Specifically, it is proposed that the "singularity" space of the black hole interior is time-like and the expansion time of the black hole interior is space-like. The resemblance of this new insider interpretation to our own expanding and redshifting big bang universe is compelling.

## Keywords

Black Holes, Complementarity, Cosmological Models, $R_h = ct$ Models, Flat Space Cosmology, Schwarzschild Cosmology, Thought Experiment, Dark Energy, Quantum Vacuum

## 1. Introduction and Background

Stephen Hawking pointed out that quantum information passing through a black hole horizon into its interior should be permanently lost at the singularity, thus apparently violating a bedrock principle of quantum physics, that quantum information cannot be destroyed [1]. This has become known as the "black hole information paradox". A hypothesis of "black hole complementarity" was subsequently introduced by Susskind [2], as a means of solving Hawking's paradox. He treated quantum information as interacting with a black hole in two different and complementary ways, only one of which could be observed from any given outside or inside perspective. Susskind's follow-up book, entitled *The Black Hole War* [3], provides a nice historical summary of his philosophical battle and apparent victory over Hawking with respect to this paradox.

The concept of complementarity in physics goes at least as far back as Emmy

Noether's strict and limiting mathematical definition in 1918. In a broader sense, differing but valid wave-and-particle interpretations of observations of double slit experiments, including Bohr's Copenhagen interpretation of quantum physics, are examples of physical complementarity. The Copenhagen interpretation withstood a barrage of challenges by Einstein, Podolsky, and Rosen (EPR) [4] and others [5]. There have since been a number of other examples of complementarity in modern physics, now including Susskind's important contribution concerning black holes.

This paper is not intended as a comprehensive review of complementarity in modern physics. Rather, the above brief summary is merely offered in order to show that the concept of physical complementarity is now over one hundred years old, pre-dating any specific applications to black holes. *In its broadest sense, a complementarity in physics can be defined as two different, but equally valid, perspectives concerning the same physical object or event.* Such complementarities rely upon underlying conservation laws of great importance. Proving this was Noether's greatest contribution to physics. As an extension of her logic, this author proposes that a deeper understanding of black hole complementarities could well be an important key to uniting general relativity with quantum physics. Thus, we would have a useful and accurate quantum cosmology.

It is the purpose of the present paper to present a somewhat different (with respect to Susskind) complementarity hypothesis concerning black holes. By means of thought experiments and a new interpretation of black hole interior "space-and-time-reversal", the reader can perhaps gain a foothold on understanding how black hole cosmological models, a distinct category of $R_h = ct$ models, can potentially resolve some cosmological conundrums [6] [7] [8] [9] [10].

## 2. The Outsider Perspective of a Black Hole (Thought Experiment)

Most readers are already familiar with the outsider perspective of a black hole. Such a perspective is all that is available to us, whether we are Earth-bound or space satellite telescope observers. We see a black hole as a finite and circumscribed spherical object emitting no visible light or other detectable electromagnetic radiation. If it does, in fact, emit Hawking radiation, as believed by nearly all black hole experts, such radiation is predicted to be so faint as to be forever beyond our means of detecting and measuring it. Furthermore, our Earth-based telescopes, as part of a planet-wide array, have revealed that selected nearby supermassive black holes (SMBHs) are bending light rays around them in exactly the way predicted by general relativity. Black holes have, so far, been highly predictable in terms of their relatively few measurable parameters. In this context, it is often said that "black holes have no hair". They are viewed, from our outside perspective, as remarkably simple spinning objects surrounded by an accretion disk of hot gases emitting x-rays and/or gamma rays. Their powerful polar mag-

netic fields can spin with great rapidity and eject concentrated beams of photons and charged particles (at nearly the speed of light) in "jets" many light-years in length. Quasars and blazars are almost-certainly some of the largest and most powerful SMBHs of the early universe, which just happen to be pointed in our general direction (as for quasars) or directly, or nearly so, at us (as for blazars).

In the present paper, we offer a thought experiment of highly-reasonable assumptions about the experience of spacecraft observers outside, but close to, a SMBH, in a somewhat similar manner to that offered by Kip Thorne in his excellent book entitled *Black Holes & Time Warps—Einstein's Outrageous Legacy* (see pages 38-48) [11]. Let us imagine that we are observers on a large spacecraft ("mother ship") hovering relatively close to the event horizon of a *truly gargantuan* supermassive black hole of 14.62 billion light-years in Schwarzschild radius. We have done our measurements and calculations and determined that our black hole, which doesn't appear to rotate or have a net charge, has an average density of approximately $8.4 \times 10^{-27}$ kg·m$^{-3}$. Thus, it appears to be a real Schwarzschild black hole! From our safe distance of observation, our black hole is so large that we and our mother ship do not experience any significant tidal effects of its gravitational field. We wish to send down a spacecraft probe to hover above the spherical horizon at various fixed distances, while returning a powerful laser pulse signal of predetermined frequency to our mother ship observers. These pulses are sent at regular time intervals according to a clock on the probe. What will we observe at the mother ship with respect to these probe signals?

The answers to such a question are a near-certainty, given our knowledge of, and extremely high confidence in, special and general relativity. At each hovering distance above the SMBH horizon we can observe frequency, wavelength, energy and timing interval of the pulses coming from the probe. At first, when the probe is nearly at the orbital height of our mother ship, we notice little, if any, change of signal properties with respect to the pre-programmed pulse signals. Frequency, wavelength, energy and timing intervals of the pulses are in-line with our on-ship calibrations prior to release of the probe. However, we gradually and then more rapidly notice, as the probe decreases its hovering distance and moves closer and closer to the horizon, the following things: the pulse frequency continuously decreases; pulse energy continuously decreases, in-line with decreasing frequency; the pulse wavelength continuously redshifts, getting longer and longer; and the pulses are more prolonged and separated by increasingly-long time intervals. If we were to plot such signal features on a graph as a function of increasing probe proximity to the horizon (or increasing hover distance from the mother ship), we would notice that frequency and pulse energy asymptote towards zero, while wavelength and timing intervals asymptote towards infinity. Although we would not be able to observe directly, due to infinite time dilation, we would expect that our probe, when embedded exactly in the horizon, would become completely undetectable to us, either by signal reception or by powerful optical, infrared or radio telescopes on the mother ship. From

our outside perspective, we mother ship observers can readily extrapolate that the clock on a horizon probe (were it possible to have an infinite quantity of fuel and infinite energy thrusters in order to maintain its position at the horizon) would be *frozen in time*! In our outside observer thought experiment, these very predictable observational phenomena would all be the result of gravitational redshift and time dilation, in exact agreement with special and general relativity.

## 3. The Insider Perspective of a Black Hole (Thought Experiment)

Now we introduce the reader to an equally valid and complementary perspective of our truly gargantuan black hole, which is the perspective of a *free-falling* (*i.e.*, not hovering) astronaut passing through the horizon and into the black hole interior. Our free-falling astronaut would have a markedly different experience in comparison to that of the hovering mother ship and probe. Let us consider this new perspective in a thought experiment.

From our astronaut's perspective, time is moving along at its usual pace, as she remembers it when she was last on the mother ship during calibrations of her watch and laser pulser with that of the aforementioned probe. She notices nothing unusual as she passes through the event horizon (according to her watch) and into the black hole. She also does not notice any frequency, wavelength or energy change in the activity of her pulser or the activity of her watch. After passing through the horizon, which now becomes her future event horizon, she puts the ticking watch up to a microphone in her helmet and hears it ticking just as loud and clear as it did back on the mother ship. She notices that, in all directions, objects more distant from her, but still inside the horizon, are more redshifted than nearby objects. She also notices, by leaning back and returning her gaze in the specific direction of where the mother ship was, that it has disappeared, and that the stars which were behind the mother ship have been replaced by an impenetrable blackness. The light of the outside universe has long ago (in comparison to her new time frame) stopped pouring into the black hole, due to the extreme time differences between her new universe (the black hole) and her old universe (the parent of the black hole in which she now finds herself). This is also a predictable time dilation effect.

Before we finish the story of our free-falling astronaut, we should take note of the following: black hole experts have shown mathematically how the interior of a black hole should have a very peculiar feature. Judging from signage changes in their mathematical formulae in the Schwarzschild metric, these experts are generally in agreement that a sudden switch takes place as one crosses the black hole event horizon into the interior:

**Space becomes time-like and time becomes space-like.**

The particular formula of interest for the Schwarzschild solution of the Einstein field equations (leaving out rotational terms because we are referring to a Schwarzschild black hole) is commonly expressed as follows [12]:

$$\Delta s^2 = \left[1/\left(1-r_s/r\right)\right]\Delta r^2 - \left[1-r_s/r\right]c^2\Delta t^2 \quad (1)$$

wherein the Schwarzschild metric term is on the left, the space-like term is in the middle and the time-like term is on the right. The symbol $r_s$ represents the Schwarzschild radius of the black hole. Notably, when Equation (1) applies to the interior of the black hole, both bracket terms switch to a negative signage, because $r_s$ suddenly becomes greater than radius $r$. General relativists interpret this signage change in terms of the space-and-time-reversal description above.

We can maybe best understand this new interior perspective by comparing it to what we observe or imagine about a black hole as outsiders. We first imagine a "singularity" of infinite properties at the geometric center of *space* within the black hole interior. This is presumably, from the outsider perspective, where all matter and information of any kind ends up. For a Schwarzschild (*i.e.*, non-rotating) black hole, this "singularity" is a point-like *spatial* object. For a Kerr-type rotating black hole, the "singularity" is ring-like and surrounding the geometric center of the black hole. Without confusing the matter further, or updating the reader on Kerr's new view on singularities of any kind, suffice it to say that a *space-like* object of "infinite" properties (*i.e.*, smallness, density and temperature) exists in the perspective of the outsider in, or very near, the geometric center of a black hole. Obviously, these properties cannot *actually* be infinite, but the fully valid outsider perspective of such a "singularity" must be left to a final theory of quantum gravity in the future.

However, according to a reasonable interpretation of the "space-and-time-reversal" math of black hole relativists described above, insiders should perceive a "singularity" of their black hole as no longer an object in space, but rather an *object in time*; this perspective resembles how we imagine our own cosmic singularity! In our own universe, there is no residual singularity within a localized point of absolute space; there is only a singularity in our most remote past. From her new "space-and-time-reversal" perspective, our free-falling astronaut might have no existing singularity to fall into. Rather, she may have fallen into an *expanding* time-like structure with an average density of approximately $8.4 \times 10^{-27}$ $kg{\cdot}m^{-3}$, very much like our own universe. As in our own expanding (*i.e.*, redshifting) universe, every point in her new space, because she can perceive it as expanding by her redshift observations, also represents a point in time; in other words, her continually expanding new environment is now time-like! Her new horizon is no longer acting as a time-less and fixed invisible spatial object, but rather acting as a dynamic, expanding, entropy-driven, time clock. The "ticking" of her new universal clock is the regular increase in horizon surface area (*i.e.*, Bekenstein-Hawking's entropy-as-time definition). Our imaginary astronaut is no longer falling towards a geographic center any more than an intergalactic astronaut in our own universe falls towards a particular absolute center of space. In an expanding universe such as ours, there is no residual center. Likewise, one can perhaps imagine in this thought experiment that her new gargantuan SMBH environment could be perceived by her in a similar way. To put it in more mod-

ern cosmological terms, the center of our free-falling astronaut's new universe is not localized, but now everywhere. She is truly free to fall wherever the new gravitation field in her new universe takes her.

## 4. Discussion

As presented, our outsider perspective of a black hole is highly-dependent upon our very limited human time perspective. Rather than perceiving a black hole as a dynamic and changing object once born, we tend to see and describe a black hole as an object almost frozen in time, other than when it ingests new matter or merges with another black hole. Although we tend to believe that, between such ingestions and mergers, a black hole continually radiates away a tiny amount of energy, complete evaporation would only occur at many times the current age of our universe. For all practical purposes, we can safely ignore the theoretical Hawking radiation and black hole evaporation.

One of the most surprising findings from recent deep telescopic observations of our past early universe is that early SMBHs have grown even faster than we could have imagined. We have even had to consider new ways in which SMBHs could have initially formed, such as "direct collapse" from gargantuan primordial gas clouds. Furthermore, the recent discovery by Farrah *et al.* [13] that the rapid growth of SMBHs appears to be *coupled* with the expansion of our own universe is astonishing. Their results and interpretations are understandingly preliminary, but they appear to imply that SMBHs could be a source of universal expansion dark energy. The present author has recently offered a quantum hypothesis on how black holes might actually *continually* grow in size and produce such dark energy [14]. A follow-up paper on likely gravitational field effects on the quantum vacuum was also published [15], and now appears to have additional theoretical support [16].

Our second thought experiment introduces the mathematical discovery by black hole experts that, within the interior of a black hole, there is a switch in space and time perspective in comparison to our own outsider perspective. Space within the black hole interior is interpreted to be time-like and time is interpreted to be space-like. This is a conclusion based upon signage changes in the terms of relativistic Schwarzschild metric equations for crossing over from outside to inside a black hole horizon.

What is still open for interpretation is the exact meaning of such a mathematical signage change. Those theorists who apply light cone analysis to the inside of a black hole take the conventional point of view that anything inside a black hole rapidly gets stretched and then crushed at the singularity; this is really no different from the outsider perspective and perhaps shows a bias in this respect. For the sake of argument, a new complementarity interpretation of black hole interior "space-and-time-reversal" is offered in the present paper, largely based upon the perspective that a SMBH is a *dynamic* object *coupled* with the expansion of our universe (see the Farrah *et al.* reference). The present author interprets the insider perspective as follows:

**The 'singularity' space becomes time-like and the expansion time becomes space-like.**

What is meant by this is that the insider perspective of a truly gargantuan black hole the size and average density ($8.4 \times 10^{-27}$ kg·m$^{-3}$) of our own universe could be that the singularity is only in the past, and that past epochs of such a black hole could perhaps be observed (by redshifting light within the SMBH) as past events of an *expanding* interior space, much like our own perceived expanding universe. In summary, in a sufficiently large black hole, there might be conditions suitable for life, rather than lethal tidal forces ending in an infinitely small, infinitely dense and hot point.

While such an insider interpretation might seem to be completely outlandish, no one can yet know *exactly* what the mathematical signage change means. Understandably, we may have been biased by our outsider perspective. It may also be that the Schwarzschild metric is not the correct metric to use for the *inside* of a black hole. The only thing which we can say for certain is that the inside of a black hole will always have some mystery about it. An inside observer will never be able to report back to us.

A subject of debate among cosmologists is whether our universe is as spatially flat as recently observed in the Planck satellite survey, or is curved in some way [17]. If our expanding universe is ultimately observed to be at its Friedmann critical density for a flat universe (*i.e.*, $k = 0$), we can call it spatially flat according to the cosmological definition of "critical density". In a similar fashion, if it turns out to be true that a supermassive or gargantuan black hole expands over the great extent of cosmic time (see the Farrah *et al.* reference), a black hole interior might also qualify for a critical density definition of spatial flatness. Obviously, this would be a radically different perspective in comparison to the outsider perspective of spatial collapse to infinite spatial curvature occurring at a geometric center "singularity". Lacking any possibility of observing a gargantuan black hole interior as an insider, one can only speculate about the true insider perspective.

One could say that such an insider interpretation cannot be considered to be within the realm of scientific interest, because it can never be verified or falsified. This is a valid point of view. Nevertheless, as discussed in other publications within this Special Issue, the meaning of recently-discovered mathematical relationships between our universe and black holes and black hole-like objects is gaining in scientific interest among reputable physicists and cosmologists [18] [19] [20] [21]. For readers with a scientific interest but an open mind, one should perhaps begin with physicist Ethan Siegel's article entitled "Are We Living in a Baby Universe that Looks Like a Black Hole to Outsiders?".

## 5. Summary and Conclusions

Following in the footsteps of Leonard Susskind, a new black hole complementarity is offered in the present paper. After first detailing the well-known outsider

perspective of a black hole, using a thought experiment, a plausible speculation on the free-falling insider perspective is offered in a second thought experiment. This second experiment incorporates a new interpretation of the meaning of black hole interior "space-and-time-reversal", owing to signage changes in the Schwarzschild metric mathematical formula, when one passes through a black hole event horizon. We can summarize this new interpretation as follows: The "singularity" space of the black hole interior is time-like and the expansion time of the black hole interior is space-like.

While the Schwarzschild metric mathematical formula of Equation (1) is generally agreed upon, the precise *meaning* of the signage change for the interior perspective of a black hole can still be subject to different interpretations. We can never observe, and can only *speculate*, what the inside of a particularly gargantuan black hole might be like. Perhaps the "singularity" of the outsider perspective is no longer an impossibly small, dense, and hot object in space when one becomes an insider, but rather an object in time only, much as many believe to be true for our own universe.

The resemblance of this new black hole insider interpretation to our own expanding and redshifting universe is intriguing. It is particularly interesting in the context of the recent Farrah *et al.* observations and physicist Ethan Siegel's article entitled "Are We Living in a Baby Universe that Looks Like a Black Hole to Outsiders?".

## Conflicts of Interest

The author declares no conflicts of interest regarding the publication of this paper.

## References

[1] Hawking, S.W. (1976) *Physical Review D*, **14**, 2460-2473. https://dx.doi.org/10.1103/PhysRevD.14.2460

[2] Susskind, L. and Lindesay, J. (2004) An Introduction to Black Holes, Information and the String Theory Revolution: The Holographic Universe. World Scientific Publishing Co., Singapore. https://doi.org/10.1142/5689

[3] Susskind, L. (2008) The Black Hole War—My Battle with Stephen Hawking to Make the World Safe for Quantum Mechanics. Little, Brown and Co., New York.

[4] Einstein, A., Podolsky, B. and Rosen, N. (1935) *Physical Review*, **47**, 777-780. https://dx.doi.org/10.1103/PhysRev.47.777

[5] Reid, M.D. *et al.* (2009) *Reviews of Modern Physics*, **81**, 1727-1751. https://dx.doi.org/10.1103/RevModPhys.81.1727

[6] Tatum, E.T. (2015) *Journal of Cosmology*, **25**, 13061-13080. https://ui.adsabs.harvard.edu/abs/2015JCos...2513063T/abstract

[7] Tatum, E.T. (2015) *Journal of Cosmology*, **25**, 13081-13111. https://ui.adsabs.harvard.edu/abs/2015JCos...2513073T

[8] Tatum, E.T., Seshavatharam,U.V.S. and Lakshminarayana, S. (2015) *International Journal of Astronomy and Astrophysics*, **5**, 116-124. http://dx.doi.org/10.4236/ijaa.2015.52015

[9] Tatum, E.T. (2018) *Journal of Modern Physics*, **9**, 1867-1882. https://doi.org/10.4236/jmp.2018.910118

[10] Tatum, E.T. (2020) A Heuristic Model of the Evolving Universe Inspired by Hawking and Penrose. In: Tatum, E.T., Ed., *New Ideas Concerning Black Holes and the Universe,* IntechOpen, London, 5-21. http://dx.doi.org/10.5772/intechopen.87019

[11] Thorne, K.S. (1994) Black Holes & Time Warps—Einstein's Outrageous Legacy. W. W. Norton & Co., New York. https://doi.org/10.1063/1.2808700

[12] Blinn, C. (2017) Schwarzschild Solution to Einstein's General Relativity. https://sites.math.washington.edu/~morrow/336_17/papers17/carson.pdf

[13] Farrah, D., *et al.* (2023) *The Astrophysical Journal Letters*, **944**, L31-L39. https://doi.org/10.3847/2041-8213/acb704

[14] Tatum, E.T. (2023) *Journal of Modern Physics*, **14**, 573-582. https://doi.org/10.4236/jmp.2023.145033

[15] Tatum, E.T. (2023) *Journal of Modern Physics*, **14**, 833-838. https://doi.org/10.4236/jmp.2023.146048

[16] Wondrak, M.F., van Suijlekom, W.D. and Falcke, H. (2023) *Physical Review Letters*, **130**, Article ID: 221502. https://dx.doi.org/10.1103/PhysRevLett.130.221502

[17] Di Valentino, E., Melchiorri, A. and Silk, J. (2020) *Nature Astronomy*, **4**, 196-203. https://doi.org/10.1038/s41550-019-0906-9

[18] Siegel, E. (2022) Are We Living in a Baby Universe that Looks Like a Black Hole to Outsiders? Forbes Archives. https://bigthink.com/hard-science/baby-universes-black-holes-dark-matter/

[19] Lineweaver, C.H. and Patel, V.M. (2023) *American Journal of Physics*, **91**, 819-825. https://doi.org/10.1119/5.0150209

[20] Rovelli, C. and Vidotto, F. (2018) *Universe*, **4**, Article 127. http://dx.doi.org/10.3390/universe4110127

[21] Poplawski, N. (2016) *The Astrophysical Journal*, **832**, Article No. 96. https://doi.org/10.3847/0004-637X/832/2/96

Journal of Modern Physics, 2024, 15, 193-238
https://www.scirp.org/journal/jmp
ISSN Online: 2153-120X
ISSN Print: 2153-1196

# A New Version of the Lambda-CDM Cosmological Model, with Extensions and New Calculations

**Jan Helm**

Department of Electrical Engineering, Technical University Berlin, Berlin, Germany
Email: jan.helm@alumni.tu-berlin.de

**How to cite this paper:** Helm, J. (2024) A New Version of the Lambda-CDM Cosmological Model, with Extensions and New Calculations. *Journal of Modern Physics*, **15**, 193-238.
https://doi.org/10.4236/jmp.2024.152011

**Received:** December 5, 2023
**Accepted:** February 20, 2024
**Published:** February 23, 2024





## Abstract

This article gives a state-of-the-art description of the cosmological Lambda-CDM model and in addition, presents extensions of the model with new calculations of background and CMB functions. Chapters 1-4 describe the background part of the model, *i.e.* the evolution of scale factor and density according to the Friedmann equations, and its extension, which results in a correction of the Hubble parameter, in agreement with new measurements (Cepheids-SNIa and Red-Giants). Based on this improved background calculation presented in chapters 5-9 the perturbation part of the model, *i.e.* the evolution of perturbation and structure according to the perturbed Einstein equations and continuity-Euler equations, and the power spectrum of the cosmic microwave background (CMB) is calculated with a new own code.

## Keywords

Lambda-DCM, Friedmann Equations, CMB, Metric Perturbation, Hubble Parameter

## 1. Introduction

The Lambda-CDM model is widely accepted as the valid description of universe on large scales and its evolution history. It is based on General Relativity and consists of two parts:

- Background part with the ansatz Robertson-Walker (RW) metric, based on Friedmann equations and equations-of-state for the different component particles. It describes the evolution of scale factor and density without perturbations, *i.e.* without local structure (like galaxies and galaxy groups);

- Perturbation part with the ansatz perturbed RW-metric and locally per-

turbed density, velocity, and pressure of the component particles. It describes the time-evolution and (quasi-random perturbed spatial distribution) of density, velocity, and pressure, *i.e.* the actual structure of the universe on inter-galactic scale.

The parameters of the perturbed model are fitted in chap. 10 with the CMB spatial spectrum measured by Planck.

We present here in chap. 2-5 the background part with Friedmann equations and equations-of-state for the components with two notable extensions: explicit temperature dependence and classical gas as baryon eos. From this follows a new solution and own calculation in chap. 5, which offers an explanation for the apparent experimental discrepancy concerning the Hubble parameter.

Based on the improved background calculation, we present the perturbation part in chap. 6-10, with the derivation of the CMB spectrum, and new calculation of it.

## 2. Friedmann Equations

In this chapter, we present in concise form the basic equations (Friedmann equations) and equations of state (eos) for density and pressure with their different components radiation $\gamma$, neutrinos $\nu$, electrons $e$, protons $p$, neutrons $n$ (respectively baryons $b$), cold-dark-matter cdm $d$. The presentation relies basically on the four monographies [1] [2] [3] [4], with two notable extensions.

-Temperature

The eos depend explicitly on temperature $T$, resp. thermal energy $E_{th} = k_B T$, and **thermal energy is introduced as a function of time** $E_{th}(t)$, as all other variables, and has to be calculated.

-Baryon eos

The baryons are **modeled as classical gas**, and not as dust with zero pressure. We shall see in the background calculation in chap. 5, that this **model increases the value of the Hubble parameter**, which basically solves the Hubble-discrepancy problem.

### 2.1. Friedmann Equations and Metric

The metric which fulfills the conditions of space homogeneity and isotropy is the Robertson-Walker (RW) metric [1] [2] [3] [4]:

$$\mathrm{d}s^2 = -c^2\mathrm{d}t^2 + a^2(t)\left(\frac{\mathrm{d}r^2}{1-kr^2/R_H^2} + r^2\mathrm{d}\Omega^2\right) \tag{1}$$

with Hubble radius $R_H = \frac{c}{H_0} = 1.37\times10^{26}\,\mathrm{m}$ (Planck value), and scale factor $a(t)$.

The Einstein equations [1] [5] [6] [7] [8] for this metric are the two original Friedmann equations a and b (with $\dot{a} = \frac{\mathrm{d}a}{\mathrm{d}t}$) and two derived equations c (acceleration eq.) and d (density equation):

$$\left(\frac{\dot{a}}{ac}\right)^2+\frac{k}{a^2}-\frac{\Lambda}{3}=\frac{\kappa}{3}\rho c^2, \tag{2a}$$

$$\frac{2\ddot{a}}{ac^2}+\left(\frac{\dot{a}}{ac}\right)^2+\frac{k}{a^2}-\Lambda=-\kappa P, \tag{2b}$$

$$\frac{\ddot{a}}{ac^2}-\frac{1}{3}\Lambda=-\frac{\kappa}{2}\left(P+\frac{\rho c^2}{3}\right) \text{ derived from a, b} \tag{2c}$$

$$\frac{\dot{\rho}a}{3}+\dot{a}\left(\frac{P}{c^2}+\rho\right)=0 \text{ derived: density equation} \tag{2d}$$

with dimensionless variables using Planck-values: Hubble constant $H_0=67.74\,\mathrm{km\cdot s^{-1}\cdot Mpc^{-1}}$, normalized Hubble constant $h=0.6774$,

Einstein constant $\kappa=\frac{8\pi G}{c^4}$, $\kappa c^2\rho_{crit,0}=\frac{\rho_{crH}}{R_H^2}$, relative pressure

$P_r=\frac{P}{c^2\rho_{crit,0}}=\frac{P}{\rho_{Ecrit,0}}=P\kappa R_H^2$, relative cosmological constant $\Lambda_1=\Lambda R_H^2$, relative density $\Omega=\frac{\rho}{\rho_{crit,0}}$ with critical density today

$$\rho_{Ecrit,0}=c^2\rho_{crit,0}=\frac{3}{\kappa R_H^2},$$

$$\rho_{crit,0}=\frac{3}{\kappa R_H^2c^2}=\frac{3H_0^2}{8\pi G}=0.862\times10^{-26}\,\mathrm{kg\cdot m^{-3}}=\frac{5.0m_p}{R_H^3}\left(1.37\times10^{26}\right)^3$$

$$=13.0\times10^{78}\frac{m_p}{R_H^3}=5.0\ \text{nucleon}/\mathrm{m^3}$$

$$\rho_{crH}=\kappa c^2R_H^2\rho_{crit,0}=3$$

$$\rho_{Ecrit,0}=5.0\times0.963\frac{\mathrm{GeV}}{\mathrm{m^3}}=4.81\frac{\mathrm{GeV}}{\mathrm{m^3}},$$

Hubble radius $R_H=\frac{c}{H_0}=1.37\times10^{26}\,\mathrm{m}$

The Friedmann equations can be reformulated dimensionless with $x_0=tc$, $a'=\frac{\mathrm{d}a}{\mathrm{d}x_0}$, $\rho_{crH}=3$

$$\left(\frac{a'}{a}\right)^2+\frac{k}{a^2}-\frac{\Lambda_1}{3R_H^2}-\frac{1}{3}\frac{\rho_{crH}}{R_H^2}\Omega=0,\ \textit{i.e.}\ \left(\frac{a'}{a}\right)^2+\frac{k}{a^2}-\frac{\Lambda_1}{3R_H^2}-\frac{\Omega}{R_H^2}=0$$

$$\frac{2a''}{a}+\left(\frac{a'}{a}\right)^2+\frac{k}{a^2}-\frac{\Lambda_1}{R_H^2}+\frac{P_r}{R_H^2}=0$$

$$\frac{\rho_r'a}{3}+a'\left(P_r+\rho_r\right)=0$$

rescaled with $\frac{a}{R_H}\to a$

$$\left(a'\right)^2+k-\frac{\Lambda_1}{3}a^2-\rho_ra^2=0 \quad \text{sF1} \tag{3a}$$

$$a"a-\frac{1}{3}\Lambda_1 a^2=-\frac{3a^2}{2}\left(P_r+\frac{\rho_r}{3}\right)\quad \text{sF2} \tag{3b}$$

$$a"a+2(a')^2+2k-\Lambda_1 a^2+\frac{3}{2}(P_r-\rho_r)a^2=0\quad \text{sF3} \tag{3c}$$

$$\frac{\rho_r' a}{3}+a'(P_r+\rho_r)=0\quad \text{sF4} \tag{3d}$$

density eq

with

$$\Omega_{mr}=\frac{\rho_{mat}+\rho_{rad}}{\rho_{Ecrit,0}},\ \Omega_{mr}=\Omega_{mr,0}\left(\frac{H}{H_0}\right)^2,\ \Omega_{Ecrit}=\frac{3}{\kappa}\left(\frac{H}{c}\right)^2,$$

$$\Omega_\Lambda=\frac{\Lambda}{3}\left(\frac{c}{H}\right)^2,\ \Omega_k=-k\left(\frac{c}{H}\right)^2 R_0^2.$$

**Conformal Friedmann equations**

In conformal time $\eta$, $\mathrm{d}\eta=\frac{\mathrm{d}t}{a}$, with comoving distance in $\eta$:

$\chi(\eta)=c\int_{t_1}^{t_0}\frac{\mathrm{d}t}{a(t)}=c\int_{\eta_1}^{\eta}\mathrm{d}\eta$, or with redshift $z=\frac{1}{a}-1$: $\chi(z)=c\int_0^z\frac{\mathrm{d}z}{H(z)}$, follow the Friedmann conformal dimensionless equations [2] [3] [4] after rescaling $\frac{a}{R_H}\to a$, $c=1$, conformal Friedmann equations:

$$(a')^2+\frac{kc^2a^2}{R_H^2}=\frac{\Lambda c^2a^4}{3}+\frac{8\pi G}{3}\rho a^4$$

$$a"+\frac{kc^2a}{R_H^2}=\frac{4\pi G}{3c^2}(\rho c^2-3P)a^3+\frac{\Lambda c^2a^3}{3}$$

and rescaled conformal:

$$(a')^2+ka^2=\frac{\Lambda_1 a^4}{3}+\frac{\rho_{crH}}{3}\rho a^4\quad \text{scF1}\quad \frac{(a')^2}{a^2}=-k+\frac{\Lambda_1 a^2}{3}+\frac{\rho_{crH}}{3}\rho a^2 \tag{4a}$$

$$a"+ka=\frac{\rho_{crH}}{6}(\rho-3P)a^3+\frac{\Lambda_1 a^3}{3}\quad \text{scF2} \tag{4b}$$

**Friedmann radial equation**

It is convenient to reformulate the first Friedmann equation in the form of velocity-potential equation, which we call here Friedmann radial equation [1] [2] [3] [4] [9].

We get the Friedmann radial equation

$$(\dot{a})^2-\frac{K_s}{a^2}-\frac{K_m}{a}-\frac{\Lambda}{3}a^2+k=0 \tag{5}$$

it follows the potential form $\frac{\dot{a}^2}{c^2}+V(a)=-k$ with $c=1$

$$V(a)=-\frac{K_s}{a^2}-\frac{K_m}{a}-\frac{\Lambda}{3}a^2$$

with Planck data we have

$$K_m = 0.423\times 10^{26}\,\mathrm{m}\,,\quad K_s = 1.01\times 10^{48}\,\mathrm{m}^2\,,\quad \Lambda = 1.1\times 10^{-52}\,\mathrm{m}^{-2}$$

dimensionless

$$K_{m1} = K_m / R_H = \Omega_{m,0} = 0.309$$

$$K_{s1} = K_s / R_H^2 = \Omega_{rad,0} = \Omega_{\gamma,0} + \Omega_{\nu,0} = 0.54\times 10^{-4} + 0.0012 = 0.00125$$

$$\Lambda_1 = \Lambda R_H^2 = 1.1\times 1.37^2 = 2.06$$

from this we get the dimensionless Friedmann radial equation

$$(\dot{a})^2 - \frac{K_{s1}}{a^2} - \frac{K_{m1}}{a} - \frac{\Lambda_1}{3}a^2 + k = 0 \tag{5a}$$

## 2.2. Relative Density and Pressure (Relative to $c^2\rho_{crit,0}$)

In the following, we present the eos for the components radiation $\gamma$, neutrinos $\nu$, electrons $e$, protons $p$, neutrons $n$, cdm $d$ [2] [3] [4] [10] [11].

**Relative density & pressure baryons $b$, CDM $c$, matter density $\rho_{m,r}$ dependent (Eth independent variable)**

With thermal energy $E_{th} = k_B T$ matter density $\rho_{m,r} = \frac{K_{m1}}{a^3}$, $b$ = baryon, $c$ = cdm (cold dark matter)

$$\rho_{m,r}(a) = \rho_b + \rho_c\,,\quad \rho_b(\rho_{m,r}) = \rho_{m,r}\frac{\Omega_{b,0}}{\Omega_{b,0}+\Omega_{c,0}}\,,\quad \rho_c(\rho_{m,r}) = \rho_{m,r}\frac{\Omega_{c,0}}{\Omega_{b,0}+\Omega_{c,0}}\,,$$

we have for the pressure before (1) and after (2) nucleosynthesis

$$P_{b,2}(\rho_b, E_{th}) = \rho_b\frac{E_{th}}{m_p c^2}\,,\quad E_{th} > E_{c,ns}\ \text{ ideal gas,}\ \ E_{mp} = m_p c^2 = 0.938\,\mathrm{GeV}\,,$$

using today's He-H-ratio $Y_{H,He} = \frac{\rho_{He}}{\rho_H} = \frac{4n_{He}}{n_H} = 0.25$, $\frac{\rho_{He}}{\rho_H} = \frac{4n_{He}}{n_H} = 0.25$

$$P_{b,1} = \frac{1+Y_{H,He}/4}{1+Y_{H,He}}\rho_b\frac{E_{th}}{m_p c^2} = 0.85\rho_b\frac{E_{th}}{m_p c^2}\,,\quad E_{th} < E_{c,ns}\,,\quad E_{c,ns} = 100\,\mathrm{keV}\,,$$

with the soft-1-0-step function for state-transition at $ns$ = nucleosynthesis with transition energy $E_{c,ns} = 100\,\mathrm{keV}$ (see chap. 9) we get the pressure

$$P_b(\rho_b, E_{th}) = P_{b,2}(\rho_b, E_{th}) + \left(P_{b,1}(\rho_b, E_{th}) - P_{b,2}(\rho_b, E_{th})\right)\Theta_{1-0}(E_{th}, E_{c,ns}, \delta_0 E_{c,ns})\,,$$

$$\delta_0 = 0.1\,,$$

$$P_c(\rho_c, E_{th}) = 0\,.$$

**Relative density & pressure neutrinos**

We have for neutrino density and pressure before (1) and after (2) neutrino decoupling [12] with threshold energy $E_{c,\nu} = 1\,\mathrm{MeV}$:

$$\rho_{\nu,1}(\rho_b, E_{th}) = \frac{\Omega_{\nu b} n_b \frac{E_{th}}{c^2}}{\rho_{crit,0}} = \Omega_{\nu b}\rho_b\frac{E_{th}}{m_p c^2}\,,\quad n_\nu = \Omega_{\nu b} n_b$$

$\rho_{\nu,2}(\rho_b, E_{th}) = \Omega_{\nu b}\rho_b \frac{E_{th}}{m_p c^2}$, $E_{th} > E_{c,\nu}$, in thermal equilibrium,

$\rho_{\nu,1}(\rho_b, E_{th}) = \Omega_{\nu b}\rho_b \frac{E_{c.\nu}}{m_p c^2}\left(\frac{E_{c.\nu}}{E_{th}}\right)^{-3}$, $E_{th} < E_{c,\nu}$ decrease with $\sim \tilde{a}^{-3}$

$P_\nu(\rho_\nu) = \frac{1}{3}\rho_\nu$, parameters today $\Omega_{\nu,0} \approx 10^{-9}$, $T_{\nu,0} = 1.95\,\mathrm{K}$,

$E_{th,\nu 0} = k_B T_{\nu,0} = \frac{1.95\,\mathrm{K}}{300\,\mathrm{K}} \times 0.026\,\mathrm{eV} = 1.69\times 10^{-4}\,\mathrm{eV}$, it follows

$$\Omega_{\nu,b} = \frac{n_{\nu,0}}{n_{b,0}} = \frac{\Omega_{\nu,0}}{\Omega_{b,0}}\frac{m_p c^2}{k_B T_{\nu,0}} = \frac{10^{-9}}{0.049}\frac{0.938\,\mathrm{GeV}}{1.69\times 10^{-4}\,\mathrm{eV}} = 1.13\times 10^5.$$

**Relative density & pressure photons**

The Stefan-Boltzmann law gives

$$\rho(T) = aT^4,\quad a = 7.56\times 10^{-16}\frac{\mathrm{J}}{\mathrm{m}^3\cdot\mathrm{K}^4} = 4.717\frac{\mathrm{MeV}}{\mathrm{m}^3\cdot\mathrm{K}^4},\quad a = 51.9\frac{4\pi k_B^4}{c^3 h^3} \qquad (6)$$

$$\rho(E_{th}) = a_{SB}E_{th}^4$$

$$a_{SB} = \frac{207.6\pi}{h^3c^3} = \frac{a}{k_B^4} = \frac{7.56\times 10^{-16}}{\left(1.38\times 10^{-23}\right)^4}\frac{1}{\mathrm{J}^3\cdot\mathrm{m}^3}$$

$$= \frac{2.08\times 10^{76}}{\left(6.24\times 10^{18}\right)^3}\frac{1}{\mathrm{eV}^3\cdot\mathrm{m}^3} = 0.856\times 10^{20}\frac{1}{\mathrm{eV}^3\cdot\mathrm{m}^3}$$

$$a_{SB} = 0.856\times 10^{20}\frac{1}{\mathrm{eV}^3\cdot\mathrm{m}^3} = \frac{1}{\mathrm{eV}^4}0.856\times 10^{11}\frac{\mathrm{GeV}}{\mathrm{m}^3} = \frac{1}{\mathrm{eV}^4}0.178\times 10^{11}\rho_{Ecrit,0}$$

$$a_{SB0} = \frac{a_{SB}}{\rho_{Ecrit,0}} = \frac{1}{\mathrm{eV}^4}0.178\times 10^{11}.$$

Before photon decoupling the photon energy density is

$$\rho_\gamma(E_{th}) = a_{SB0}E_{th}^4,\quad P_\gamma(\rho_\gamma) = \frac{1}{3}\rho_\gamma$$

after photon decoupling at $E_{th} = E_{c,dc}$, $E_{c,dc} = 0.25\,\mathrm{eV}$, Planck $z_{dc} = 1090$, it becomes

$$\rho_\gamma(a, E_{th}) = a_{SB}\left(E_{c,dc}\frac{a(t_{c,dc})}{a}\right)^4,\quad E_{th} < E_{c,dc},\quad a(t_{c,dc}) = \frac{1}{z_{dc}+1} = \frac{1}{1091}$$

at e-pair production and above photons lose energy and keep a mean energy

$$E \geq m_e c^2,\quad E_{th} \approx 2m_e c^2$$

at p-pair production and above photons lose energy and keep a mean energy

$$E \geq m_p c^2,\quad E_{th} \approx 2m_p c^2.$$

**Temperature jumps at phase transitions**

At recombination $E_{th} = E_{c,re}$, $E_{c,re} = 0.29\,\mathrm{eV}$ temperature goes up due to free electrons forming atoms with baryons,

before recombination:

$$n = n_b + n_e = 2n_b\,,\quad n_b = n_e\,,\quad E_{th} = E_{c,re}\frac{a\left(t_{c,re}\right)}{a(t)}\,,\quad a\left(t_{c,re}\right) = \frac{1}{z_{re}+1} = \frac{1}{1271}\,,$$

$$z_{re} = 1270\,,\quad t_{c,re} = 1.16\times 10^{13}$$

after recombination: Saha equation:

$$X_e\left(E_{th}\right) = \frac{n_e}{n_e + n_H} = \frac{n_e}{n_b} = \frac{-1+\sqrt{1+4f\left(E_{th}\right)}}{2f\left(E_{th}\right)} \tag{7}$$

$$n = n_b + n_e = n_b\left(1 + X_e\left(E_{th}\right)\right),\quad E_{H,re} = 13.6\text{ eV}$$

$$f\left(E_{th}\right) = 4\zeta(3)\sqrt{\frac{2}{\pi}}\eta\left(\frac{E_{th}}{m_e c^2}\right)^{3/2}\exp\left(\frac{E_{H,re}}{E_{th}}\right) = 2.26\times 10^{-9}\left(\frac{E_{th}}{m_e c^2}\right)^{3/2}\exp\left(\frac{E_{H,re}}{E_{th}}\right).$$

The equation for $E_{th}$ after recombination with $E_H = E_{H,re}$, $E_m = m_e c^2$ is:

$$\frac{\mathrm{d}E_{th}}{\mathrm{d}a} = -\frac{E_{th0}}{a^2} - E_{H,re}\frac{\mathrm{d}X_e}{\mathrm{d}f}\frac{\mathrm{d}f}{\mathrm{d}a}\frac{\mathrm{d}E_{th}}{\mathrm{d}a}\,,\quad \frac{\mathrm{d}E_{th}}{\mathrm{d}a}\left(1 + E_{H,re}\frac{\mathrm{d}X_e}{\mathrm{d}f}\frac{\mathrm{d}f}{\mathrm{d}a}\right) = -\frac{E_{th0}}{a^2}$$

with solution $E_{th,a}(a)$ [13] shown in **Figure 1**.

$$E_{th,a}(1) = E_{th,0} = 0.000663\text{ eV}\,,\quad E_{th,a}\left(a_{re} = 1/\left(z_{re}+1\right)\right) = 0.2842\text{ eV} \approx E_{c,re}\,.$$

At nucleo-synthesis $E_{th} = E_{c,ns}$, $E_{c,ns} = 100\text{ keV}$ temperature goes up due to helium synthesis with energy released $E_{He,ns} = 12\text{ MeV}$, thermal energy behavior is analogously for $E_{c,re} < E_{th} < E_{He,ns}$, $z_{re} = 4\times 10^8$

$$E_{th} \approx E_{c,ns}\frac{a\left(t_{c,ns}\right)}{a(t)}\left(1 + 0.021\left(\left(\frac{E_{c,ns}a\left(t_{c,ns}\right)}{m_p c^2 a(t)}\right)^{-3/4}\exp\left(-\frac{E_{He,ns}a(t)}{2E_{c,ns}a\left(t_{c,ns}\right)}\right)\right.\right.$$

$$\left.\left. -\left(\frac{E_{c,ns}a\left(t_{c,ns}\right)}{m_p c^2 a\left(t_{He,ns}\right)}\right)^{-3/4}\exp\left(-\frac{E_{He,ns}a\left(t_{He,ns}\right)}{2E_{c,ns}a\left(t_{c,ns}\right)}\right)\right)\right)$$

where the baryon temperature depends on the photon temperature

$$T_b' = -2\frac{a'}{a}T_b + \frac{8}{3}\frac{m_b}{m_e}\frac{\bar{\rho}_\gamma}{\bar{\rho}_b}a n_e \sigma_T\left(T_\gamma - T_b\right)\quad\text{with}\quad a' = \frac{\mathrm{d}a}{\mathrm{d}\eta}\quad [14].$$

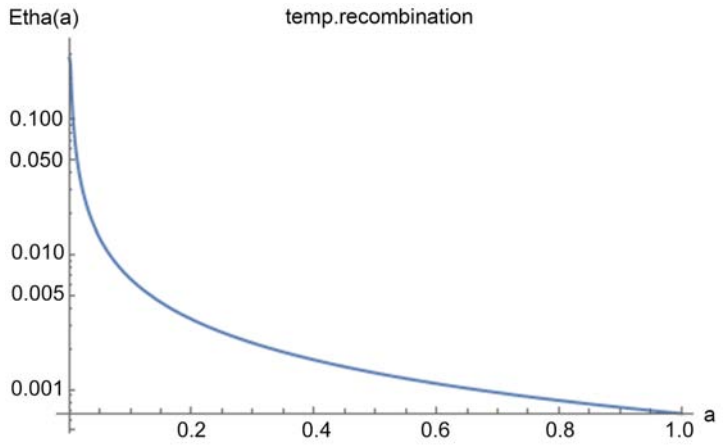


**Figure 1.** Temperature after recombination $E_{th,a}(a)$ in eV.

**Density electrons**

The density of electrons is described by the Peebles equation with the parameters

$$C_r(T) \equiv \frac{\Lambda_{2\gamma} + \Lambda_\alpha}{\Lambda_{2\gamma} + \Lambda_\alpha + \beta_\alpha}, \quad \Lambda_{2\gamma} = 8.227\ \mathrm{s}^{-1},$$

$$\Lambda_\alpha = \frac{27}{128\zeta(3)} \frac{H(T)}{(1-X_e)(n_b/n_\gamma)(k_B T/E_I)^3}, \quad \beta_\alpha = \beta(T)\exp\left(\frac{3E_I}{4k_B T}\right),$$

$E_I = 13.6\ \mathrm{eV}$ = hydrogen ionization energy, 1s ionization rate, $n_{1s} \approx (1-X_e)n_b$,

$n_b = \eta n_\gamma$, $\lambda_\alpha = \dfrac{8\pi\hbar c}{3E_I}$ Lyman wavelength,

$$\beta(T) = \langle \sigma v \rangle \left(\frac{m_e c^2 k_B T}{2\pi\hbar^2 c^2}\right)^{3/2} \exp\left(-\frac{E_I}{k_B T}\right)$$

$$\alpha(T) \approx 9.8 \frac{\alpha^2}{(m_e c^2)^2} \left(\frac{E_I}{k_B T}\right)^{1/2} \log\left(\left(\frac{E_I}{k_B T}\right)\right)$$

we get the Peebles equation ([4] 3.153) for the hydrogen ionization percentage

$$\frac{\mathrm{d}X_e}{\mathrm{d}z} = -\frac{C_r(T)}{H(z)(1+z)}\left(\left(\frac{m_e c^2 k_B T}{2\pi}\right)^{1/2}(1-X_e)\exp\left(-\frac{E_I}{k_B T}\right) - \alpha(T)\frac{n_b}{n_\gamma}\frac{2\zeta(3)}{\pi^2}(k_B T)^3 X_e^2\right) \tag{8}$$

where

$$H(z) = \sqrt{\Omega_m} H_0 (1+z)^{3/2}\left(1 + \frac{1+z}{1+z_{eq}}\right), \quad H_0 \approx 1.5\times 10^{-33}\ \mathrm{eV}$$

$$T = (1+z)0.235\ \mathrm{eV}.$$

We get for the electron density before (1) and after (2) recombination

$$\rho_{e,1}(\rho_b, E_{th}) = \rho_b \frac{E_{th}}{m_p c^2}, \quad E < E_{c,ep}, \quad E_{c,ep} = m_e c^2 = 511\,\mathrm{keV}$$

$$n_{e+} \approx \frac{n_b^2}{n_\gamma} 0.17\alpha \left(\frac{E_{th}}{m_e c^2}\right)^2 = \frac{n_b^2}{n_\gamma}\left(\frac{E_{th}}{m_e c^2}\right)^2 1.2\times 10^{-3}, \quad n_b = \Omega_{b,0}\frac{\rho_{crit,0}}{m_p}$$

$$\frac{n_b}{n_\gamma} = \frac{n_{b,0}}{n_{\gamma,0}} \frac{a^3 E_{th,0}^3}{a^3 E_{th}^3} = \frac{n_{b,0}}{n_{\gamma,0}} = \frac{0.242\ \mathrm{m}^{-3}}{0.41\times 10^{-3}\ \mathrm{m}^{-3}} = 590 \quad \text{scale-independent}$$

follows $\dfrac{n_{e+}}{n_b} \approx \dfrac{n_b}{n_\gamma} 0.17\alpha \left(\dfrac{E_{th}}{m_e c^2}\right)^2 = \left(\dfrac{E_{th}}{m_e c^2}\right)^2 0.708$,

$$\rho_{e,2}(\rho_b, E_{th}) = \rho_b\left(1 + \frac{2n_{e+}}{n_b}\right)\frac{E_{th} + m_e c^2}{m_p c^2}, \quad E > E_{c,ep}$$

due to Saha equation

$$\rho_{e,0}\left(\rho_b, E_{th}\right) \approx \rho_{e,1}\left(\rho_b\left(t_{c,re}\right), E_{c,re}\right)\exp\left(E_{H,re}\left(\frac{1}{E_{c,re}}-\frac{1}{E_{th}}\right)\right)$$

$$= \rho_b\left(a\left(t_{c,re}\right)\right)\frac{m_e}{m_p}\exp\left(E_{H,re}\left(\frac{1}{E_{c,re}}-\frac{1}{E_{th}}\right)\right)$$

alternatively

$$n_e = n_b X_e\left(E_{th}\right), \quad \rho_e = \frac{m_e c^2}{m_p c^2}\rho_b X_e\left(E_{th}\right)$$

$$E < E_{c,re}, \quad E_{c,re} = 0.29\,\text{eV}, \quad \rho_b\left(t_{c,re}, E_{c,re}\right) = \Omega_{b,0} z_{re},$$

$$\Omega_{b,0} = 0.0486, \quad z_{re} = 1270, \quad a\left(t_{c,re}\right) = \frac{1}{z_{re}+1} = \frac{1}{1271}.$$

**Fermi pressure electrons**

The pressure of electrons is the Fermi pressure $P_{Fe}$ of a (spin_1/2) fermion gas

$$P_e\left(\rho_e, E_{th}\right) = P_{Fe}\left(\rho_e, E_{th}\right)$$

with low- and high-density limits $P_1 = \frac{1}{5}np_F c$, $P_2 = \frac{2}{5}nE_F$.

Fermi energy $E_F = \sqrt{\left(p_F c\right)^2 + \left(m_e c^2\right)^2}$, $p_F c = \hbar c\left(3\pi^2 n\right)^{1/3}$

$$P_{Fe}\left(\rho, E\right) = P_2\left(\rho\right) + \left(P_1\left(\rho\right) - P_2\left(\rho\right)\right)\Theta_{1-0}\left(E, m_e c^2, \delta_0 m_e c^2\right) \tag{9}$$

$$\rho_{cr} = \rho_{crit,0}c^2 = 0.77\times10^{-10}\,\text{J}\cdot\text{m}^{-3} = 0.484\times10^3\,\text{MeV}\cdot\text{m}^{-3}$$

$$n_{p,0} = \frac{\rho_{crit,0}c^2\Omega_{b,0}}{m_p c^2} = \frac{0.484\times10^3\,\text{MeV}\cdot\text{m}^{-3}\times0.047}{0.938\,\text{GeV}} = 0.0242\,\text{m}^{-3}$$

$$\hbar c = 1.96\times10^{-16}\,\text{GeV}\cdot\text{m} = 1.96\times10^{-5}\,\text{eV}\cdot\text{m}$$

$$n_e = \frac{\rho_{crit,0}c^2\rho_e}{m_e c^2} = n_{p,0}\frac{m_p}{\Omega_{b,0}m_e}\rho_e = 0.0242\,\text{m}^{-3}\rho_e 39.0\times10^3 = 943.8\rho_e$$

$$\frac{n_e}{n_{p,0}} = \frac{m_p}{\Omega_{b,0}m_e}\rho_e = 339055.6\rho_e.$$

For electrons we get the expressions

$$P_1 = \frac{1}{5}\frac{np_F c}{\rho_{crit,0}} = \frac{1}{5}\left(\frac{n_e\Omega_{b,0}}{n_{p,0}}\right)\frac{p_F c}{m_p c^2} = \frac{1}{5}\left(\frac{m_p}{m_e}\rho_e\right)\frac{p_F c}{m_p c^2} = \frac{1}{5}\left(\frac{m_p}{m_e}\rho_e\right)\frac{201.78\left(\rho_e\right)^{1/3}}{m_p c^2}$$

$$P_2 = \frac{2}{5}\frac{nE_F}{\rho_{crit,0}} = \frac{1}{5}\left(\frac{n_e\Omega_{b,0}}{n_{p,0}}\right)\frac{E_F}{m_p c^2} = \frac{1}{5}\left(\frac{m_p}{m_e}\rho_e\right)\frac{\sqrt{\left(p_F c\right)^2 + \left(m_e c^2\right)^2}}{m_p c^2}$$

$$p_F c = \hbar c\left(3\pi^2 n_{e,0}\right)^{1/3}\left(\rho_e\right)^{1/3}33.91$$

$$= 1.96\times10^{-5}\,\text{eV}\cdot\text{m}\left(3\pi^2 0.947\times10^3\,\text{m}^{-3}\right)^{1/3}33.91\left(\rho_e\right)^{1/3}$$

$$= 201.78\left(\rho_e\right)^{1/3}\,\text{eV}$$

$$p_F c = 201.78\left(\rho_e\right)^{1/3}\,\text{eV}.$$

**State transitions** radiation $\gamma$, neutrinos $\nu$, electrons $e$, protons $p$, neutrons $n$, cdm $d$.

Generally, the density state transition from $\rho_1$ to $\rho_2$ at transition temperature $T_c$ (transition thermal energy $E_c = k_B T_c$) has the form

$\rho(E) = \rho_2 + (\rho_1 - \rho_2)\Theta_{1-0}(E, E_c, \delta E_c)$,

with soft-0-1-step function $\Theta_{0-1}(E, E_c, \delta E_c) = \dfrac{1}{1+\exp\left(\dfrac{E_c - E}{\delta E_c}\right)}$,

with soft-1-0-step function $\Theta_{1-0}(E, E_c, \delta E_c) = \dfrac{1+\exp\left(-\dfrac{E_c}{\delta E_c}\right)}{1+\exp\left(\dfrac{E - E_c}{\delta E_c}\right)}$,

where $\delta E_c$ is the standard deviation of $E_c$.

We can set approximately $\dfrac{\delta E_c}{E_c} = \dfrac{\delta T_c}{T_c} \approx \dfrac{\delta T_0}{T_0}$, where (measured in CMB) $\dfrac{\delta T_0}{T_0} = \dfrac{\Delta T_{\gamma,0}}{T_{\gamma,0}} \approx \dfrac{30\,\mu\text{K}}{2.72\,\text{K}} = 1.1\times 10^{-5}$.

## 2.3. Transition Thermal Energies and Eos

**-neutrino decoupling** $E_{c,\nu} = 1\,\text{MeV}$, $t_{c,\nu} = 1\,\text{s}$, $\rho_{1c,\nu} = \rho_{1,\nu}(t_{c,\nu})$,

$\rho_{1,\nu}(E_{th}) = E_{th}$, $\rho_{2,\nu}(E_{th}, a) = \rho_{1c,\nu}\left(\dfrac{a}{a(t_{c,\nu})}\right)^4$;

**-e-p-annihilation**

$E_{c,ep} = 0.5\,\text{MeV}$, $t_{c,ep} = 6\,\text{s}$, $n_\gamma = a_{SB} E_{th}^4$ for all $t$ $a = 7.56\times 10^{-16}\,\text{J}/\text{m}^2\cdot\text{K}^4$,

$a = 51.9\dfrac{4\pi k_B^4}{c^3 h^3}$

$\rho_{1,e} = \left(n_b + n_{e+}(t_{c,ep})\right)m_e$, $\rho_{2,e} = n_b m_e$ with

$n_{e+} \approx \dfrac{n_b^2}{n_\gamma} 0.17\alpha\left(\dfrac{E_{th}}{m_e c^2}\right)^2 = \dfrac{n_b^2}{n_\gamma}\left(\dfrac{E_{th}}{m_e c^2}\right)^2 1.2\times 10^{-3}$;

**-photon recombination**

$E_{c,re} = 0.29\,\text{eV}$, $t_{c,re} = 290\,\text{ky}$, $\rho_{2c,re} = \rho_{1c,re} + n_b(t_{c,re})E_{c,re}$

$\rho_{1,e} = n_b m_e$, $\rho_{2,e} = \dfrac{1}{2}\rho_{1,e}\exp\left(\dfrac{E_{th} - E_{c,re}}{E_{th}}\right)$;

**-photon decoupling**

$E_{c,\gamma} = 0.25\,\text{eV}$, $t_{c,\gamma} = 370\,\text{ky}$, $\rho_{1c,\gamma} = \rho_{1,\gamma}(t_{c,\gamma})$,

$\rho_{1,\gamma}(E_{th}) = E_{th}$, $\rho_{2,\gamma}(E_{th}, a) = \rho_{1c,\gamma}\left(\dfrac{a}{a(t_{c,\gamma})}\right)^4$;

**-nucleo-synthesis helium**

$E_{c,ns} = 100\,\text{keV}$ , $t_{c,ns} = 3\,\text{min}$ , $4p^+ + 2e^- \to He^{2+}$ , ratio $\frac{\rho_{He}}{\rho_p} = 0.25$ , eos transition $1 \to 2$ with ideal gas $P_1 = n_b E_{th} = \rho_b \frac{E_{th}}{m_p}$ , $t < t_{c,ns}$ , with ideal gas $P_2 = n_{b,1}(0.75 + 0.25/4)E_{th} = n_{b,1}0.81E_{th} = 0.81\rho_b \frac{E_{th}}{m_p}$ , $t < t_{c,ns}$ .

## 3. Parameters

The simple ΛCDM model is based on seven parameters: physical baryon density parameter $\Omega_b h^2$; physical matter density parameter $\Omega_m h^2$; the age of the universe $t_0$; scalar spectral index $n_s$; curvature fluctuation amplitude $A_s$; and reionization optical depth $\tau$, dark energy density $\Omega_\Lambda$.

The parameters of the ΛCDM are given in the following table (Table 1).

11 independent parameters: $\Omega_b h^2$, $\Omega_c h^2$, $t_0$, $n_s$, $\Delta_R^2$, $\tau$, $\Omega_\rho$, $w$, $\Sigma m_\nu$, $N_{eff}(\nu)$, $A_s$;

7 fixed parameters $r$, $\mathrm{d}n_s/\mathrm{d}\ln k$, $H_0$, $\Omega_b$, $\Omega_c$, $\Omega_m$, $\Omega_\Lambda$;

5 calculated parameters $\rho_{crit}$, $\sigma_8$, $z_{dec}$, $t_{dec}$, $z_{re}$;

13 total parameters $\Omega_b$, $\Omega_c$, $t_0$, $n_s$, $A_s$, $\tau$, $\Omega_\Lambda$, $w$, $\Sigma m_\nu$, $N_{eff}(\nu)$, $r$, $\mathrm{d}n_s/\mathrm{d}k$, $H_0$;

derived parameters $\rho_{crit}$, $\sigma_8$, $z_{dec}$, $t_{dec}$, $z_{re}$, $\omega_b = \Omega_b h^2$, $\omega_m = \Omega_m h^2$.

**Table 1.** Planck Collaboration Cosmological parameters [15].

| | Description | Symbol | Value |
|---|---|---|---|
| **Independent parameters 11** | Physical baryon density parameter | $\Omega_b h^2$ | 0.02230 ± 0.00014 |
| | Physical dark matter density parameter | $\Omega_c h^2$ | 0.1188 ± 0.0010 |
| | Age of the universe | $t_0$ | 13.799 ± 0.021 × $10^9$ years |
| | Scalar spectral index | $n_s$ | 0.9667 ± 0.0040 |
| | Curvature fluctuation amplitude, $k_0 = 0.002$ $\text{Mpc}^{-1}$ | $\Delta_R^2$ | 2.441 + 0.088 − 0.092 × $10^{-9}$ |
| | Reionization optical depth | $\tau$ | 0.066 ± 0.012 |
| **Fixed parameters 7** | Total density parameter | $\Omega_{tot}$ | 1 |
| | Equation of state of dark energy | $w$ | −1 |
| | Sum of three neutrino masses | $\Sigma m_\nu$ | 0.06 eV/$c^2$ |
| | Effective number of relativistic degrees of freedom | $N_{eff}$ | 3.046 |
| | Scalar amplitude | $A_s$ | (2.215 ± 0.13) |
| | Tensor/scalar ratio | $r$ | 0 |
| | Running of spectral index | $\mathrm{d}n_s/\mathrm{d}\ln k$ | 0 |
| **Calculated values 5** | Hubble constant | $H_0$ | 67.74 ± 0.46 $\text{km}\cdot\text{s}^{-1}\cdot\text{Mpc}^{-1}$ |
| | Baryon density parameter | $\Omega_b$ | 0.0486 ± 0.0010 |
| | Dark matter density parameter | $\Omega_c$ | 0.2589 ± 0.0057 |
| | Matter density parameter | $\Omega_m$ | 0.3089 ± 0.0062 |
| | Dark energy density parameter | $\Omega_\Lambda$ | 0.6911 ± 0.0062 |
| | Critical density | $\rho_{\text{crit}}$ | (8.62 ± 0.12) × $10^{-27}$ $\text{kg/m}^3$ |
| | Fluctuation amplitude at 8 $h^{-1}$ Mpc | $\sigma_8$ | 0.8159 ± 0.0086 |
| | Redshift at decoupling | $z_*$ | 1089.90 ± 0.23 |
| | Age at decoupling | $t_*$ | 377,700 ± 3200 y |
| | Redshift of reionization (with uniform prior) | $z_{re}$ | 8.5 + 1.0 − 1.1 |

The additional parameters of the extended ΛCDM are given in the second table (Table 2).

**Some specifications**

The amplitude $A_s$, is determined by the CMB power spectrum

$$\Delta_R^2\left(k^2\right)=A_s\left(\frac{k}{k_0}\right)^{n_s-1},\quad k_0\approx 0.05\ \text{Mpc}^{-1}.$$

The relative current Hubble parameter is $h=\frac{H_0}{100}$.

The fluctuation amplitude is defined by $\sigma_8=\sigma\left(\rho_{mat},R\right)_{R=8h^{-1}\text{Mpc}}$, where $\sigma\left(\rho_{mat},R\right)=\text{stdev}\left(\rho_{mat}\right)$ smoothed by distance $R$ ([2]).

**Key cosmological events**

Key cosmological events calculated from the ΛCDM model with temperature, energy scale and cosmic time are given below [4] [16] in Table 3.

Table 2. Extended model parameters [15].

| Description | Symbol | Value |
|---|---|---|
| Total density parameter | $\Omega_{tot}$ | 1.0023 + 0.0056 − 0.0054 |
| Equation of state of dark energy | $w$ | −0.980 ± 0.053 |
| Tensor-to-scalar ratio | $r$ | <0.11, $k_0$ = 0.002 Mpc$^{-1}$ ($2\sigma$) |
| Running of the spectral index | $\mathrm{d}n_s/\mathrm{d}\ln k$ | −0.022 ± 0.020, $k_0$ = 0.002 Mpc$^{-1}$ |
| Physical neutrino density parameter | $\Omega_\nu h^2$ | <0.0062 |
| Sum of three neutrino masses | $\Sigma m_\nu$ | <0.58 eV/$c^2$ ($2\sigma$) |

Table 3. Key cosmological events ([4], chap. 2).

| Event | Temperature | Energy | Time |
|---|---|---|---|
| Inflation ends | $10^{29}$ K | $10^{16}$ GeV | $10^{-35}$ s |
| CDM decouples, GUT scale | $10^{29}$ K | $10^{15}$ GeV | $10^{-36}$ s |
| Baryons form | $10^{16}$ K | 1 TeV? | $10^{-12}$ s |
| El-weak force | $10^{15}$ K | 100 GeV | $10^{-11}$ s |
| Hadrons form | $10^{12}$ K | 150 MeV | $10^{-5}$ s |
| Neutrinos decouple | $10^{10}$ K | 1 MeV | 1 s |
| Nuclei form | $10^{9}$ K | 100 keV | 200s |
| Atoms form | 3460 K | 0.29 eV | 290 ky |
| Photons decouple | 2970 K | 0.25 eV | 370 ky |
| First stars | 50 K | 4 meV | 100 My |
| First galaxies | 12 K | 1 meV | 400 My |
| Dark energy domination | 3.8 K | 0.33 meV | 9 Gy |
| Now | 2.7 K | 0.24 meV | 13.8 Gy |

## 4. Inflation

The "naive" so called Hot-Big-Bang model has several aspects, which are in disagreement with cosmological observations.

**Hot Big-bang problems**

- the observed homogeneity of the present universe (distances > 200 Mly) should arise from arbitrary initial conditions: **horizon problem**;

- the observed curvature is small: **flatness problem**;

- the observed correlation regions in the CMB have supraluminal distance: **superhorizon correlations**.

**Cosmological inflation**

In the approximation that the expansion is exactly exponential, the horizon is static, *i.e.* $H=\frac{\dot{a}}{a}\approx const$, and we have an inflating universe [17]. This inflating universe can be described by the de-Sitter metric [1] [2] [3] [5]

$$\mathrm{d}s^2=-\left(1-\Lambda r^2\right)c^2\mathrm{d}t^2+\frac{1}{1-\Lambda r^2}\mathrm{d}r^2+r^2\mathrm{d}\Omega^2 \tag{10a}$$

For the case of exponential expansion, the equation of state is $P=-\rho$, with world radius

$$R(t)=R_0\exp\left(ct\sqrt{\frac{\Lambda}{3}}\right) \tag{10b}$$

The expansion generates an almost-flat and large-scale-homogeneous universe, as it is observed today.

Furthermore, horizon $R_H=\dot{a}^{-1}=(Ha)^{-1}$ reaches a minimum at the end of inflation, and then rises again, this explains superluminal correlations in the present universe.

**Inflation in Ashtekar-Kodama quantum gravity** [18]

Inflation takes place between $r_i=l_p=1.61\times10^{-35}\,\mathrm{m}$ and $R_{\mathrm{inf}}=r_{gr}=3.1\times10^{-5}\,\mathrm{m}$ with expansion factor $f_{\mathrm{inf}}=\exp\left(r_{\mathrm{inf}}\sqrt{\frac{\Lambda}{3}}\right)=1.9\times10^{30}$, $r_{\mathrm{inf}}=2\times10^{-26}\,\mathrm{m}$,

$E_{\mathrm{inf}}=\frac{\hbar c}{r_{\mathrm{inf}}}=\frac{1.96\times10^{-16}\,\mathrm{GeV}}{2\times10^{-26}\,\mathrm{m}}=0.98\times10^{10}\,\mathrm{GeV}$, $t_{\mathrm{inf}}=\frac{r_{\mathrm{inf}}}{c}=0.66\times10^{-34}\,\mathrm{s}$,

$R_{\mathrm{inf}}=10^{-2}\,\mathrm{m}$.

Inflation with standard assumptions ([4], chap. 4)

$$r_i=3\times10^{-28}\,\mathrm{m},\quad t_{\mathrm{inf}}=10^{-36}\,\mathrm{s},\quad f_{\mathrm{inf}}=10^{30},\quad a_{\mathrm{inf}}=10^{-28},\quad R_{\mathrm{inf}}=3\times10^{2}\,\mathrm{m},$$

$$f_{\mathrm{inf}}=\exp\left(r_{\mathrm{inf}}\sqrt{\frac{\Lambda}{3}}\right),\quad \Lambda=3\left(\frac{\log(f_{\mathrm{inf}})}{r_{\mathrm{inf}}}\right)^2=1.4\times10^{60}\,\mathrm{m}^{-2},$$

$$H=\sqrt{\frac{\Lambda}{3}}=\frac{\log(f_{\mathrm{inf}})}{r_{\mathrm{inf}}}=6.9\times10^{29}\,\mathrm{m}^{-1}.$$

**Assessment of the inflation factor** ([3], chap. 4),

*f* = end inflation, *i* = start inflation, *eq* = matter-radiation-equality, *0* = today, *ER* = *f* = expansion rate

$$\frac{a(t_f)}{a(t_{in})} = \exp N\,,\quad N \gg \log\left(\frac{T_f}{T_{eq}}\right) + \frac{1}{2}\log\left(\frac{T_{eq}}{T_0}\right),$$

$$T_f \simeq 10^{16}\,\text{GeV}\,,\quad T_{eq} \simeq 1\,\text{eV}\,,\quad T_0 \simeq 10^{-4}\,\text{eV}$$

$$N \geq 60\,,\quad \Delta t \geq \frac{60}{H(t_f)} \simeq 60\sqrt{\frac{3}{8\pi G\rho_{ER}}}\left(\frac{T_0}{T_f}\right)^2 \approx 10^{-37}\,\text{s}\,.$$

**Inflaton model $\phi(t,x)$ with GR-action**

The action is ([3], chap. 4)

$$S = \int \mathrm{d}^4x\sqrt{-g}\left(L_{EH} + L_\phi\right)$$

with the Einstein-Hilbert action of GR

$$S_{EH} = \int\left(\frac{R-2\Lambda}{2\kappa}\right)\sqrt{-g}\,\mathrm{d}^4x$$

$$L_{EH} = \frac{R-2\Lambda}{2\kappa}$$

and the inflaton action

$$S_\phi = \int \mathrm{d}^4x\sqrt{-g}\left(\frac{\hbar c}{2}g^{\mu\nu}\partial_\mu\phi\partial_\nu\phi - V(\phi)\right)$$

$$L_\phi = \frac{\hbar c}{2}g^{\mu\nu}\partial_\mu\phi\partial_\nu\phi - V(\phi)$$

with energy-momentum $T_{\mu\nu} = \hbar c\partial_\mu\phi\partial_\nu\phi - g_{\mu\nu}\left(\frac{\hbar c}{2}g^{\mu\nu}\partial_\mu\phi\partial_\nu\phi - V(\phi)\right)$

$$T_0^0 = \hbar c\frac{\dot\phi^2}{2} + V(\phi)\,,\quad T_i^{\,j} = -\delta_i^j\left(\hbar c\frac{\dot\phi^2}{2} - V(\phi)\right).$$

For RW-metric the action is $S = \int \mathrm{d}^4x\sqrt{-g}\left(\hbar c\left(-\frac{\dot\phi^2}{2} + \frac{1}{2a^2}(\nabla\phi)^2\right) - V(\phi)\right)$

with eom = Klein-Gordon equation $\ddot\phi + 3H\dot\phi + \frac{1}{\hbar c}\frac{\mathrm{d}V(\phi)}{\mathrm{d}\phi} = 0$

which represents an oscillator with Hubble-friction $3H\dot\phi$

and energy density $\rho_\phi = \hbar c\frac{\dot\phi^2}{2} + V(\phi)$,

and pressure $P_\phi = \hbar c\frac{\dot\phi^2}{2} - V(\phi)$ (4.50).

If $E_{kin} \equiv \frac{1}{2}\dot\phi^2 \ll E_{pot} \equiv V(\phi)$, $E_{kin} = \hbar c\frac{\dot\phi^2}{2} \ll E_{pot} = V(\phi)$, we have $P_\phi \approx -\rho_\phi$ *i.e.* equation-of-state of dark energy $\Omega_\Lambda$ generating temporary inflation.

We get the **Friedmann equations** (radiation-matter density $\rho_{rm}$ added)

$$H^2 = \frac{\kappa}{3}\rho_E = \frac{\kappa}{3}\left(\hbar c\frac{\dot\phi^2}{2} + V(\phi) + \rho_{rm}\right) \tag{11a}$$

$$\dot H = -\frac{\kappa}{2}\left(\rho_\phi + P_\phi - \rho_{rm} - P_{rm}\right) = -\frac{\kappa}{2}\left(\hbar c\dot\phi^2 - \frac{4}{3}\rho_{rm}\right) \tag{11b}$$

and the **Klein-Gordon equation**

$$\ddot{\phi}+3H\dot{\phi}+\frac{1}{\hbar c}\frac{\mathrm{d}V(\phi)}{\mathrm{d}\phi}=0 \tag{11c}$$

**We get dimensionless 2 equations** in Planck-units $l_{Pl}=1.62\times10^{-35}\,\mathrm{m}$,

$$\rho_{rm}=\frac{3}{8\pi}H^2-\frac{\dot{\phi}^2}{2}-V(\phi)$$

Friedmann $\dot{H}=-4\pi\left(\dot{\phi}^2-\frac{4}{3}\left(\frac{3}{8\pi}H^2-\frac{\dot{\phi}^2}{2}-V(\phi)\right)\right)=-4\pi\left(\frac{3\dot{\phi}^2}{2}-\frac{H^2}{2\pi}+\frac{4}{3}V(\phi)\right)$.

Klein-Gordon $\ddot{\phi}+3H\dot{\phi}+\frac{\mathrm{d}V(\phi)}{\mathrm{d}\phi}=0$.

**Slow-roll approximation**

If $E_{kin}\equiv\frac{1}{2}\dot{\phi}^2\ll E_{pot}\equiv V(\phi)$ or $\varepsilon_H\ll1$, $\varepsilon_H\equiv-\frac{\dot{H}}{H^2}$ (slow-roll parameter 1), and almost constant velocity, $\eta_H=-\frac{\ddot{\phi}}{H\dot{\phi}}\ll1$ (slow-roll parameter 2), we have persisting slow-roll condition $\varepsilon_H\ll1$, $\eta_H\ll1$ (**slow-roll approximation**), which yields approximate fundamental equations with approximations $3H\dot{\phi}\approx-V'$ and $3H^2\approx8\pi GV$ and $\varepsilon_H=-\frac{\dot{H}}{H^2}=-\frac{V'}{2V}\frac{\dot{\phi}}{H}=\frac{1}{16\pi G}\left(\frac{V'}{V}\right)^2$ and $\eta_H=-\frac{\ddot{\phi}}{H\dot{\phi}}=\frac{V''}{3H^2}=\frac{1}{8\pi G}\left(\frac{V''}{V}\right)$ and for the scale factor

$$a(t)=a(t_{in})\exp\left(\int_{t_{in}}^{t}H(t)\mathrm{d}t\right)=a(t_{in})\exp\left(-8\pi G\int_{t_{in}}^{t}\frac{V}{V'}\mathrm{d}\phi\right).$$

**Square potential**

We use the square potential $V(\phi)=c_1+c_2(\phi-\phi_0)^2$, $c_1=1.16\times10^{-124}$, slow-roll condition: $c_1\ll c_2$ with the minimum value $V(\phi_0)=c_1=\frac{\Lambda}{\kappa}=1.16\times10^{-124}$ and $r_{\inf}=2\times10^{-26}\,\mathrm{m}$, we get the following relations:

$$a(t)=a(t_{in})\exp\left(\int_{t_{in}}^{t}H(t)\mathrm{d}t\right)=a(t_{in})\exp\left(-8\pi\int_{t_{in}}^{t}\frac{V}{V'}\mathrm{d}\phi\right)$$

$$a(t)=a(t_{in})\exp\left(4\pi\int_{0}^{\phi_0}(\phi-\phi_0)\mathrm{d}\phi\right)=a(t_{in})\exp\left(2\pi\phi_0^2\right)$$

$$\phi_0=\sqrt{\frac{1}{2\pi}\log\left(\frac{a(t)}{a(t_{in})}\right)}=\sqrt{\frac{1}{2\pi}\log(f_{\inf})}=3.31$$

$$\varepsilon_H=\frac{1}{16\pi}\left(\frac{V'}{V}\right)^2=\frac{1}{16\pi}\left(\frac{2}{\frac{c_1}{c_2(\phi-\phi_0)}+(\phi-\phi_0)}\right)^2\approx\frac{1}{4\pi}\frac{1}{(\phi-\phi_0)^2}$$

$$\eta_H = \frac{1}{8\pi}\left(\frac{V''}{V}\right) = \frac{1}{8\pi}\left(\frac{2c_2}{c_1 + c_2(\phi-\phi_0)^2}\right) \approx \frac{1}{4\pi}\frac{1}{(\phi-\phi_0)^2}$$

$$\rho_{rm} = \frac{3}{8\pi}H^2 - \frac{\dot{\phi}^2}{2} - V(\phi)$$

for $t \to \infty$, $\dot{\phi} = \delta c_1 \ll 1$, $H = H_0$, $\phi \to \phi_0$, $\rho_{rm} = \left(\frac{3}{8\pi}H_0^2 - c_1\right) = 0$,

so condition for convergence is: $c_1 = \frac{3}{8\pi}H_0^2$.

The fundamental equations become

Friedmann $\dot{H} = -4\pi\left(\dot{\phi}^2 - \frac{4}{3}\left|\frac{3}{8\pi}H^2 - \frac{\dot{\phi}^2}{2} - V(\phi)\right|\right)$;

Klein-Gordon $\ddot{\phi} + 3H\dot{\phi} + \frac{\mathrm{d}V(\phi)}{\mathrm{d}\phi} = 0$;

slow-roll $\dot{H} \approx -6\pi\dot{\phi}^2$;

3 boundary conditions for $t = l_{Pl} = 1$: $H(1) = H_1$, $\phi(1) = \phi_1$, $\dot{\phi}(1) = \phi_{d1}$;

with 3 potential parameters $c_1$, $c_2$, $\phi$.

Example: $\delta c_1 = 0.05$, $H_0 = 5$, $\phi_0 = 2.3$, $c_1 = 3$, $c_2 = 1$ [13].

Below in Figure 2 and Figure 3 are inflaton amplitude and Hubble parameter.

## 5. Background Calculations

There are basically two possible ways for background calculation:

-numerical solution of two Friedmann equations in two variables, calculating backward from boundary conditions at present time $x_0$;

-analytical solution, where the second equation is solved analytically, and inserted into the first, which gives an integral, which is calculated numerically.

The numerical solution encounters the problem of limited convergence: it stops at some time $x_c$.

The analytical solution avoids the convergence problem, and **this solution scheme is used in the calculation** of results presented below.

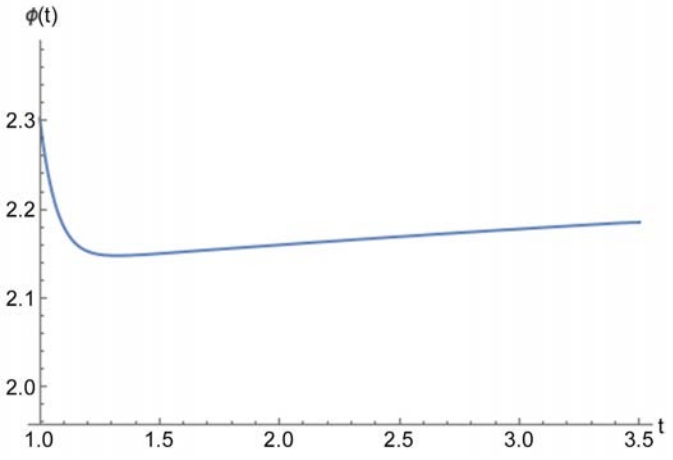


Figure 2. Inflaton amplitude $\phi(t)$.

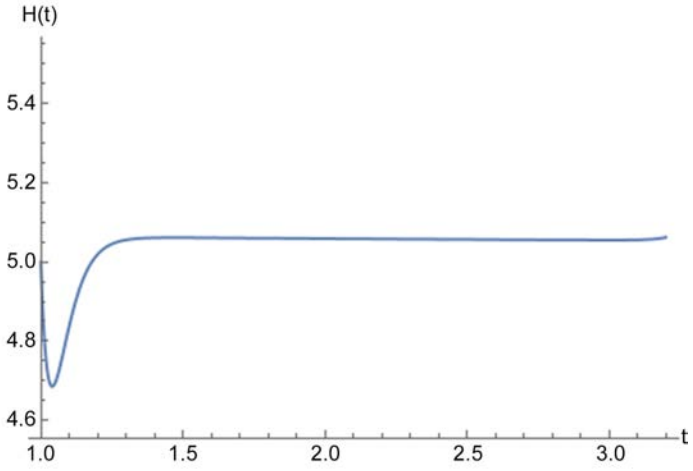


**Figure 3.** Hubble parameter $H(t)$.

## 5.1. Numerical Solution

We solve for dimensionless function variables $a, \rho_r$, in dimensionless relative time variable $x = \frac{tc}{R_H}$, limits $0 \le x \le x_{00} = 0.96$, where the upper limit is the relative cosmic time today $x_{00} = \frac{ct_0}{R_H} = \frac{R_0}{R_H} = 0.96$, from Planck data $t_0 = 13.9 \times 10^9$ y, with boundary conditions: $\rho_r(x_0) = \Omega_{m,0} + \Omega_{rad,0}$, $a(x_0) = 1$, $a'(x_0) = 1$ (because $H(x_0) = R_H$) from $a'(x_0) = 1$ follows $k_0 = -0.0042$ which is compatible with Planck data

$$(a')^2 + k_0 - \frac{\Lambda_1}{3}a^2 - \rho_r a^2 = 0 \quad \text{sF1} \tag{3a}$$

$$a''a - \frac{1}{3}\Lambda_1 a^2 = -\frac{a^2 \rho_{crH}}{2}\left(P_r + \frac{\rho_r}{3}\right) \quad \text{sF2} \tag{3b}$$

$$a''a + 2(a')^2 + 2k - \Lambda_1 a^2 + \frac{\rho_{crH}}{2}(P_r - \rho_r)a^2 = 0 \quad \text{sF3} \tag{3c}$$

$$\frac{\rho_r' a}{3} + a'(P_r + \rho_r) = 0 \quad \text{sF4} \tag{3d}$$

The two independent (3c and 3d is derived) Equations (3a, 3d) are non-linear second-order differential equations quadratic in the variables $a, \rho_r$.

Alternatively, one can solve for function variables $a$, $E_{th} = k_B T$, the latter with thermal energy $E_{th} = k_B T$, photon density $\rho_\gamma = a_{SB0} E_{th}^4$, $P_\gamma(\rho_\gamma) = \frac{1}{3}\rho_\gamma$, matter density $\rho_{mat} = \rho_b + \rho_c = \frac{K_m a}{K_s + K_m a}\rho_r$, baryon density $\rho_b = \rho_{mat}\frac{\Omega_{b,0}}{\Omega_{b,0} + \Omega_{c,0}}$, cold-dark-matter (cdm) density $\rho_c = \rho_{mat}\frac{\Omega_{c,0}}{\Omega_{b,0} + \Omega_{c,0}}$

$$P_b(\rho_b, E_{th}) = \rho_b \frac{E_{th}}{m_p c^2}.$$

The additional equation for pressure is the equation-of-state (eos) for the pressure $P_r$: $P_r = P(a, \rho_r)$.

**Solution 1**

One solves numerically [9] [13] [19] (3ac) with boundary conditions $a(x_0)=1$, $a'(x_0)=1$ as algebraic-differential equations for function variables *a*, $E_{th} = k_B T$. The solution exists until $x_{1c} = 0.14$, where numerical integration stops converging.

**Solution 2**

One solves numerically [9] [13] [19] (3ad) with boundary conditions $a(x_0)=1$, $a'(x_0)=1$ as differential equations for function variables $a, \rho_r$. The solution exists until $x_{1c} = 0.0196$, where numerical integration stops converging.

Plot *a*(*x*) is shown below [13] in **Figure 4**.

The solution limit $x_{1c} = 0.0196$ indicates the transition from matter-dominated to the radiation-dominated regime, which happens approximately at photon decoupling time $t_{re} = 370$ ky, $x_{re} = 0.000026$. For $x \le x_{1c}$ solution is continued by pure radiation density ([13]).

**Solution 3**

One solves numerically [13] (3a) with boundary conditions $a(x_0)=1$, $a'(x_0)=1$ as differential equation for function variable *a*, with ansatz for $\rho_r = \frac{K_s}{a^4} + \frac{K_m}{a^3}$. This is the usual solution method for background functions, used in CAMB [20] and in CMBquick ([21] [22]).

The solution exists until $x_{1c} = 0.0055$, where numerical integration stops converging, and the solution becomes complex (*i.e.* $\mathrm{Im}(a) \neq 0$).

Plot *a*(*x*) is shown below [13] in **Figure 5**.

The solution limit $x_{1c} = 0.0055$ indicates the transition from matter-dominated to the radiation-dominated regime, which happens approximately at photon decoupling time $t_{re} = 370$ ky, $x_{re} = 0.000026$. For $x \le x_{1c}$ solution is continued by pure radiation density ([13] [20] [22]).

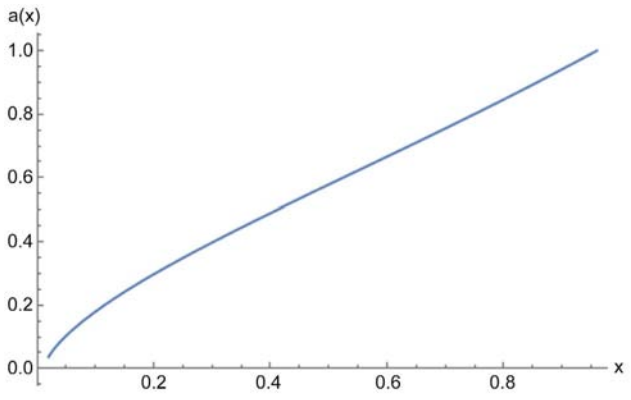


**Figure 4.** The scale factor *a(x)* in dependence of relative time $x = \frac{tc}{R_H}$, numerical solution 2.

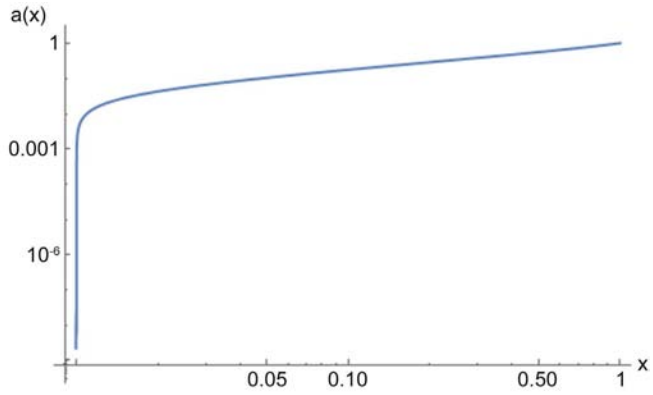


**Figure 5.** The scale factor *a(x)* in dependence of relative time $x = \frac{tc}{R_H}$, numerical solution 3.

## 5.2. Analytic Solution

The analytic solution scheme transforms the two basic equations into a parameterized integral $x(a)$, which is the inverted scale factor $a(x)$.

In order to calculate the thermal energy, we apply an iteration, we calculate the temperature $E_{th}(a)$ from $\rho_{rad} \equiv \rho_\gamma + \rho_\nu = \frac{K_s}{K_s + K_m a}\rho_r$, using the solution $a(x)$ in the next iteration: $E_{th}^{(n+1)} = E_{th}^{(n)}\left(a^{(n)}(x)\right)$, as shown in the schematic in chap. 11.

The zero iteration is the "naive" thermal energy $E_{th}^{(0)} = E_{th,0}/a$.

The variables are scale factor and density $a, \rho_r$.

The boundary conditions are $\rho_r(x_0) = \Omega_{m,0} + \Omega_{rad,0}$, $a(x_0) = 1$, $a'(x_0) = 1$, from $a'(x_0) = 1$ follows $k = -0.0042$ which is compatible with Planck data

$$(a')^2 + k_0 - \frac{\Lambda_1}{3}a^2 - \rho_r a^2 = 0 \quad \text{sF1} \tag{3a}$$

$$\frac{\rho_r' a}{3} + a'(P_r + \rho_r) = 0 \quad \text{sF4} \tag{3d}$$

The two Equations (3ad) are non-linear first-order differential equations quadratic in the variables $a, \rho_r$.

The third equation is the equation-of-state (eos) for the pressure $P_r$: $P_r = P(a, \rho_r)$.

The density and pressure have the form: relative energy density $\rho_r = \rho_b + \rho_\gamma + \rho_c + \rho_e + \rho_\nu$ for baryons, photons, dark matter, free electrons, neutrinos, relative pressure $P_r = P_b + P_\gamma + P_c + P_e + P_\nu$, where radiation pressure $P_{rad} = P_\gamma + P_\nu = \frac{\rho_\gamma + \rho_\nu}{3}$, and matter pressure (neglecting electrons) is the baryon ideal gas pressure $P_{mat} = P_b = \rho_b \frac{k_B T}{m_b c^2}$, for under-nuclear temperature $k_B T \ll m_b c^2 = 0.94\,\text{GeV}$ the baryon matter is dust-like, *i.e.* pressure is almost zero.

The densities have the form

$$\rho_r = \rho_{mat} + \rho_{rad}$$

$$\rho_{mat} = \rho_b + \rho_c = \frac{K_m a}{K_s + K_m a}\rho_r, \quad \rho_{rad} = \rho_\gamma + \rho_\nu = \frac{K_s}{K_s + K_m a}\rho_r$$

$$\rho_c = \rho_{mat}\frac{\Omega_{c,0}}{\Omega_{b,0} + \Omega_{c,0}}, \quad \rho_b = \rho_{mat}\frac{\Omega_{b,0}}{\Omega_{b,0} + \Omega_{c,0}}$$

$$\rho_\gamma = a_{SB0}E_{th}^4, \quad \rho_\nu = \frac{\Omega_{\nu,0}}{a^3}$$

We calculate the temperature $E_{th}(a)$ from $\rho_{rad} \equiv \rho_\gamma + \rho_\nu = \frac{K_s}{K_s + K_m a}\rho_r$ (12a)

$$i.e. \quad E_{th}(a) = \frac{1}{a_{SB0}^{1/4}}\left(\frac{K_s}{K_s + K_m a}\rho_r(a) - \frac{\Omega_{\nu,0}}{a^3}\right)^{1/4} \tag{12a1}$$

and all the pressure becomes a function of $a$,

$$P_r(a, \rho_r) = P_{rad} + P_{mat} = \left(\frac{K_s}{K_s + K_m a} + \frac{K_m a}{K_s + K_m a}\frac{\Omega_{b,0}}{\Omega_{b,0} + \Omega_{c,0}}\frac{E_{th}(a)}{m_b c^2}\right)\rho_r \tag{12b}$$

$$i.e. \quad \frac{P_r}{\rho_r} = P_\rho(a) = \left(\frac{K_s}{K_s + K_m a} + \frac{K_m a}{K_s + K_m a}\frac{\Omega_{b,0}}{\Omega_{b,0} + \Omega_{c,0}}\frac{E_{th}(a)}{m_b c^2}\right)$$

then we can integrate (3d) in $a$:

$$\log(\rho_r(a)) = \frac{\rho_r' a}{3} + a'(P_r + \rho_r) = -\int_0^a da\left(\frac{3 + P_\rho(a)}{a}\right) + c_1 \tag{12c}$$

and then can integrate (3a) in $a$:

$$x(a) = \int_0^a da\, a\sqrt{\frac{\Lambda_1}{3} + \rho_r(a) - \frac{k_0}{a^2}} + c_2, \tag{12d}$$

where $c_1$ and $c_2$ are set to fulfill the boundary conditions

$$\rho_r(x_0) = \Omega_{m,0} + \Omega_{rad,0}, \quad a(x_0) = 1, \quad \Omega = \frac{\rho}{\rho_{crit,0}}$$

### 5.3. Background Results

Results for density and relative time in dependence of scale factor $\rho_r(a)$, $x(a)$, are shown below [13].

Relative density in $\rho_{crit,0}$ units is shown over scale factor $a$, in double-logarithmic plot **Figure 6**.

There is a **critical point** $a_T \approx 0.5\times 10^{-4}$, where the density changes its behavior, it coincides roughly with the critical point in temperature. The corresponding time is $x_T \approx 10^{-8}$, thermal energy $E_{th} \approx 1\,\text{eV}$.

The analytic solution yields directly the inverse scale factor function $x(a)$, it shown in **Figure 7**.

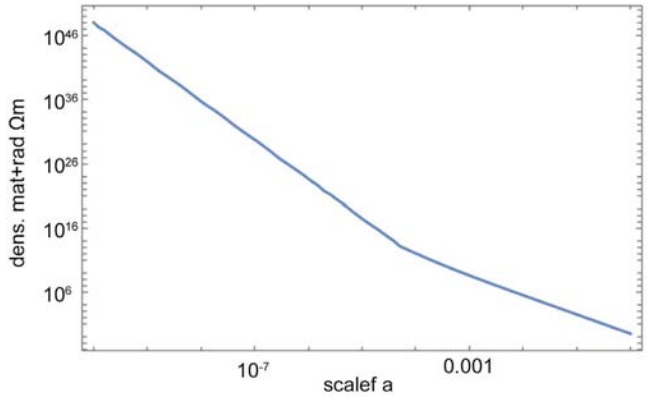


**Figure 6.** The density $\rho_r(a)$ in dependence of scale factor *a*, analytic solution.

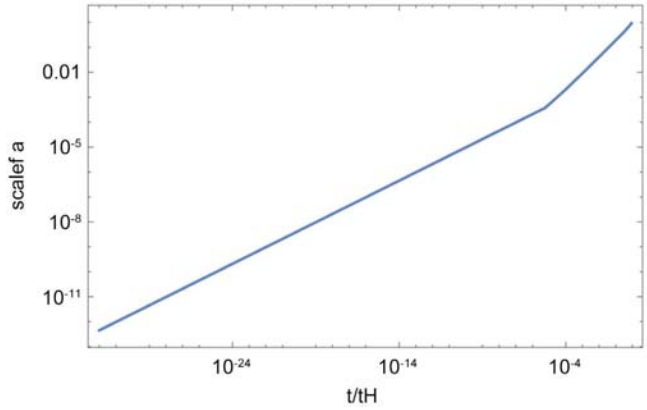


**Figure 7.** Relative time $x = \frac{tc}{R_H}$ and scale factor *a*, analytic solution.

There is a **critical point at photon decoupling**, $a_{dec} = 0.9 \times 10^{-3}$, $x_{dec} = 0.3 \times 10^{-4} \triangleq 370$ ky, redshift $z_{dec} = 1090$, thermal energy $E_{th} = 0.25$ eV.

The scale factor changes its power-law dependence on time:

$$a(x) \cong \begin{cases} x, & x > x_{dec} \\ x^{1/2}, & x < x_{dec} \end{cases}$$

It is useful to compare the result for $x(a)$ from the analytical solution and the standard CAMB solution ([13] [20]) **Figure 8**. The two curves separate roughly at $a_{dec} = 0.9 \times 10^{-3}$, the CAMB curve continues approximately linearly, whereas in the analytical solution time decreases quadratically, $x(a) \cong a^2$.

The plots of density $\rho_r(a)$ (blue) and radiation density $\rho_{rad}(a)$ are shown in comparison below ([13]) in **Figure 9**. As expected, we have radiation dominance roughly for $a < a_{dec}$, and matter dominance for $a > a_{dec}$.

The Hubble parameter is approximately linear in *x*, as it should be. However, there is a small deviation at critical point $x_{cH} \approx 10^{-8}$, scale factor $a_{cH} \approx 0.5 \times 10^{-4}$, redshift $z_{cH} \approx 1/a \approx 20000$.

This is apparently responsible for the small correction of the present Hubble

constant $H_0$, compared to CAMB solution.

The plot of the Hubble parameter is shown in Figure 10.

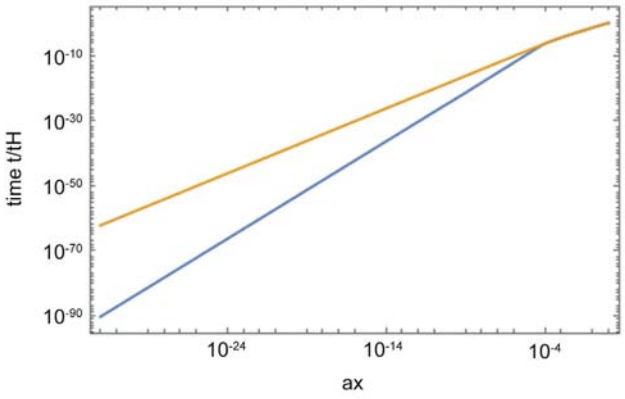


**Figure 8.** Relative time $x=\frac{tc}{R_H}$ in dependence of scale factor *a*, analytic solution (blue), CAMB-solution (orange).

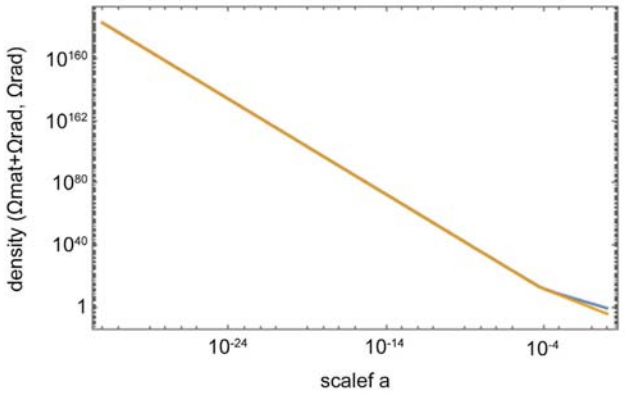


**Figure 9.** The density $\rho_r(a)$ (blue) and radiation density $\rho_{rad}(a)$ (orange), in dependence of scale factor *a*, analytic solution.

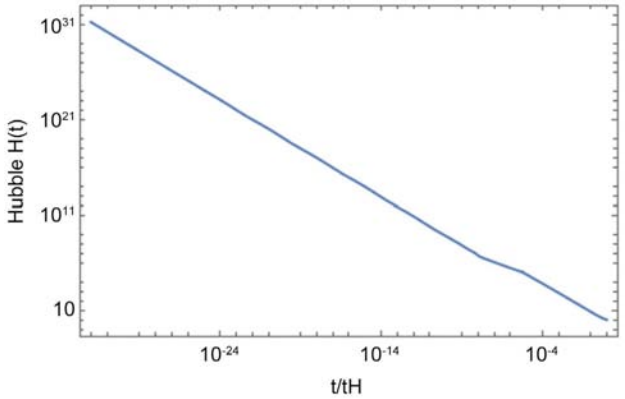


**Figure 10.** The Hubble parameter $H(x)$, in dependence of relative time $x=\frac{tc}{R_H}$, analytic solution.

The "naive" temperature $E_{th}^{(0)}(a)$ from (12a) is compared to the iterated temperature $E_{th}^{(1)}(a)$ calculated from the first analytic solution in (12a1) is shown in **Figure 11**. The point of deviation is $a_T \approx 0.5\times 10^{-4}$, the corresponding time is $x_T \approx 10^{-8}$, thermal energy $E_{th} \approx 1\,\text{eV}$. This point coincides roughly with the critical point in density **Figure 6**.

**Hubble parameter**

**Baryon pressure correction**

Baryon pressure correction yields $t_{0c} = t_0/1.043t_0$, so $H_{0c} = 1.043H_0$, the corrected Planck-value is $H_{0Pc} = H_{0P} \times 1.043 = 70.6 \pm 0.4$;

$H_{0R} = 69.8 \pm 1.7$ Red-Giants Freedmann 09/21;

$H_{0S} = 73.04 \pm 1.04$ Cepheids-SNIa SHOES 12/21;

$H_{0P} = 67.66 \pm 0.42$ Planck 07/18.

$H_{0R}$ Red-Giants is in agreement with corrected Planck within error margin.

**Assessed correction of the Cepheids-SNIa-measurement**

Cepheids-SNIa-measurement based on time-brightness calibration for small redshift *z*, peak power $P_{\max} \sim T(t_{cr}) \sim \bar{m}_b$, with average nucleus mass $\bar{m}_b$ percentage of higher-mass nuclei at present: $r(O) = 1.04\%$, $r(C) = 0.46\%$, so $\frac{P_{\max}(z \gg 1)}{P_{\max}(z \ll 1)} \approx (1 + r(O) + r(C)) = 1.015$ so z-corrected Cepheids-SNIa becomes 73.04/1.015 = 72. $H_{0Sc} = H_{0S}/1.015 = 72. \pm 1.$, which is at error margin.

## 6. Relativistic Perturbations and the Perturbed Lambda-CDM Model

The Lambda-CDM model is locally homogeneous, but during inflation the quantum fluctuations are "blown-up", and the universe becomes inhomogeneous on small (galactic) scales and remains homogeneous on large scales. These local inhomogeneities generate structure, which we observe today.

In order to reproduce these local inhomogeneities in the *perturbed Lambda-CDM model*, we introduce small perturbations in the metric and in the density distribution. These perturbations are functions of conformal time $\eta$ (defined by $\mathrm{d}\eta = \frac{\mathrm{d}t}{a}$), and space location vector $x^i$, and are not random variables. The randomness is introduced by initial conditions for perturbations (see chap. 8).

We introduce metric perturbations $A, B_i, E_{ij}$ in the RW-metric [2] [3] [4]

$$\mathrm{d}s^2 = a^2(\eta)\left(-(1+2A)\mathrm{d}\eta^2 + 2B_i \mathrm{d}x^i \mathrm{d}\eta + (\delta_{ij} + 2E_{ij})\mathrm{d}x^i \mathrm{d}x^j\right) \tag{13}$$

and split-up in scalar, vector, tensor parts:

scalar $A$

$B_i = \partial_i B + \hat{B}_i$, scalar $B$, vector $\hat{B}_i$

$E_{ij} = C\delta_{ij} + \partial_i\partial_j E + \left(\partial_i \hat{E}_j - \partial_j \hat{E}_i\right) + \hat{E}_{ij}$, scalar $C$ $E$, vector $\hat{E}_i$, tensor $\hat{E}_{ij}$, where $\sum_i E_i^i = 3C$

Furthermore, we form the **gauge-invariant Bardeen variables** with 8 = 1scalar ($A$) + 3vector ($B_i$) + 4tensor ($E_{ij}$) degrees-of-freedom (dof's)

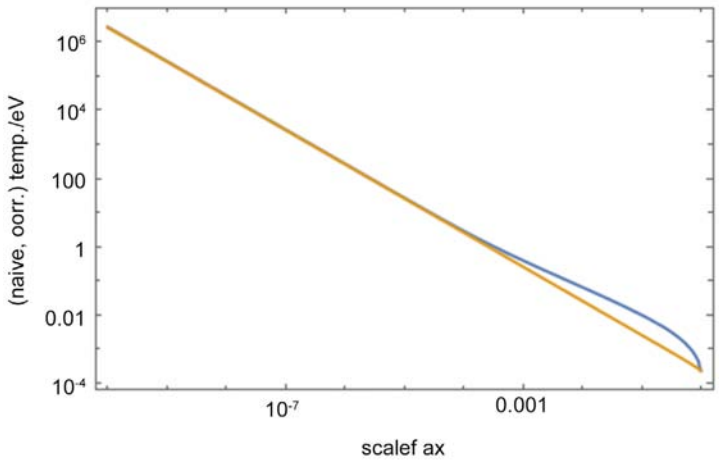


**Figure 11.** The naive temperature $E_{th}^{(0)}(a)$ compared to the iterated temperature $E_{th}^{(1)}(a)$, in dependence of scale factor *a*, analytic solution.

$$\Psi = A + H(B - E') + (B - E')', \quad \Phi = -C + \frac{1}{3}\nabla^2 E - H(B - E'),$$

$$\hat{\Phi}_i = \hat{B}_i - \hat{E}_i', \quad \hat{E}_{ij}$$

Since we have 6 Einstein equations, we can remove the 8 − 6 = 2 dof's by **gauge-fixing**.

- Newtonian gauge $B = E = 0$

$$ds^2 = a^2(\eta)\left(-(1+2\Psi)d\eta^2 + (1-2\Phi)\delta_{ij}dx^i dx^j\right)$$

$$A = \Psi, \quad C = -\Phi \tag{6.30}$$

- Spatially flat gauge $C = E = 0$
- Synchronous gauge $A = B = 0$

From now on, **we use the Newtonian gauge**.

We get for the energy-density tensor

$$T_0^0 = -(\bar{\rho} + \delta\rho)$$

$$T_0^i = -(\bar{\rho} + \bar{P})v^i$$

$$T_j^i = -(\bar{P} + \delta P)\delta_j^i + \Pi_j^i, \quad \Pi_i^i = 0 \ \forall i \tag{14}$$

**The relativistic Euler** equation is

$$\left(\frac{\rho c^2}{\sqrt{1-(v/c)^2}} + p\right)\frac{1}{c^2\sqrt{1-(v/c)^2}}\frac{d}{dt}\left(\frac{v_i}{\sqrt{1-(v/c)^2}}\right) + \partial_i p + \frac{1}{c^2\sqrt{1-(v/c)^2}}\frac{dp}{dt}v_i = 0,$$

**The Euler equation** in the RW metric becomes

$$v_i' = -\left(H + \frac{\bar{P}'}{\bar{P} + \bar{\rho}}\right)v_i - \frac{1}{\bar{P} + \bar{\rho}}\left(\partial_i \delta P + \partial^j \Pi_{ij}\right) - \partial_i \Psi \tag{6.76}$$

where $\Pi_{ij}$ is the anisotropic stress with the decomposition

$$\Pi_{ij} = \partial_i\partial_j\Pi + \left(\partial_i\hat{\Pi}_j - \partial_j\hat{\Pi}_i\right) + \hat{\Pi}_{ij} \tag{6.39}$$

**Finally, we get 10 fundamental equations:**

**6 Einstein equations**

[4]

$$\nabla^2\Phi - 3H\left(\Phi' + H\Psi\right) = \pi G a^2 \delta\rho$$

$$\Phi' + H\Psi = \pi G a^2 \frac{a''}{a'H}$$

$$\partial_i\partial_j\left(\Phi - \Psi\right) = 8\pi G a^2 \Pi_{ij},\ i < j$$

$$\Phi'' + H\Psi' + 2H\Phi' + \frac{1}{3}\nabla^2\left(\Phi - \Psi\right) + \left(2H' + H^2\right)\Psi = \pi G a^2 \delta P \qquad (15a\text{-}d)$$

**4 conservation equations: continuity +Euler**

[4]

$$\delta' = -\left(1 + \frac{\bar{P}}{\bar{\rho}}\right)\left(\partial^i v_i - 3\Phi'\right) - 3H\left(\frac{\delta P}{\delta\rho} - \frac{\bar{P}}{\bar{\rho}}\right)\delta$$

$$v_i' = -\left(H + \frac{\bar{P}'}{\bar{P} + \bar{\rho}}\right)v_i - \frac{1}{\bar{P} + \bar{\rho}}\left(\partial_i\delta P + \partial^j\Pi_{ij}\right) - \partial_i\Psi \qquad (15ef)$$

$q^i = \left(\bar{\rho} + \bar{P}\right)v^i$, $\delta = \frac{\delta\rho}{\bar{\rho}}$ decelaration conformal $q = -\frac{a''}{a'\mathcal{H}}$, $T_i^0 = \partial_i q$,

for **10 variables** 4 scalar $\Phi, \Psi, \delta, \delta P$, 3 vector $v^i$, 3 tensor $\Pi_j^i$;

**initial conditions** 6

$\Phi$ 2c, $\Psi$ 1c, $v^i$ 3c, $\left(\delta, \delta P\right)$ 0c;

**background parameters**

$$\mathcal{H} = \frac{a'}{a},\ q = -\frac{a''}{a'\mathcal{H}},\ a,\ \bar{\rho},\ \bar{P}.$$

**Fundamental equations in k-space ([14] Ma)**

In the following, we transform the fundamental equations via Fourier-transform into k-space.

We use Newtonian gauge, conformal time $\eta$, $a' = \frac{\mathrm{d}a}{\mathrm{d}\eta}$, the metric in Newtonian gauge reduces to

$$\mathrm{d}s^2 = a(\eta)\left(-\left(1 + 2\Psi\right)\mathrm{d}\eta^2 + \left(1 - 2\Phi\right)\mathrm{d}x^i\mathrm{d}x_i\right)$$

We get 4 Einstein equations in k-space

$$k^2\Phi - 3H\left(\Phi' + H\Psi\right) = \pi G a^2 \delta\rho$$

$$k^2\left(\Phi' + H\Psi\right) = \pi G a^2\left(\bar{P} + \bar{\rho}\right)\theta$$

$$k^2\left(\Phi - \Psi\right) = 12\pi G a^2\left(\bar{P} + \bar{\rho}\right)\sigma$$

$$\Phi'' + H\left(\Psi' + 2\Phi'\right) + \frac{1}{3}k^2\left(\Phi - \Psi\right) + \left(2H' + H^2\right)\Psi = 4\pi G a^2 \delta P \qquad (16a\text{-}d)$$

and 2 continuity-Euler equs in k-space

$$\delta' = -\left(1 + \frac{\bar{P}}{\bar{\rho}}\right)\left(\theta - 3\Phi'\right) - 3H\left(\frac{\delta P}{\bar{\rho}\delta} - \frac{\bar{P}}{\bar{\rho}}\right)\delta \quad \text{density equ}$$

$$\theta' = -\left(H + \frac{\bar{P}'}{\bar{P}+\bar{\rho}}\right)\theta - \frac{\delta P}{\bar{P}+\bar{\rho}}k^2 - k^2\sigma + k^2\Psi \quad \text{velocity equ} \qquad (16ef)$$

with the definitions

$$\delta = \frac{\delta\rho}{\bar{\rho}}, \quad \theta = ik^j v^j, \quad \sigma = -\frac{\left(\hat{k}_i\hat{k}_j - \frac{\delta_{ij}}{3}\right)\Pi_{ij}}{\bar{P}+\bar{\rho}},$$

where $\hat{k} = \frac{\vec{k}}{k}$ is the k-unit-vector, $\Pi^i_j$ anisotropic stress

and the relations

$$T^0_0 = -(\bar{\rho}+\delta\rho), \quad T^0_i = (\bar{\rho}+\bar{P})v_i, \quad T^i_j = (\bar{P}+\delta P)\delta^i_j + \Pi^i_j, \quad \delta = \frac{\delta\rho}{\bar{\rho}} = -\frac{T^0_0}{\bar{\rho}}$$

$$\Pi^i_i = 0, i = 1,2,3, \quad \Pi^i_j \equiv T^i_j - T^k_k\delta^i_j$$

$$\theta = ik^j v_j, \quad (\bar{\rho}+\bar{P})\theta = ik^j\delta T^0_j, \quad (\bar{\rho}+\bar{P})\sigma = -\left(\hat{k}^i\hat{k}^j - \frac{1}{3}\delta_{ij}\right)\Pi^i_j.$$

We have here 6 variables $\Phi, \Psi, \theta, \sigma, \delta, \delta P$, $\delta P = \delta T^i_i$, $\delta\rho = \delta T^0_0$, which are functions of $(k,\eta)$.

## 7. Evolution of Distribution Momenta

We introduce here density distribution momenta for density components radiation $\gamma$, neutrinos $\nu$, electrons *e*, baryons *b*, cold-dark-matter *d*. The densities acquire their random nature from random initial conditions, and have therefore a (Gaussian) probability distribution. These distribution momenta are used in the calculation of CMB spectrum in chap. 10.

**Evolution of distribution function momenta (Ma [14])**

We have for Newtonian gauge, conformal time $\eta$, $a' = \frac{da}{d\eta}$

$$ds^2 = a(\eta)\left(-(1+2\Psi)d\eta^2 + (1-2\Phi)dx^i dx_i\right).$$

**Phase space distribution**

With phase space element $dx^1dx^2dx^3dP_1dP_2dP_3$

$dN = f\left(x^i, P_j, \eta\right)dx^1dx^2dx^3dP_1dP_2dP_3$ particle number in element (32)

$P_i = a(1-\Phi)p_i$ co-moving disturbed momentum

density distribution for matter fermions (Fermi-Dirac distribution +), density distribution for radiation bosons (Bose-Einstein distribution -)

$$f_0(\varepsilon, T) = \frac{g_s}{h^3}\frac{1}{\exp\left(\frac{\varepsilon}{k_B T}\right)\pm 1} \qquad (17)$$

energy $\varepsilon = a\sqrt{p^2+m^2} = \sqrt{P^2+a^2m^2}$, temperature $T$, today temperature $T_0$.

We change variables: $x^iP_j$ to $x^iq_j$, and get the expressions:

scaled momentum $q_j = ap_j = qn_j$, unit momentum vector $\hat{n}$ with $n^in_i = 1$

energy $\varepsilon = \sqrt{q^2+a^2m^2}$;

change distribution $f\left(x^i,P_j,\eta\right)$ to $f\left(x^i,q,n_j,\eta\right)$.

Finally we get for the neutrino distribution perturbation function $\psi\left(x^i,q,n_j,\eta\right)$ (not equal to the metric perturbation $\Psi$)

$$f\left(x^i,P_j,\eta\right)=f_0\left(\varepsilon,T\right)\left(1+\psi\left(x^i,q,n_j,\eta\right)\right) \quad (35)$$

for the distribution of energy tensor

$$T_0^0=a^{-4}\int \mathrm{d}q\mathrm{d}\Omega\, q^2\varepsilon f_0\left(\varepsilon,T\right)\left(1+\psi\right)$$

$$T_i^0=a^{-4}\int \mathrm{d}q\mathrm{d}\Omega\, qn_i f_0\left(\varepsilon,T\right)\left(1+\psi\right)$$

$$T_j^i=a^{-4}\int \mathrm{d}q\mathrm{d}\Omega\frac{n_in_jq^2}{\varepsilon} f_0\left(\varepsilon,T\right)\left(1+\psi\right)$$

Boltzmann equation in $\left(x^i,q,n_j,\eta\right)$, with collision term $\frac{\partial f_C}{\partial\eta}$ becomes

$$\frac{Df}{d\eta}=\frac{\partial f}{\partial\eta}+\frac{\partial x^i}{\partial\eta}\frac{\partial f}{\partial x^i}+\frac{\partial q}{\partial\eta}\frac{\partial f}{\partial q}+\frac{\partial n_i}{\partial\eta}\frac{\partial f}{\partial n_i}=\frac{\partial f_C}{\partial\eta}$$

GR geodesic equation $P^0\frac{\mathrm{d}P^\mu}{\mathrm{d}\eta}+\Gamma^\mu_{\alpha\beta}P^\alpha P^\beta=0$ gives

$$\frac{\mathrm{d}q}{\mathrm{d}\eta}=q\dot{\Phi}-\varepsilon\left(q,\eta\right)n_i\partial_i\Psi \quad (39)$$

and **Boltzmann equation** becomes

$$\frac{\partial\psi}{\partial\eta}+i\frac{q}{\varepsilon}\left(\vec{k}\cdot\hat{n}\right)\psi+\frac{\mathrm{d}\ln f_0}{\mathrm{d}\ln q}\left(\dot{\Phi}-i\frac{\varepsilon}{q}\left(\vec{k}\cdot\hat{n}\right)\Psi\right)=\frac{1}{f_0}\frac{\partial f_C}{\partial\eta} \quad (18)$$

with **fluid equations cdm**

$$\delta_c'=-\theta_c+3\Phi',\quad \theta_c'=-\frac{a'}{a}\theta_c+k^2\Psi \quad (19a)$$

**Component evolution equations**

In the following we present the evolution equations for *l*-momenta in *k*-space for important components.

**Evolution equations massive neutrinos**

We have for (average) background density, pressure

$$\bar{\rho}_h=a^{-4}\int \mathrm{d}q\mathrm{d}\Omega\, q^2\varepsilon f_0\left(\varepsilon,T\right),\quad \bar{P}_h=\frac{1}{3}a^{-4}\int \mathrm{d}q\mathrm{d}\Omega\, q^2\frac{q^2}{\varepsilon} f_0\left(\varepsilon,T\right)$$

the perturbations

$$\delta\rho_h=a^{-4}\int \mathrm{d}q\mathrm{d}\Omega\, q^2\varepsilon f_0\left(\varepsilon,T\right)\psi,\quad \delta P_h=\frac{1}{3}a^{-4}\int \mathrm{d}q\mathrm{d}\Omega\, q^2\frac{q^2}{\varepsilon} f_0\left(\varepsilon,T\right)\psi$$

$$\delta T_h{}^0{}_i=a^{-4}\int \mathrm{d}q\mathrm{d}\Omega\, qn_i f_0\left(\varepsilon,T\right)\psi,$$

$$\delta\Pi_h{}^0{}_i=\frac{1}{3}a^{-4}\int \mathrm{d}q\mathrm{d}\Omega\, q^2\frac{q^2}{\varepsilon}\left(n_in_j-\frac{1}{3}\delta_{ij}\right) f_0\left(\varepsilon,T\right)\psi$$

distribution perturbation function are developed in Legendre polynomials of the angle $\left(\hat{k}\cdot\hat{n}\right)$

$$\psi\left(\vec{k},\hat{n},q,\eta\right)=\sum_{l=0}^{\infty}\left(-i\right)^l\left(2l+1\right)\psi_l\left(\vec{k},q,\eta\right)P_l\left(\hat{k}\cdot\hat{n}\right) \quad (54)$$

$$\delta\rho_h = 4\pi a^{-4}\int \mathrm{d}q\, q^2 \varepsilon\, f_0(\varepsilon,T)\psi_0\,,\quad \delta P_h = \frac{4\pi}{3}a^{-4}\int \mathrm{d}q\, q^2 \frac{q^2}{\varepsilon}\, f_0(\varepsilon,T)\psi_0$$

$$\left(\bar{\rho}_h + \bar{P}_h\right)\theta_h = 4\pi k a^{-4}\int \mathrm{d}q\, q^3 f_0(\varepsilon,T)\psi_1\,,$$

$$\left(\bar{\rho}_h + \bar{P}_h\right)\sigma_h = \frac{4\pi}{3}a^{-4}\int \mathrm{d}q\, q^2 \frac{q^2}{\varepsilon}\, f_0(\varepsilon,T)\psi_0\,.$$

Boltzmann equation yields for evolution of perturbation momenta

$$\psi_0' = -\frac{qk}{\varepsilon}\psi_1 - \Phi'\frac{\mathrm{d}\ln f_0}{\mathrm{d}\ln q},\quad \psi_1' = \frac{qk}{3\varepsilon}\left(\psi_0 - 2\psi_2\right) - \frac{\varepsilon k}{3q}\Psi\frac{\mathrm{d}\ln f_0}{\mathrm{d}\ln q}$$

$$\psi_l' = \frac{qk}{(2l+1)\varepsilon}\left(l\psi_{l-1} - (l+1)\psi_{l+1}\right),\quad l \geq 2 \tag{19b}$$

truncating order $l_{\max}$

$$\psi_{l_{\max}+1} = \frac{(2l_{\max}+1)\varepsilon}{qk\eta}\psi_{l_{\max}} - \psi_{l_{\max}-1}\,.$$

**Evolution equations photons**

We assume $\gamma - e$ Thomson scattering with the Thomson cross-section

$$\frac{\mathrm{d}\sigma}{\mathrm{d}\Omega} = 3\sigma_T\frac{1+\cos^2\theta}{16\pi},\quad \sigma_T = 0.665\times 10^{-24}\ \mathrm{cm}^2$$

with $F_\gamma(k,\hat{n},\eta)$ distribution total intensity

with $G_\gamma(k,\vec{n},\eta)$ distribution difference polarization components

with collision terms

$$\left(\frac{\partial F_\gamma}{\partial\eta}\right)_C = an_e\sigma_T\left(-F_\gamma + F_{\gamma 0} + 4\left(\hat{n}\cdot\vec{v}_e\right) - \left(F_{\gamma 2} + G_{\gamma 0} + G_{\gamma 2}\right)P_2\right)$$

$$\left(\frac{\partial G_\gamma}{\partial\eta}\right)_C = an_e\sigma_T\left(-G_\gamma + \frac{1}{2}\left(F_{\gamma 2} + G_{\gamma 0} + G_{\gamma 2}\right)\left(1 - P_2\right)\right)$$

with expansion

$$\left(\frac{\partial F_\gamma}{\partial\eta}\right)_C = an_e\sigma_T\left(\frac{4i}{k}\left(\theta_\gamma - \theta_b\right)P_1 + \left(9\sigma_\gamma - \frac{1}{2}G_{\gamma 0} - \frac{1}{2}G_{\gamma 2}\right)P_2 - \sum_{l=3}^{\infty}(-i)^l(2l+1)F_{\gamma l}P_l\right)$$

$$\left(\frac{\partial G_\gamma}{\partial\eta}\right)_C = an_e\sigma_T\left(\frac{1}{2}\left(F_{\gamma 2} + G_{\gamma 0} + G_{\gamma 2}\right)\left(1 - P\right)_2 - \sum_{l=0}^{\infty}(-i)^l(2l+1)G_{\gamma l}P_l\right).$$

Resulting fluid equations are then

$$\delta_\gamma' = -\frac{4}{3}\theta_\gamma + 4\Phi',\quad \theta_\gamma' = k^2\left(\frac{1}{4}\delta_\gamma - \sigma_\gamma\right) + k^2\Psi + an_e\sigma_T\left(\theta_b - \theta_\gamma\right) \tag{19c1}$$

and momenta evolution becomes

$$F_{\gamma 2}' = 2\sigma_\gamma' = \frac{8}{15}\theta_\gamma - \frac{3}{5}kF_{\gamma 3} - \frac{9}{5}an_e\sigma_T\sigma_\gamma\left(\theta_\gamma - \theta_b\right) + \frac{1}{10}an_e\sigma_T\left(\theta_\gamma - \theta_b\right)\left(G_{\gamma 0} + G_{\gamma 2}\right)$$

$$F_{\gamma l}' = \frac{k}{2l+1}\left(lF_{\gamma(l-1)} - (l+1)F_{\gamma(l+1)}\right) - an_e\sigma_T F_{\gamma l}, \quad l \geq 3 \tag{19c2}$$

$$\begin{aligned} G_{\gamma l}' = {} & \frac{k}{2l+1}\left(lG_{\gamma(l-1)} - (l+1)G_{\gamma(l+1)}\right) \\ & + an_e\sigma_T\left(-G_{\gamma l} + \frac{1}{2}\left(F_{\gamma 2} + G_{\gamma 0} + G_{\gamma 2}\right)\left(\delta_{l0} + \frac{\delta_{l2}}{5}\right)\right) \end{aligned} \tag{19c3}$$

**Evolution equations baryons**

We have the fluid equations

$$\delta_b' = -\theta_b + 3\Phi', \quad \theta_b' = -\frac{a'}{a}\theta_b + c_s^2 k^2\delta_b - \frac{4\bar{\rho}_\gamma}{3\bar{\rho}_b}an_e\sigma_T\left(\theta_b - \theta_\gamma\right) + k^2\Psi \tag{19d1}$$

with sound speed $c_s^2 = \frac{k_B T_b}{\mu}\left(1 - \frac{1}{3}\frac{\mathrm{d}\ln T_b}{\mathrm{d}\ln a}\right)$, $\mu$ mean baryon mass.

The temperature equation becomes

$$T_b' = -2\frac{a'}{a}T_b + \frac{8}{3}\frac{\mu}{m_e}\frac{\bar{\rho}_\gamma}{\bar{\rho}_b}an_e\sigma_T\left(T_\gamma - T_b\right)$$

Before recombination tight-coupling $\gamma - b$, we have

$$\theta_b - \theta_\gamma = \tau_c\left(\theta_\gamma' - k^2\left(\frac{1}{4}\delta_\gamma - \sigma_\gamma\right) - k^2\Psi\right) \tag{19d2}$$

$$\sigma_\gamma = \frac{\tau_c}{9}\left(\frac{8}{3}\theta_\gamma - 10\sigma_\gamma' - 3kF_{\gamma 3}\right) \tag{19d3}$$

$$\theta_\gamma' = -\frac{3}{4}\frac{\bar{\rho}_b}{\bar{\rho}_\gamma}\left(\theta_b' + \frac{a'}{a}\theta_b - c_s^2 k^2\delta_b\right) + k^2\left(\frac{1}{4}\delta_\gamma - \sigma_\gamma\right) + \left(1 + \frac{3}{4}\frac{\bar{\rho}_b}{\bar{\rho}_\gamma}\right)k^2\Psi \tag{19d4}$$

## 8. Initial Conditions

Initial conditions in k-space for density components (radiation $\gamma$, neutrinos $\nu$, electrons $e$, baryons $b$, cold-dark-matter $c$) and metric perturbations $\Psi, \Phi$ generate the random (Gaussian distributed) inhomogeneities required for structure formation.

**Initial conditions k-space**

For Newtonian gauge in conformal time $\eta$, initial conditions are chosen in such a way, that only the largest order in $k\eta$ is present (Ma [14])

$$\delta_\gamma = -\frac{40C}{3\left(\bar{P} + \bar{\rho}\right)} = -2\Psi$$

$$\delta_c = \delta_b = \frac{3}{4}\delta_\nu = \frac{3}{4}\delta_\gamma$$

$$\theta_\gamma = \theta_\nu = \theta_b = \theta_c = \frac{10C}{15 + 4R_\nu}\left(k^2\eta\right) = \frac{k^2\eta}{2}\Psi$$

$$\sigma_\nu = \frac{4C}{3\left(15 + 4R_\nu\right)}\left(k\eta\right)^2 = \frac{\left(k\eta\right)^2}{15}\Psi$$

$$\Psi = \frac{20C}{15+4R_\nu}, \quad \Phi = \left(1+\frac{2}{5}R_\nu\right)\Psi$$

with neutrino density ratio $R_\nu = \frac{\bar{\rho}_\nu}{\bar{\rho}_\gamma + \bar{\rho}_\nu}$

## 9. Structure Formation

In the following, we present in concise form cross sections, reaction rates and densities for important cosmological particle processes [2] [3] [4] [11] [23]. They are used in the background eos equations in chap. 2, and in the evolution equations of density distribution momenta in chap. 7.

**Cosmic neutrino background**

The reaction is $\nu_e + \bar{\nu}_e \leftrightarrow e^+ + e^-$, $e^- + \bar{\nu}_e \leftrightarrow e^- + \bar{\nu}_e$

with reaction rate $\Gamma = n\sigma v \approx G_F^2 T^5$, $G_F \approx 1.2\times 10^{-5}\,\mathrm{GeV}^{-2}$ (3.58)

and corresponding Hubbble rate $H \approx \frac{T^2}{M_{Pl}}$, $\frac{\Gamma}{H} \approx \left(\frac{T}{1\,\mathrm{MeV}}\right)^3$,

neutrinos decouple at $T_{\nu,d} = 1\,\mathrm{MeV}$, $t_{\nu,d} = 1\,\mathrm{s}$,

the number density $n_\nu \propto a^{-3}\int \mathrm{d}^3 q \frac{1}{\exp\left(\frac{q}{aT_\nu}+1\right)}$,

with $T_\nu \propto a^{-1}$ for $T_\nu > T_{\nu,d}$.

**Gamma pair production**

The gamma-pair production reaction is $\gamma + A \to e^+ + e^- + A$ [24] [25]

with the cross-section $\sigma = \alpha r_e^2 Z^2 P(E,Z)$, where $Z$ = atomic number of material $A$, $k = \frac{E_\gamma}{E_e}$, $\alpha$ fine-structure-constant, and

$$P(E,Z) \approx \frac{2\pi}{3}\left(\frac{|k-2|}{k}\right)^3, \quad 2 < k < 4,$$

$$P(E,Z) \approx \frac{28}{9}\ln(2k) - \frac{218}{27} = 3.11\ln\left(2\frac{E_\gamma}{E_e}\right) - 8.07, \quad k > 4,$$

wih reaction rate $\Gamma = n\sigma c$.

**Electron-positron annihilation**

The ep-annihilation reaction is $e^+ + e^- \to \gamma + \gamma$ shown in **Figure 12.**

wih the cross-section

$$\sigma_{e^+e^-}(\omega_0) = \left(1+\frac{\pi\alpha}{v}\right)\sigma_0(\beta) - \frac{2\alpha}{\pi}\left(-\frac{1+\beta^2}{2\beta}\log\left(\frac{1+\beta}{1-\beta}\right)-1\right)\log\left(\frac{\sqrt{s}}{2\omega_0}\right)\sigma_0(\beta) \quad [24]$$

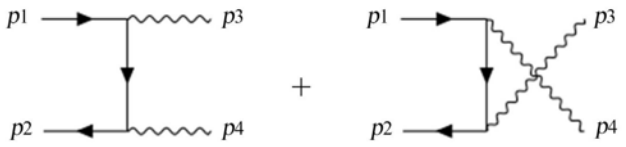


**Figure 12.** e-p annihilation.

where $\sigma_0(\beta)=\frac{\pi\alpha^2}{s\beta}\left(-\frac{3-\beta^4}{\beta}\log\left(\frac{1+\beta}{1-\beta}\right)-2\left(2-\beta^2\right)\right)$ Born cross-section, and Mandelstamm variables $s=(p_1+p_2)^2$, $t=(p_1-p_3)^2$, $u=(p_1-p_4)^2$, where

$$\beta=\sqrt{1-4\left(mc^2\right)^2/s}\,,\quad z=\frac{1+\beta}{1-\beta}$$

$\omega_0$ soft cut-off, $v=\frac{2\beta}{1+\beta^2}$ relative velocity, dof number

$$g_S=\begin{cases}2+\frac{7}{8}\times 4=\frac{11}{2} & T\geq m_e\\ 2 & T<m_e\end{cases}$$ with photons decoupling at $T_{e,d}=0.5\,\text{MeV}$,

$t_{e,d}=6\,\text{s}$, duration $\Delta t_{e,d}=\frac{\alpha^2}{m_e}=10^{-18}\,\text{s}$

$T_\nu=\left(\frac{4}{11}\right)^{1/3}T_\gamma$, $t>t_{e,d}$ after ep-annihilation, so $T_{\gamma,0}=2.73\,\text{K}$, $T_{\nu,0}=1.95\,\text{K}$.

Planck data yield $\sum_i m_{\nu i}<0.13\,\text{eV}$, $\Omega_\nu<0.003$.

**General photon eos**

For $T>T_{an}$ in pair-production regime, we have in equilibrium (relativistic)

$$\sigma_0(\beta)=\frac{2\pi\alpha^2}{s\beta},\quad \beta=\frac{v_e}{c}$$

$$\Gamma_{ee\gamma}=2n_{e+}v\sigma\approx 2n_{e+}\beta c\frac{2\pi\alpha^2\hbar^2c^2}{s\beta}\left(1+\frac{\pi\alpha}{\beta}\right)$$

$$\Gamma_{\gamma ee}=2n_\gamma c\sigma\approx 2n_\gamma c\alpha r_e^2Z_{ef}^2\left(3.1\ln\left(\frac{E_\gamma}{E_e}\right)-8.1\right)\ \text{with}\ Z_{ef}=1\frac{n_b}{n_\gamma},\ s=4E_{th}^2$$

$\Gamma_{ee\gamma}=\Gamma_{\gamma ee}$ results $n_\gamma=\frac{n_b^2}{n_{e+}}E_{th}^2\frac{r_e^2 3.1\ln\left(\frac{E_\gamma}{E_e}\right)}{4\pi\alpha\hbar^2c^2\left(1+\frac{\pi\alpha c}{v_e}\right)}$, *i.e.* $n_\gamma\sim\frac{n_b}{n_{e+}}n_bE_{th}^2\sim E_{th}^4$,

with thermal energy $E_{th}=k_BT$.

In the black-body regime we have the Stefan-Boltzmann relation $n_\gamma=a_{SB}E_{th}^4$.

The positron density $n_{e+}$ results from equality of both $n_\gamma$ from pair-production-annihilation and Stefan-Boltzmann

$$n_{e+}\approx\frac{n_b^2}{n_\gamma}0.17\alpha\left(\frac{E_{th}}{m_ec^2}\right)^2=\frac{n_b^2}{n_\gamma}\left(\frac{E_{th}}{m_ec^2}\right)^2 1.2\times10^{-3}.$$

**Thomson scattering ([26] Hu)**

We get density of free electrons

$n_e=\left(1-\frac{Y_p}{2}\right)X_en_b\approx\Omega_bh^2(1+z)^3\times10^{-5}\,\text{cm}^{-3}$, ionization fraction $X_e\approx1$,

where $Y_p\approx0.24$ Helium mass fraction.

The optical depth $\tau$ results from the Thomson equation $\frac{\mathrm{d}\tau}{\mathrm{d}\eta}=n_e\sigma_Ta$,

where $\sigma_T = \frac{8\pi\alpha^2}{3m_e^2} = 6.65\times10^{-25}\,\mathrm{cm}^2$ is the Thomson cross-section in photon-electron scattering.

**Photons and neutrinos**

After photon decoupling we have the relation for neutrino and photon temperature

$$T_\nu = \left(\frac{4}{11}\right)^{1/3} T_\gamma \tag{3.62}$$

**Hydrogen recombination** ([4], chap. 2)

For hydrogen recombination we have the reaction $e^- + p^+ \to H + \gamma$,

and number density $\left(\frac{n_H}{n_e^2}\right) = \left(\frac{2\pi}{m_e T}\right)^{3/2} \exp\left(\frac{E_{ion}}{T}\right)$,

with ionization energy $E_{ion} = m_p + m_e - m_H = 13.6\,\mathrm{eV}$, $E_{H,re} = 13.6\,\mathrm{eV}$

and free electron fraction $X_e \equiv \frac{n_e}{n_p + n_H} = \frac{n_e}{n_b}$.

The free electron fraction obeys Saha equation

$$\frac{1-X_e}{X_e^2} = \frac{2\zeta(3)}{\pi^2}\left(\frac{2\pi}{m_e T}\right)^{3/2} \eta \exp\left(\frac{E_{ion}}{T}\right) \quad (3.78) \quad \zeta(3) = 1.202$$

where $\frac{n_b}{n_\gamma} = \frac{n_{b,0}}{n_{\gamma,0}} = \frac{0.242\ \mathrm{m}^{-3}}{0.41\times10^9\ \mathrm{m}^{-3}} = 0.59\times10^{-9}$, and baryon-photon ratio $\eta \approx 6\times10^{-10}$.

The solution is $X_e = \frac{-1+\sqrt{1+4f(E_{th})}}{2f(E_{th})}$,

$$f(E_{th}) = 4\zeta(3)\sqrt{\frac{2}{\pi}}\eta\left(\frac{E_{th}}{m_e c^2}\right)^{3/2} \exp\left(\frac{E_{H,re}}{E_{th}}\right) = 2.26\times10^{-9}\left(\frac{E_{th}}{m_e c^2}\right)^{3/2} \exp\left(\frac{E_{H,re}}{E_{th}}\right),$$

with limits

$$f \gg 1,\ X_e \approx \frac{1}{\sqrt{f(E_{th})}},\ n_e = n_b,\ \frac{n_b}{n_H} \ll 1$$

$$f \ll 1,\ X_e \approx 1,\ n_e = n_b,\ n_H = 0,$$

and recombination temperature $T_{rec} \approx 0.32\,\mathrm{eV} = 3760\,\mathrm{K}$, $t_{rec} \approx 290\,\mathrm{ky}$.

**Photon decoupling**

The photon decoupling reaction is $e^- + \gamma \leftrightarrow e^- + \gamma$, with reaction rate $\Gamma_\gamma \approx n_e \sigma_T$, $\sigma_T \approx 2\times10^{-3}\,\mathrm{MeV}^{-2}$, and decoupling temperature

$$\Gamma_\gamma(T_{dec}) \approx H(T_{dec}),\quad X_e(T_{dec}) T_{dec}^{3/2} \approx \frac{\pi^2}{2\zeta(3)} \frac{H_0\sqrt{\Omega_m}}{\eta\sigma_T T_0^{3/2}},\quad T_{dec} \approx 0.25\,\mathrm{eV} = 2970\,\mathrm{K}$$

for $t_{dec} \approx 370\,\mathrm{ky}$.

The Boltzmann equation is $\frac{\partial f}{\partial t} + \frac{\vec{p}}{m}\nabla f + \vec{F}\cdot\frac{\partial f}{\partial \vec{p}} = C(f)$, for reaction

$1+2 \leftrightarrow 3+4$ collision term is $C_i\left[\left\{n_j\right\}\right]=-\alpha_c n_1 n_2+\alpha_c \beta_c n_3 n_4$, where $\alpha_c=\langle\sigma v\rangle$ thermally averaged cross-section, $\beta_c=\left(\frac{n_1 n_2}{n_3 n_4}\right)_{eq}$ detailed balanced coefficient.

From this follows **cosmic Boltzmann equation** with collision term

$$\frac{1}{a^3}\frac{\mathrm{d}\left(n_i a^3\right)}{\mathrm{d}t}=-\langle\sigma v\rangle\left(n_1 n_2-\beta_c n_3 n_4\right) \tag{3.96}$$

where the particle number is $N_i \equiv \frac{n_i}{s} \propto n_i a^3$, $\frac{\mathrm{d}(\log N_1)}{\mathrm{d}(\log a)}=-\frac{\Gamma_1}{H}\left(1-\left(\frac{N_1 N_2}{N_3 N_4}\right)_{eq}\frac{N_3 N_4}{N_1 N_2}\right)$, where $\Gamma_1 \equiv n_2\langle\sigma v\rangle$ (1,2) interaction rate.

**Dark matter cdm decoupling**

The reaction for cdm particle $X$, light particle $l$: $X+\bar{X} \leftrightarrow l+\bar{l}$ with Boltzmann equation $\frac{1}{a^3}\frac{\mathrm{d}\left(n_X a^3\right)}{\mathrm{d}t}=-\langle\sigma v\rangle\left(n_X^2-\left(n_X\right)_{eq}^2\right)$, with $Y_X \equiv \frac{n_X}{T^3}$ particles in co-moving volume, and reduced mass $x \equiv \frac{M_X}{T}$, $\frac{\mathrm{d}x}{\mathrm{d}t}=Hx$.

Using $\lambda \equiv \frac{\Gamma\left(M_X\right)}{H\left(M_X\right)}=\frac{M_X^3\langle\sigma v\rangle}{H\left(M_X\right)}$, we get the Riccati equation

$\frac{\mathrm{d}Y_X}{\mathrm{d}x}=-\frac{\lambda}{x^2}\left(Y_X^2-\left(Y_X\right)_{eq}^2\right)$.

The asympotic value is $Y_{X,\infty} \approx \frac{x_f}{\lambda}$ with $x_f$ reduced mass at freeze-out.

The cdm density is $\Omega_X \sim 0.1\frac{x_f}{\sqrt{g_s\left(M_X\right)}}\frac{10^{-8}\,\mathrm{GeV}^{-2}}{\langle\sigma v\rangle}$ with reaction rate $\sqrt{\langle\sigma v\rangle} \sim 10^{-8}\,\mathrm{GeV}^{-2} \sim 0.1\sqrt{G_F}$ (≈weak interaction).

**Baryo-genesis**

In the following we present important cosmological processes of nuclei, with density evolution equation, cross-section, and charasteristic (freeze-out) time.

**Neutron-proton decay**

The reaction here is $n+\nu_e \leftrightarrow p^+ + e^-$, $n+e^+ \leftrightarrow p^+ + \bar{\nu}_e$ with density ratio $\left(\frac{n_n}{n_p}\right)_{eq}=\exp\left(-\frac{E_{np}}{k_B T}\right)$, $E_{np}=\left(m_n-m_p\right)c^2=1.30\,\mathrm{MeV}$, and with $X_n \equiv \frac{n_n}{n_n+n_p}$ relative n-abundance.

For $X_n$ we get the equation

$$\frac{\mathrm{d}X_n}{\mathrm{d}t}=-\Gamma_n(x)\left(X_n-(1-X_n)\exp\left(-\frac{E_{np}}{k_B T}\right)\right)$$

where

$\Gamma_n(x)=\frac{255}{\tau_n}\frac{12+6x+x^2}{x^5}$, $x=\frac{E_{np}}{k_B T}$, $\tau_n=886.7\pm0.8\,\mathrm{s}$ neutron lifetime.

With freeze-out abundance $X_{n,\infty}=0.15$ it becomes $X_n(t)=X_{n,\infty}\exp\left(-\frac{t}{\tau_n}\right)$.

**Deuterium**

The density ratio is $\left(\frac{n_D}{n_p}\right)_{eq} = \frac{3}{4} n_{n,eq} \left(\frac{4\pi\hbar^2 c^2}{m_p c^2 k_B T}\right)^{3/2} \exp\left(\frac{E_{npD}}{k_B T}\right)$, with $E_{npD} = \left(m_n + m_p - m_D\right)c^2 = 2.22\ \text{MeV}$ and temperature $T_{nuc} = 0.06\ \text{MeV}$ at $\left(\frac{n_D}{n_p}\right)_{eq}\left(T = T_{nuc}\right) = 1$, the corresponding time is $t_{nuc} = \left(\frac{0.1\ \text{MeV}}{T_{nuc}}\right)^2 120\ \text{s} \approx 330\ \text{s}$.

**Helium**

The reactions are

$$D + p^+ \leftrightarrow He^3 + \gamma, \quad H^3 + p^+ \leftrightarrow He^3 + n$$

$$D + D \leftrightarrow H^3 + p^+, \quad H^3 + D \leftrightarrow He^4 + p^+$$

$$D + D \leftrightarrow He^3 + n, \quad He^3 + D \leftrightarrow He^4 + p^+$$

helium-hydrogen ratio is then

$Y_P = \frac{4n_{He}}{n_H} = \frac{4n_{He}}{n_p} \approx \frac{2X_n\left(t_{nuc}\right)}{1 - X_n\left(t_{nuc}\right)} \sim 0.25$, which is observed.

**Lithium beryllium**

The reactions are

$Be^7 + n \leftrightarrow Li^7 + p^+, \quad Li^7 + p^+ \leftrightarrow He^4 + He^4, \quad Be^7 + e^- \leftrightarrow Li^7 + \nu_e$

$He^3 + He^4 \leftrightarrow Be^7 + \gamma, \quad H^3 + He^4 \leftrightarrow Li^7 + \gamma$.

**Hydrogen recombination**

The process of hydrogen recombination is shown in Figure 13.

We have the Peebles equation for free electron density $X_e$ with an improved calculation in redshift $z$ [27]

$$\frac{\mathrm{d}X_e}{\mathrm{d}z} = -\frac{C_r(T)}{H(z)(1+z)}\left(\left(\frac{m_e c^2 k_B T}{2\pi}\right)^{1/2}\left(1 - X_e\right)\exp\left(-\frac{E_I}{k_B T}\right) - \alpha(T)\frac{n_b}{n_\gamma}\frac{2\zeta(3)}{\pi^2}\left(k_B T\right)^3 X_e^2\right) \tag{20}$$

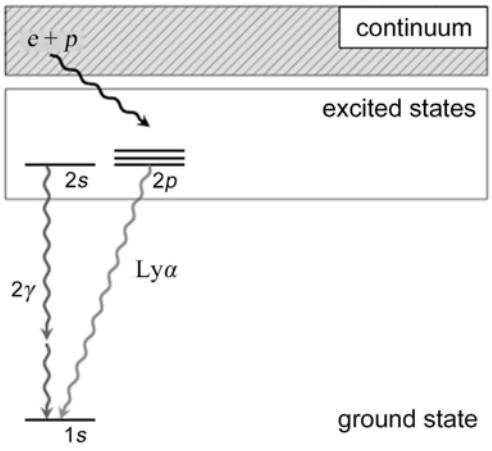


Figure 13. Hydrogen recombination state diagram [4].

with

$$C_r(T) \equiv \frac{\Lambda_{2\gamma} + \Lambda_\alpha}{\Lambda_{2\gamma} + \Lambda_\alpha + \beta_\alpha},$$

$$\Lambda_\alpha = \frac{27}{128\zeta(3)} \frac{H(T)}{(1-X_e)(n_b/n_\gamma)(k_B T/E_I)^3},$$

$$\Lambda_{2\gamma} = 8.227\ \mathrm{s}^{-1},$$

$\lambda_\alpha = \frac{8\pi\hbar c}{3E_I}$ Lyman wavelength, $\beta_\alpha = \beta(T)\exp\left(\frac{3E_I}{4k_B T}\right)$,

$$\alpha(T) \approx 9.8 \frac{\alpha^2}{(m_e c^2)^2} \left(\frac{E_I}{k_B T}\right)^{1/2} \log\left(\frac{E_I}{k_B T}\right),$$

$$H(z) = \sqrt{\Omega_m} H_0 (1+z)^{3/2} \left(1 + \frac{1+z}{1+z_{eq}}\right),$$

$H_0 \approx 1.5 \times 10^{-33}$ eV, $T = (1+z)0.235$ eV.

## 10. CMB Spectrum

In this chapter, we present first in concise way the contributions to the temperature anisotropy of the cosmic microwave background CMB.

Then we describe the scheme for the calculation of the CMB spectrum coefficients $C_l$.

The schematic of the calculation is shown in chap. 11.

Finally, we present the self-calculated results and a comparison with data.

### 10.1. CMB Spectrum Theory

**CMB spectrum today**

CMB as measured today has the parameters [28]:

temperature $T_{\gamma,0} = 2.7255 \pm 0.0006$ K.

CMB dipole is around 3.3621 ± 0.0010 mK

relative density $\Omega_\gamma = 6 \times 10^{-5}$

temperature anisotropy $\Delta T_{\gamma,0} \approx 30\ \mu\mathrm{K}$, so $\frac{\Delta T_{\gamma,0}}{T_{\gamma,0}} \approx \frac{30\ \mu\mathrm{K}}{2.72\ \mathrm{K}} = 1.1 \times 10^{-5}$.

**Temperature anisotropy**

The temperature anisotropy of the CMB has the following contributions:

$$\frac{\delta T}{\bar{T}}(\hat{n}) = \left(\mathrm{SW} = \left(\frac{1}{4}\delta_\gamma + \Psi\right)_*\right) + \left(\mathrm{Dop} = -(\hat{n}\cdot\vec{v}_b)_*\right) + \left(\mathrm{ISW} = \int_{\eta_*}^{\eta_0} \mathrm{d}\eta\left(\Phi' + \Psi'\right)\right) \quad (7.29)$$

at conformal time $\eta = \eta_* = \eta_{dec}$.

▪ **SW** The first term is the so-called Sachs–Wolfe term. It represents the intrinsic temperature fluctuations associated to the photon density fluctuations $\delta_\gamma/4$ and the metric perturbation $\Psi$ at last scattering.

▪ **Doppler** The second term is the Doppler term $\hat{n}\cdot\vec{v}_b$ caused by local veloc-

ity, this contribution is small on large scales.

▪ **ISW** The last term describes the additional gravitational redshift $\int_{\eta_*}^{\eta_0} \mathrm{d}\eta\left(\Phi'+\Psi'\right)$ due to the evolution of the metric.

The temperature anisotropy has the form

$$\Theta\left(\hat{n}\right)\equiv\frac{\delta T}{\bar{T}}\left(\hat{n}\right)=\int\frac{\mathrm{d}^3k}{\left(2\pi\right)^3}\exp\left(i\vec{k}\cdot\hat{n}ct\left(\eta_*\right)\right)\left(F\left(\eta_*,\vec{k}\right)+i\left(\vec{k}\cdot\hat{n}\right)G\left(\eta_*,\vec{k}\right)\right),$$

where $F\left(\eta_*,\vec{k}\right)=\left(\frac{1}{4}\delta_\gamma+\Psi\right)$, $G\left(\eta_*,\vec{k}\right)=v_b$, $F_*\left(k\right)=\frac{F\left(\eta_*,\vec{k}\right)}{R\left(\eta=0,\vec{k}\right)}$,

$G_*\left(k\right)=\frac{G\left(\eta_*,\vec{k}\right)}{R\left(\eta=0,\vec{k}\right)}$ and $R\left(\eta=0,\vec{k}\right)$ are the initial curvature anisotropies.

We get for the anisotropy the series in Legendre polynomials

$$\Theta\left(\hat{n}\right)=\sum_l i^l\left(2l+1\right)\int\frac{\mathrm{d}^3k}{\left(2\pi\right)^3}\Theta_l\left(k\right)R\left(0,\vec{k}\right)P_l\left(\vec{k}\cdot\hat{n}\right)$$

with the transfer function including ISW

$$\Theta_l\left(k\right)=\Theta_l\left(k\right)=\left(F_*\left(k\right)j_j\left(\chi_*k\right)-G_*\left(k\right)j_j{}'\left(\chi_*k\right)\right)+\int_{\eta_*}^{\eta_0}\mathrm{d}\eta\left(\Phi'+\Psi'\right)j_j\left(ct\left(\eta\right)k\right),$$

with $\chi_*=ct\left(\eta_*\right)$.

The two-point temperature correlation (scalar TT-correlation) spectrum measured in CMB is $C\left(\theta\right)=\left\langle\Theta\left(\hat{n}\right)\Theta\left(\hat{n}'\right)\right\rangle$, with directions $\hat{n},\hat{n}'$, angle $\cos\theta=\hat{n}\cdot\hat{n}'$, and the series in Legendre polynomials

$$C\left(\theta\right)=\sum_l\frac{2l+1}{4\pi}C_lP_l\left(\cos\theta\right)$$

with series coefficients $C_l$

$$C_l=2\pi\int_{-1}^{1}\mathrm{d}\left(\cos\theta\right)C\left(\theta\right)P_l\left(\cos\theta\right)=4\pi\int\frac{\mathrm{d}k}{k}\Theta_l^2\left(k\right)\Delta_R^2\left(k\right)\tag{7.6}$$

where $\Delta_R^2\left(k\right)=A_s\left(\frac{k}{k_0}\right)^{n_s-1}$ is the power amplitude, and where sound horizon is

$r_s=\int\frac{\mathrm{d}\eta}{\sqrt{3\left(1+R\left(\eta\right)\right)}}$, with curvature $R\left(\eta\right)$.

**Weinberg semi-analytic solution** [29]

Weinberg proposed a semi-analytic solution for photon density perturbations

$$\delta_\gamma=\frac{4}{5}R\left(\eta=0,\vec{k}\right)\left(\frac{S\left(k\right)}{\left(1+R\left(\eta,\vec{k}\right)\right)^{1/4}}\cos\left(kr_s+\theta\left(k\right)\right)-\left(1+3R\left(\eta,\vec{k}\right)\right)T\left(k\right)\right)$$

with Weinberg semi-analytic transfer functions for SW and Doppler with

$$F_*\left(k\right)=\frac{1}{5}\left(\exp\left(-\frac{k^2}{k_{D^*}{}^2}\right)\frac{S\left(k\right)}{\left(1+R\left(\eta_*,\vec{k}\right)\right)^{1/4}}\cos\left(kr_{s*}+\theta\left(k\right)\right)-3R\left(\eta_*,\vec{k}\right)T\left(k\right)\right)$$

$$G_*(k) = -\frac{\sqrt{3}}{5}\exp\left(-\frac{k^2}{k_{D^*}{}^2}\right)\frac{S(k)}{\left(1+R\left(\eta_*,\vec{k}\right)\right)^{1/4}}\sin\left(kr_{s^*}+\theta(k)\right) \quad \text{where}$$

$k_{D^*}^{-1} = 8.8\,\text{Mpc}$

and the resulting CMB power spectrum

$$\frac{l(l+1)}{2\pi}C_l = \int_1^\infty \frac{\mathrm{d}\beta}{\beta^2\sqrt{\beta^2-1}}\left(F_*^2\left(\frac{l\beta}{\chi_*}\right)+\frac{\beta^2-1}{\beta^2}G_*^2\left(\frac{l\beta}{\chi_*}\right)\right)\Delta_R^2\left(\frac{l\beta}{\chi_*}\right) \quad \text{with}$$

$\chi_* = ct(\eta_*)$

where

$$S(\kappa) = \left(\frac{1+(1.209\kappa)^2+(0.5611\kappa)^4+\sqrt{5}(0.1567\kappa)^6}{1+(0.9459\kappa)^2+(0.4249\kappa)^4+(0.167\kappa)^6}\right)^2$$

$$T(\kappa) = \frac{\log\left(1+(0.124\kappa)^2\right)}{(0.124\kappa)^2}\left(\frac{1+(1.257\kappa)^2+(0.4452\kappa)^4+(0.2197\kappa)^6}{1+(1.606\kappa)^2+(0.8568\kappa)^4+(0.3927\kappa)^6}\right)^{1/2}$$

$$\theta(\kappa) = \left(\frac{(1.1547\kappa)^2+(0.5986\kappa)^4+\sqrt{5}(0.2578\kappa)^6}{1+(1.723\kappa)^2+(0.8707\kappa)^4+(0.4581\kappa)^6+(0.2204\kappa)^8}\right)^{1/2}.$$

**Calculation of CMB spectrum coefficients $C_l$ ([30] Hu)**

The temperature and photon polarization Stokes parameters anisotropy are expanded in a series in angular momentum ($l$, $m$),

$$\Theta(\eta,\vec{x},\hat{n}) = \int\frac{\mathrm{d}^3k}{(2\pi)^3}\sum_{l=0}^{\infty}\sum_{m=-2}^{2}\Theta_{lm}G_{lm} \tag{21a}$$

$$(Q\pm iU)(\eta,\vec{x},\hat{n}) = \int\frac{\mathrm{d}^3k}{(2\pi)^3}\sum_{l=0}^{\infty}\sum_{m=-2}^{2}(E_{lm}\pm iB_{lm})G_{lm}$$

with temperature ($l$, $m$)-moments

$$\Theta_l^{(m)} = \int \mathrm{d}nY_{lm}^*(\vec{n})\Theta(\vec{n}) \tag{21b}$$

and with temperature basis functions

$$G_{lm} = (-i)^l\sqrt{\frac{4\pi}{2l+1}}Y_{lm}(\hat{n})\exp\left(i\vec{k}\cdot\vec{x}\right) = \sum_l(-i)^l\sqrt{4\pi(2l+1)}j_l(kr)Y_{l0}(\theta,\varphi),$$

$$G_{l'm} = \sum_l(-i)^l\sqrt{4\pi(2l+1)}j_{ll'm}(kr)Y_{lm}(\theta,\varphi),$$

where

$$\exp\left(i\vec{k}\cdot\vec{x}\right) = \sum_l(-i)^l\sqrt{4\pi(2l+1)}j_l(kr)Y_{l0}(\theta,\varphi).$$

In this representation, the spectrum coefficients $C_l$ are

$$\left\langle\Theta_l^{(m)},\Theta_{l'}^{(m')}\right\rangle_\eta \equiv \int \mathrm{d}\eta\,\Theta*_l^{(m)}\Theta_{l'}^{(m')} = \delta_{ll'}\delta_{mm'}C_l \tag{21c}$$

where the power spectrum on the angular momentum $l$ is

$$\Delta_T^2(l) = \frac{l(l+1)}{2\pi}C_lT^2 \quad \text{in } \mu\text{K}^2 \tag{21d}$$

We use the variables:

averaged pressure $V(\eta',k)=-\frac{8\pi G}{ka^2}\int_0^{\eta'}\mathrm{d}\eta\, a^4\delta P$, $V'(\eta,k)=-\frac{8\pi G}{k}a^2\delta P$

optical depth $\tau(\eta')=\sigma_T\int_0^{\eta'}\mathrm{d}\eta\, n_e a$, $\tau'(\eta)=n_e\sigma_T a$.

The temperature ($l$, $m$)-moments are calculated from the evolution equations

$$\Theta'_{lm}=k\left(\frac{\kappa^m_{0l}}{2l-1}\Theta_{lm}-\frac{\kappa^m_{0l+1}}{2l+3}\Theta_{l+1m}\right)-\tau'\Theta_{lm}+S_{lm} \tag{21e}$$

with sources

$$S_{00}=\tau'\Theta_{00}-\Phi',\quad S_{10}=\tau' v_{b0}+k\Psi,\quad S_{11}=\tau' v_{b1}+V'$$

$$S_{20}=\frac{1}{10}\tau'\left(\Theta_{20}-\sqrt{6}E_{20}\right),\quad S_{21}=\frac{1}{10}\tau'\left(\Theta_{21}-\sqrt{6}E_{21}\right),$$

$$S_{22}=\frac{1}{10}\tau'\left(\Theta_{22}-\sqrt{6}E_{22}\right)-\Phi'$$

$$S_{20}=\frac{1}{10}\tau'\left(\Theta_{20}-\sqrt{6}E_{20}\right),\quad S_{21}=\frac{1}{10}\tau'\left(\Theta_{21}-\sqrt{6}E_{21}\right),$$

$$S_{22}=\frac{1}{10}\tau'\left(\Theta_{22}-\sqrt{6}E_{22}\right)-\Phi'$$

$$\frac{\Theta_{lm}(\eta_0,k)}{2l+1}=\int_0^{\eta_0}\mathrm{d}\eta\exp(-\tau)\sum_{l'}S_{l'm}(\eta)\,j_{ll'm}\left(k(\eta_0-\eta)\right)$$

and $j_{ll'm}$ are spherical Bessel functions

$$j_{l00}(x)=j_l(x),\quad j_{l10}(x)=j_l'(x),\quad j_{l20}(x)=\frac{1}{2}\left(3j_l''(x)+j_l(x)\right)$$

$$j_{l11}(x)=\sqrt{\frac{l(l+1)}{2}}\frac{j_l(x)}{x},\quad j_{l21}(x)=\sqrt{\frac{3l(l+1)}{2}}\frac{\mathrm{d}}{\mathrm{d}x}\left(\frac{j_l(x)}{x}\right),$$

$$j_{l22}(x)=\sqrt{\frac{3}{8}\frac{(l+2)!}{(l-2)!}}\frac{j_l(x)}{x^2}.$$

## 10.2. CMB Calculation Results

The metric perturbations $\Psi,\Phi$ in k-space for $k=5$ are shown in **Figure 14**, as a function of relative scale factor $a/a_{eq}$, where $a_{eq}=a_{dec}=0.9\times10^{-3}$ at photon decoupling. Note the transition from high to low amplitude at decoupling.

Density fluctuations for baryons, radiation, cdm $\delta_b$, $\delta_r$, $\delta_c$, for $k=5$ are shown in **Figure 15**, as a function of relative scale factor $a/a_{eq}$. The matter fluctuations decay before or after decoupling, whereas radiation fluctuation stabilizes at a higher level.

The calculated normalized scalar TT-correlation power spectrum of CMB, $\Delta_T^2(l)=\frac{l(l+1)}{2\pi}C_l T^2$, is shown in **Figure 16**, in $\mu\mathrm{K}^2$ over multipole order $l$, calculated for the original Planck Hubble value $H_{0,P}=67.74\,\mathrm{km}\cdot\mathrm{s}^{-1}\cdot\mathrm{Mpc}$. Note

the characteristic decrease from the first to the second maximum and from the third to the following maxima.

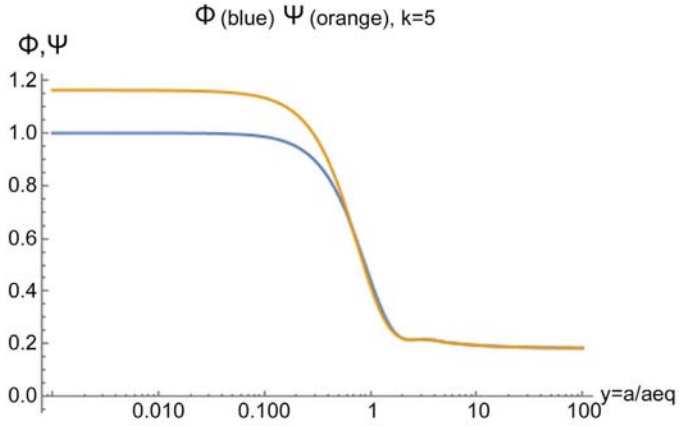


**Figure 14.** Metric perturbations, Ψ, $k = 5$ [31].

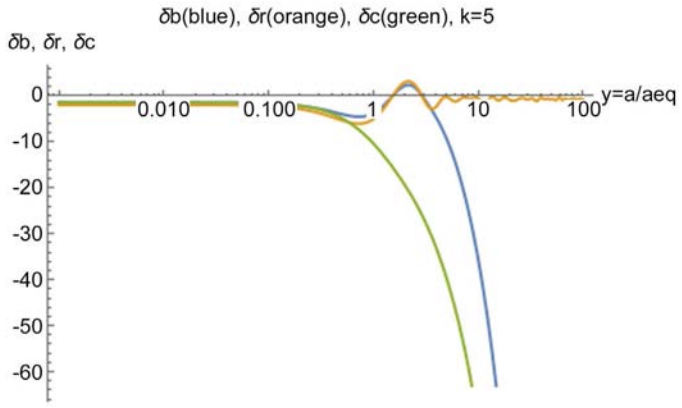


**Figure 15.** Density fluctuations $\delta_b$, $\delta_r$, $\delta_c$, $k = 5$ [31], double logarithmic plot.

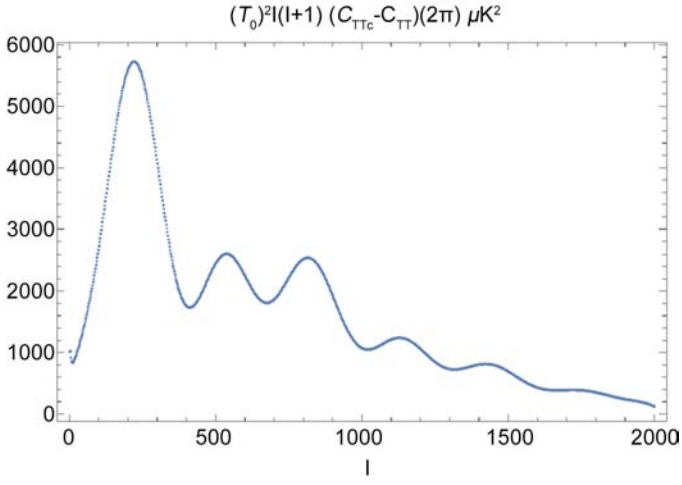


**Figure 16.** Temperature scalar TT-correlation spectrum $y = T^2 \frac{l(l+1)}{2\pi} C_l$, $[y] = \mu\mathrm{K}^2$, $x = l$ [31].

The background Hubble parameter $H_0$ influences the CMB spectrum, but the deviation $\delta$ = 1.3% caused by the calculated correction from chap. 5 is within measurement error.

The plot in Figure 17 shows the difference between the power spectrum for Planck-Hubble-parameter $\Delta_T^2\left(l,H_{0,P}\right)=\frac{l(l+1)}{2\pi}C_lT^2$, and for the background-corrected Hubble-parameter $\Delta_T^2\left(l,H_{0,Pc}\right)=\frac{l(l+1)}{2\pi}C_lT^2$, where $H_{0,Pc}=H_{0,P}\times 1.043=70.6\pm 0.4$, with maximum deviation of $\delta$ = 1.3%.

In Figure 18 is shown the scalar TT-correlation power spectrum from Figure 16, together with measurement data and its error bars.

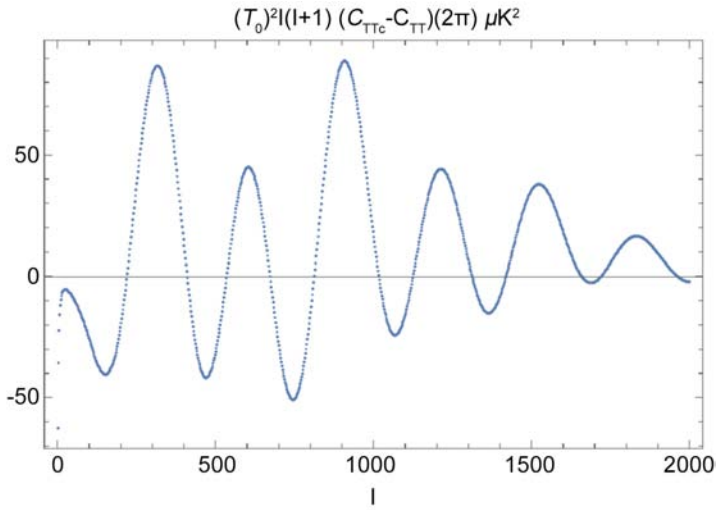


Figure 17. Power TT spectrum Hubble correction, max rel.dev. $\delta$ = 1.3% [31].

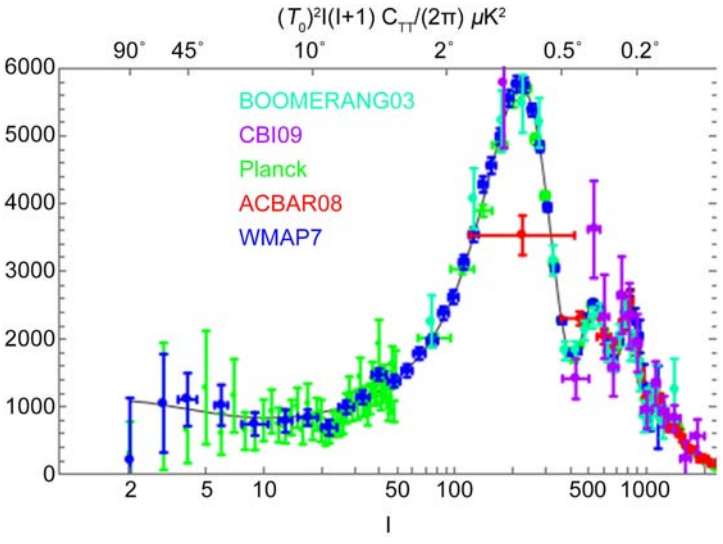


Figure 18. Temperature scalar TT-correlation power spectrum with measured data [22] [31], for measurements Planck, WMAP, ACBAR, CBI, and BOOMERANG.

## 11. Concise Presentation

In the following, we present the fundamental equations, the solution process and results in form of schematic diagrams for the background calculation and for the CMB calculation.

Lambda-CDM background calculation:

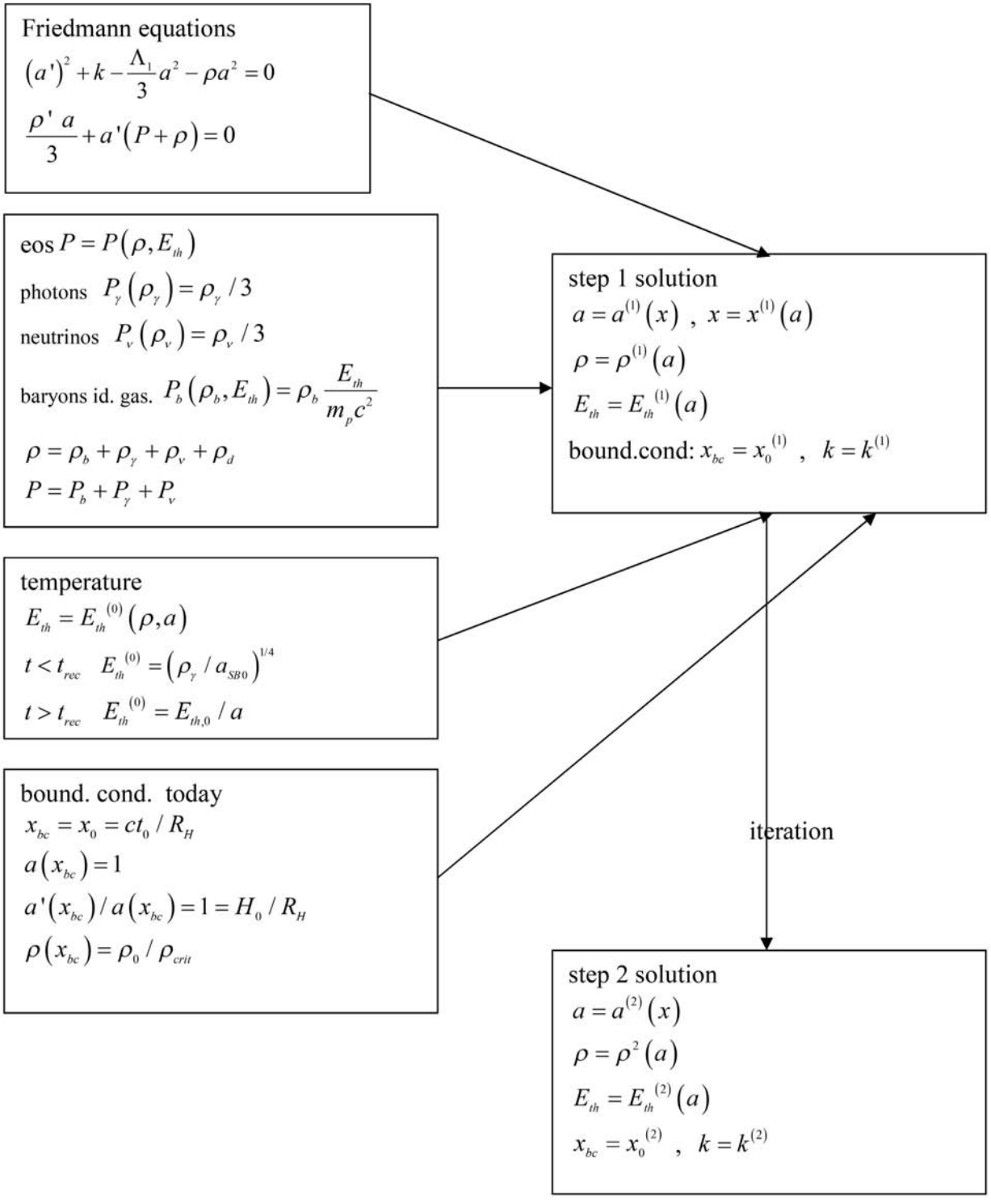

Lambda-CDM CMB calculation:

perturbations

$ds^2 = a(\eta)\left(-(1+2\Psi)d\eta^2 + (1-2\Phi)dx^i dx_i\right)$

$\Phi, \Psi, \theta, \sigma, \delta, \delta P$ perturbations

$\delta P$ pressure

$\theta = ik^j v_j$ velocity

$\delta = \delta\rho / \bar{\rho}$ relative density

$\sigma = -\left(\hat{k}^i\hat{k}^j - \frac{1}{3}\delta_{ij}\right)\Pi^i{}_j / \left(\bar{\rho} + \bar{P}\right)$ stress

$\bar{\rho}, \bar{P}, a, E_{th}, \tau$ background

Einstein equations k-space

$k^2\Phi - 3H\left(\Phi' + H\Psi\right) = \pi G a^2 \delta\rho$

$k^2\left(\Phi' + H\Psi\right) = \pi G a^2 \left(\bar{P} + \bar{\rho}\right)\theta$

$k^2\left(\Phi - \Psi\right) = 12\pi G a^2 \left(\bar{P} + \bar{\rho}\right)\sigma$

$\Phi'' + H\left(\Psi' + 2\Phi'\right) + \frac{1}{3}k^2\left(\Phi - \Psi\right)$

$+\left(2H' + H^2\right)\Psi = 4\pi G a^2 \delta P$

thermodynamic: density+Euler

$\delta' = -\left(1 + \frac{\bar{P}}{\bar{\rho}}\right)\left(\theta - 3\Phi'\right) - 3H\left(\frac{\delta P}{\bar{\rho}\,\delta} - \frac{\bar{P}}{\bar{\rho}}\right)\delta$

$\theta' = -\left(H + \frac{\bar{P}'}{\bar{P} + \bar{\rho}}\right)\theta - \frac{\delta P}{\left(\bar{P} + \bar{\rho}\right)}k^2 - k^2\sigma + k^2\Psi$

initial conditions

$\Phi, \Psi, \theta, \sigma, \delta, \delta P$ = variables $\xi_i$

$\xi_i\left(a = 0\right) = \xi_{i,1}$

CMB power spectrum coef $C_l$

$\Theta(\eta, \vec{x}, \hat{n}) = \int \frac{d^3k}{(2\pi)^3} \sum_{l=0}^{\infty} \sum_{m=-2}^{2} \Theta_{lm} G_{lm}$

$\left\langle \Theta_l^{(m)}, \Theta_{l'}^{(m')} \right\rangle_\eta \equiv \int d\eta\, \Theta^{*(m)}_l \Theta_{l'}^{(m')} = \delta_{ll'}\delta_{mm'} C_l$

$\Theta_l^{(m)} = \int dn Y_{lm}^{*}\left(\vec{n}\right)\Theta\left(\vec{n}\right)$

$\Theta'_{lm} = k\left(\frac{\kappa^m_{0l}}{2l-1}\Theta_{lm} - \frac{\kappa^m_{0l+1}}{2l+3}\Theta_{l+1m}\right) - \tau'\Theta_{lm} + S_{lm}$

measurement temperature correlations

$C(\theta) = \left\langle \Theta(\hat{n})\Theta(\hat{n}') \right\rangle$

$C(\theta) = \sum_l \frac{2l+1}{4\pi} C_l P_l(\cos\theta)$

measured, calculated coef $C_l$

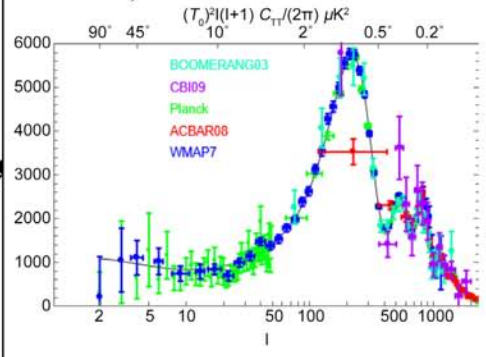


13 fitted parameters

$\Omega_b, \Omega_c, \Omega_\Lambda, t_0, H_0, A_s, n_s, \tau, w, \Sigma m_\nu, N_\nu, r_t, \frac{dn_s}{dk}$

## 12. Conclusions

The results for the background part are presented in schematic form in chap. 11 Lambda-CDM background calculation.

We start with the Friedmann equations

$$(a')^2 + k - \frac{\Lambda_1}{3}a^2 - \rho a^2 = 0$$

$$\frac{\rho' a}{3} + a'(P + \rho) = 0$$

with the variables in dependence of the scale factor *a* (inverting the scalefactor-time relation $a = a(x)$,

$x(a)$ time,

$\rho_i(a)$ density of component *i*,

$E_{th}(a)$ temperature,

for components radiation *γ*, neutrinos $\nu$, electrons *e*, protons *p*, neutrons *n*, cdm *d*, where the pressure $P_i(a)$ is eliminated using the component eos $P_i = P_i(\rho_i, E_{th})$.

In difference to the conventional ansatz,

-the temperature resp. **thermal energy is introduced as explicit function of time** $E_{th}(t)$;

-we use **the ideal gas eos for baryons**, instead of the usual setting $P_b = 0$ (dust eos).

As we show in chap. 5, this leads to a correction of 4.3% for the present value of Hubble parameter $H_{0c} = 1.043 H_0$, which brings it into agreement with the measured Red-Giant-result, and within error margin with the Cepheids-SNIa-measurement.

We carry out an iterated calculation with two steps *i* = 1 and *i* = 2, the results are shown graphically in chap. 10.2.

Note the deviation of the temperature from the conventional linear behavior (brown) to the calculated first-iteration-value (blue) for later times. This produces also a slight "bump" for the Hubble parameter $H(a)$, and there is a slight "kink" in $x(a)$.

The results for the perturbation part are presented in schematic form in chap. 11 Lambda-CDM CMB calculation.

We start with the perturbed metric

$$\mathrm{d}s^2 = a(\eta)\left(-(1+2\Psi)\mathrm{d}\eta^2 + (1-2\Phi)\mathrm{d}x^i \mathrm{d}x_i\right)$$

perturbations $\Phi, \Psi, \theta, \sigma, \delta, \delta P$, where

$\delta P$ pressure

$\theta = ik^j v_j$ velocity

$\delta = \delta\rho/\bar{\rho}$ relative density

$\sigma = -\left(\hat{k}^i \hat{k}^j - \frac{1}{3}\delta_{ij}\right)\Pi^i_j / \left(\bar{\rho} + \bar{P}\right)$ stress

$\bar{\rho}, \bar{P}, a, E_{th}$ are background functions calculated already in the background

part.

And $\tau$ = reionization optical depth is a parameter used for the CMB calculation.

The perturbations result from (random) initial conditions and represent the random nature of structure formation.

The resulting fundamental equations are transformed to *k*-space (*i.e.* Fourier transformed), and consist of two parts.

The Einstein equations in *k*-space resulting from the perturbed metric ansatz

$$k^2\Phi - 3H\left(\Phi' + H\Psi\right) = \pi G a^2 \delta\rho$$

$$k^2\left(\Phi' + H\Psi\right) = \pi G a^2 \left(\bar{P} + \bar{\rho}\right)\theta$$

$$k^2\left(\Phi - \Psi\right) = 12\pi G a^2 \left(\bar{P} + \bar{\rho}\right)\sigma$$

$$\Phi'' + H\left(\Psi' + 2\Phi'\right) + \frac{1}{3}k^2\left(\Phi - \Psi\right) + \left(2H' + H^2\right)\Psi = 4\pi G a^2 \delta P$$

and the thermodynamic: density and Euler (relativistic fluid) equation, resulting from the relativistic Boltzmann transport equation

$$\delta' = -\left(1 + \frac{\bar{P}}{\bar{\rho}}\right)\left(\theta - 3\Phi'\right) - 3H\left(\frac{\delta P}{\bar{\rho}\,\delta} - \frac{\bar{P}}{\bar{\rho}}\right)\delta$$

$$\theta' = -\left(H + \frac{\bar{P}'}{\bar{P} + \bar{\rho}}\right)\theta - \frac{\delta P}{\bar{P} + \bar{\rho}}k^2 - k^2\sigma + k^2\Psi$$

The CMB power spectrum coefficients $C_l$ depend on the angular moments of temperature correlation $\Theta_{lm}$, which obey the iterative differential equation in *k*-space

$$\Theta'_{lm} = k\left(\frac{\kappa^m_{0l}}{2l-1}\Theta_{lm} - \frac{\kappa^m_{0l+1}}{2l+3}\Theta_{l+1m}\right) - \tau'\Theta_{lm} + S_{lm}$$

with parameters, which are calculated from the fundamental equations.

The actual numerical calculation is performed in program [31], based on a function library from [22].

Then a fit is carried out between the calculated parameterized coefficients $C_l\left(p_i\right)$ and tthe measured values $C_{l,exp}$.

The 13 fitted parameters

$p_i = \left(\Omega_b, \Omega_c, \Omega_\Lambda, t_0, H_0, A_s, n_s, \tau, w, \Sigma m_\nu, N_\nu, r_t, \frac{\mathrm{d}n_s}{\mathrm{d}k}\right)$ are calculated by the Planck collaboration [32], and are not recalculated here.

The fitted [32] and measured coefficients $C_l$ are shown in a plot.

## Conflicts of Interest

The author declares no conflicts of interest regarding the publication of this paper.

## References

[1] Fliessbach, T. (1990) Allgemeine Relativitätstheorie. Bibliographisches Institut, Leipzig.

[2] Dodelson, S. and Schmidt, F. (2021) Modern Cosmology. Academic Press, Cambridge.

[3] Vittorio, N. (2018) Cosmology. CRC Press, Boca Raton. https://doi.org/10.1201/b22176

[4] Baumann, D. (2022) Cosmology. Cambridge University Press, Cambridge. https://doi.org/10.1017/9781108937092

[5] Ciufolini, I. and Wheeler, A. (1996) Gravitation and Inertia. Princeton University Press, Princeton. https://doi.org/10.1515/9780691190198

[6] Soff, G. (1993) Allgemeine Relativitätstheorie. Univ. Frankfurt/M, Frankfurt.

[7] Blau, M. (2000) Lecture Notes on General Relativity. Bern University, Bern.

[8] Stefani, H., *et al.* (2003) Exact Solutions of Einstein's Field Equations. Cambridge University Press, Cambridge.

[9] Steiner, F. (2008) Solution of the Friedmann Equation Determining the Time Evolution. Ulm University, Ulm.

[10] Armendariz-Picon, C. and Neelakanta, J. (2014) *Journal of Cosmology and Astroparticle Physics*, **3**, 49. https://doi.org/10.1088/1475-7516/2014/03/049

[11] Particle Data Group (2022). https://pdg.lbl.gov/2011/reviews/rpp2011-rev-cosmological-parameters.pdf

[12] Shaw, J.R. and Lewis, A. (2010) *Physical Review D*, **81**, Article ID: 043517. https://doi.org/10.1103/PhysRevD.81.043517

[13] Helm, J. (2023) LamCDM.nb Mathematica Program. https://www.researchgate.net/profile/Jan-Helm/publications

[14] Ma, C.-H. and Bertschinger, E. (1995) Cosmological Perturbation Theory.

[15] Planck Collaboration (2022). https://www.cosmos.esa.int/web/planck/planck-collaboration

[16] Aydiner, E. (2022) *The European Physical Journal*, **82**, 39. https://doi.org/10.1140/epjc/s10052-022-09996-2

[17] Davis, T.M. and Lineweaver, C.H. (2003) Expanding Confusion.

[18] Helm, J. (2018) A Covariant Formulation of the Ashtekar-Kodama Quantum Gravity and Its Solutions. https://www.researchgate.net

[19] Crevecoeur, G.U. (2016) Evolution of the Distance Scale Factor and the Hubble Parameter.

[20] Lewis, A. and Challinor, A. (2013) Code for Anisotropies in the Microwave Background CAMB Fortran-Python Code.

[21] Bernardeau, F., Pitrou, C. and Uzan, J.-P. (2010) CMB Spectra and Bispectra Calculations: Making the Flat-Sky Approximation Rigorous. arXiv: astro-ph/1012.2652.

[22] Pitrou, C. (2018) CMBquick Mathematica Program. https://www2.iap.fr/users/pitrou

[23] Croswell, K. (1996) Alchemy of the Heavens. Anchor, New York.

[24] Lee, R. (2020) *Nuclear Physics B*, **860**, Article ID: 115200.

[25] Maximon, L.C. (1968) *Journal of Research of the National Bureau of Standards B*, **72**, 79-88. https://doi.org/10.6028/jres.072B.011

[26] Hu, W. (2017) CMB. Lecture, University of Chicago, Chicago.

[27] Peebles, P.J.E. (1968) *The Astrophysical Journal*, **153**, 1. https://doi.org/10.1086/149628

[28] Hu, W. (2001) Cosmic Microwave Background. University of Chicago, Chicago. https://background.uchicago.edu

[29] Weinberg, S. (2008) Cosmology. Oxford University Press, Oxford. https://doi.org/10.1093/oso/9780198526827.001.0001

[30] Hu, W. and White, M. (1997) CMB Anisotropies: Total Angular Momentum Method.

[31] Helm, J. (2023) LamCDMcmb.nb Mahematica Program. https://www.researchgate.net/profile/Jan-Helm/publications

[32] Planck Collaboration (2016) *Astronomy & Astrophysics*, **594**, A13.

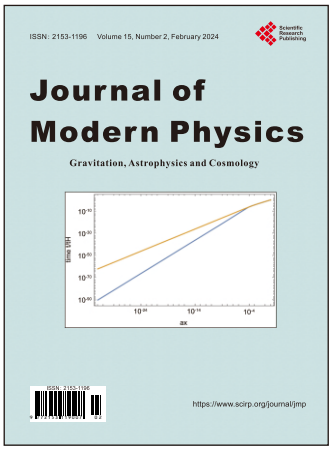


# Call for Papers

# Journal of Modern Physics

**ISSN: 2153-1196 (Print) ISSN: 2153-120X (Online)**
**https://www.scirp.org/journal/jmp**

***Journal of Modern Physics*** **(JMP)** is an international journal dedicated to the latest advancement of modern physics. The goal of this journal is to provide a platform for scientists and academicians all over the world to promote, share, and discuss various new issues and developments in different areas of modern physics.

## Subject Coverage

Journal of Modern Physics publishes original papers including but not limited to the following fields:

Biophysics and Medical Physics
Complex Systems Physics
Computational Physics
Condensed Matter Physics
Cosmology and Early Universe
Earth and Planetary Sciences
General Relativity
High Energy Astrophysics
High Energy/Accelerator Physics
Instrumentation and Measurement
Interdisciplinary Physics
Materials Sciences and Technology
Mathematical Physics
Mechanical Response of Solids and Structures
New Materials: Micro and Nano-Mechanics and Homogeneization
Non-Equilibrium Thermodynamics and Statistical Mechanics
Nuclear Science and Engineering
Optics
Physics of Nanostructures
Plasma Physics
Quantum Mechanical Developments
Quantum Theory
Relativistic Astrophysics
String Theory
Superconducting Physics
Theoretical High Energy Physics
Thermology

We are also interested in: 1) Short Reports—2-5 page papers where an author can either present an idea with theoretical background but has not yet completed the research needed for a complete paper or preliminary data; 2) Book Reviews—Comments and critiques.

## Notes for Intending Authors

Submitted papers should not have been previously published nor be currently under consideration for publication elsewhere. Paper submission will be handled electronically through the website. All papers are refereed through a peer review process. For more details about the submissions, please access the website.

## Website and E-Mail

**https://www.scirp.org/journal/jmp** **E-mail: jmp@scirp.org**

## What is SCIRP?

Scientific Research Publishing (SCIRP) is one of the largest Open Access journal publishers. It is currently publishing more than 200 open access, online, peer-reviewed journals covering a wide range of academic disciplines. SCIRP serves the worldwide academic communities and contributes to the progress and application of science with its publication.

## What is Open Access?

All original research papers published by SCIRP are made freely and permanently accessible online immediately upon publication. To be able to provide open access journals, SCIRP defrays operation costs from authors and subscription charges only for its printed version. Open access publishing allows an immediate, worldwide, barrier-free, open access to the full text of research papers, which is in the best interests of the scientific community.

- High visibility for maximum global exposure with open access publishing model
- Rigorous peer review of research papers
- Prompt faster publication with less cost
- Guaranteed targeted, multidisciplinary audience


Scientific Research Publishing

**Website: https://www.scirp.org**
**Subscription: sub@scirp.org**
**Advertisement: service@scirp.org**